https://www.mdc-berlin.de/de/veroeffentlichungstypen/clinical-journal-club

Als gemeinsame Einrichtung von MDC und Charité fördert das Experimental and Clinical Research Center die Zusammenarbeit zwischen Grundlagenwissenschaftlern und klinischen Forschern. Hier werden neue Ansätze für Diagnose, Prävention und Therapie von Herz-Kreislauf- und Stoffwechselerkrankungen, Krebs sowie neurologischen Erkrankungen entwickelt und zeitnah am Patienten eingesetzt. Sie sind eingeladen, uns beizutreten. Bewerben Sie sich!

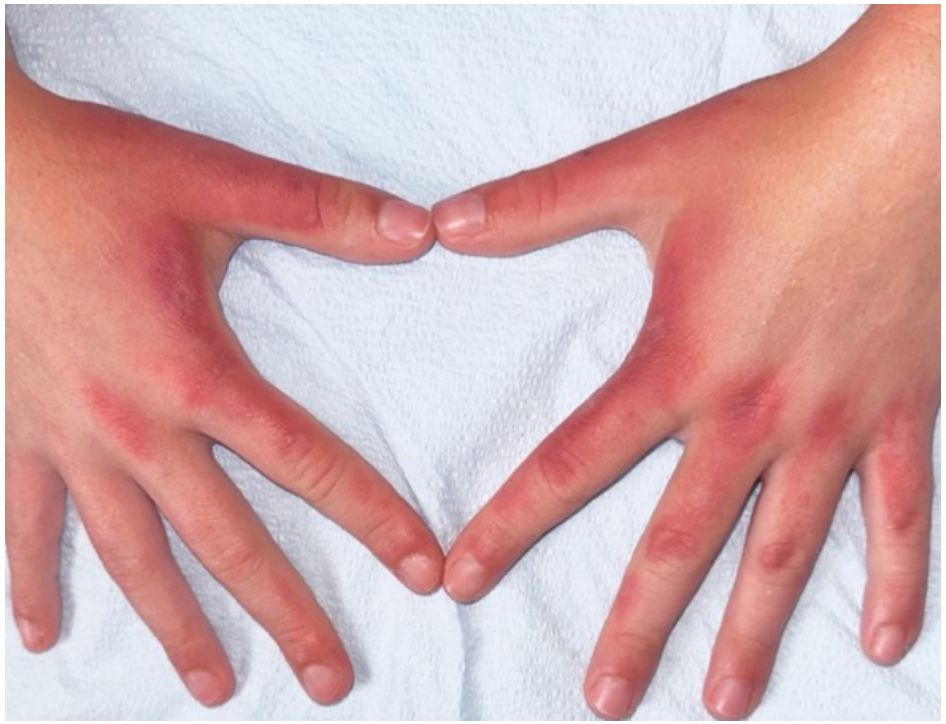

A 44-year-old man presented with a 4-day history of an itchy rash and a 2-day history of fever and malaise. The rash had first appeared on the scalp and then spread across the body within 24 hours. What is the most likely diagnosis?

Cutaneous t-cell lymphoma

Dengue fever

Disseminated gonococcal infection

➔ Primary varicella infection

Small pox

A polymerase-chain-reaction assay of fluid from a vesicle was positive for varicella–zoster virus. The patient reported no history of chicken pox or varicella vaccination. Primary varicella infection, or chicken pox, in adults is often more severe than in children, which highlights the importance of childhood vaccination. Adults with varicella infection — even immunocompetent ones, such as this patient — have an increased risk of complications, such as pneumonia and encephalitis.

Primary varicella infection, also known as chickenpox, is the initial illness caused by the varicella-zoster virus (VZV). It typically presents with an itchy, fluid-filled rash that starts on the body and spreads, often accompanied by fever, fatigue, and headache. While mild in healthy children, the infection can be more severe in adults, immunocompromised individuals, and pregnant women, potentially leading to complications like pneumonia or bacterial skin infections. After recovery, the virus lies dormant in the nerves and can reactivate later in life to cause shingles

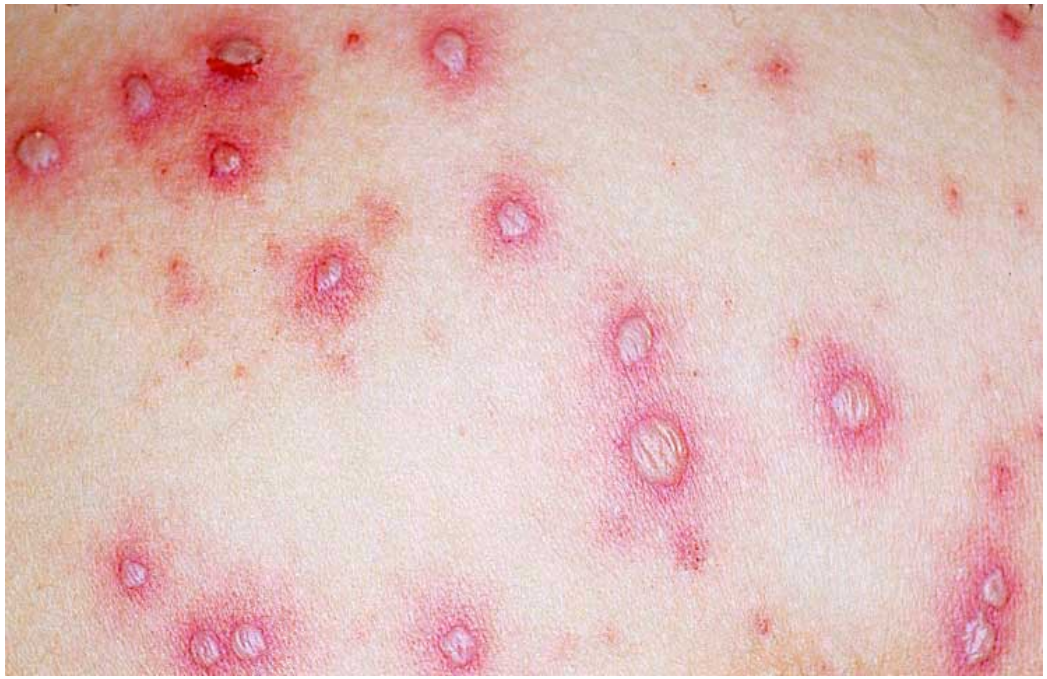

Aspirin hemmt sowohl Cyclooxygenase-1 (COX-1) als auch Cyclooxygenase-2 (COX-2) durch irreversible Acetylierung der Serinreste in ihrem aktiven Zentrum, was die Umwandlung von Arachidonsäure in Prostaglandine verhindert. Obwohl Aspirin beide Enzyme hemmt, ist die Hemmung von COX-1 stärker, was zu seinen kardiovaskulären Wirkungen führt. Bei der langfristigen Anwendung kann Aspirin jedoch auch das Risiko für bestimmte Krebsarten, insbesondere Dickdarmkrebs, durch die Hemmung von COX-2 senken.

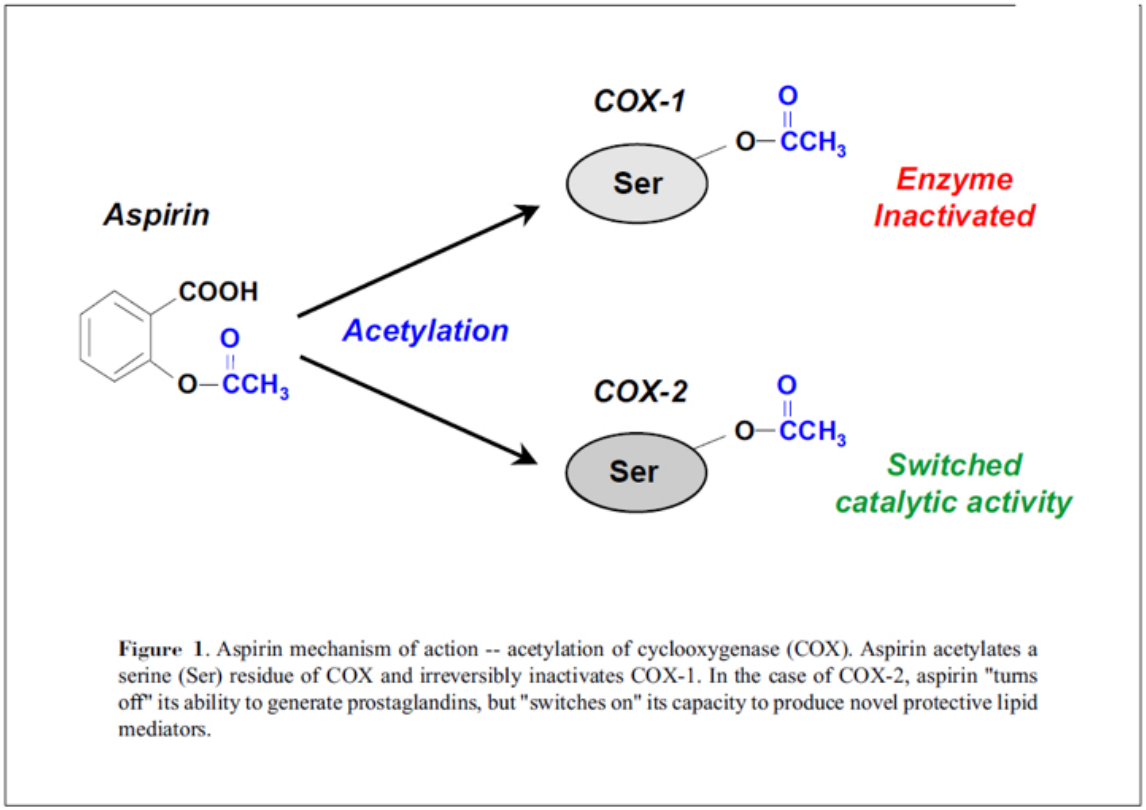

Figure 1. Aspirin mechanism of action -- acetylation of cyclooxygenase (COX). Aspirin acetylates a serine (Ser) residue of COX and irreversibly inactivates COX-1. In the case of COX-2, aspirin "turns off" its ability to generate prostaglandins, but "switches on" its capacity to produce novel protective lipid mediators.

Der PI3K/Akt-Signalweg ist ein wichtiger intrazellulärer Signalweg, der bei vielen Zellvorgängen eine Rolle spielt, die das Wachstum, die Proliferation und den Stoffwechsel der Zellen regulieren. Seine genauen Abläufe sind bislang (2022) noch nicht vollständig geklärt.

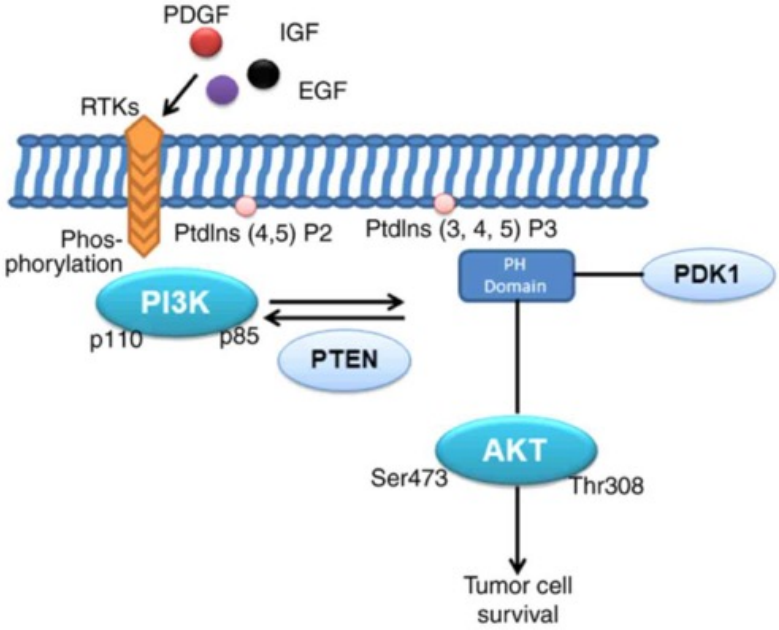

Die Phosphatase PTEN (Phosphatase and Tensin homolog) ist ein multifunktionelles Enzym in Eukaryoten. Es katalysiert die Hydrolyse von verschiedenen Phosphorsäureestern (Phospholipide und Phosphoproteine).

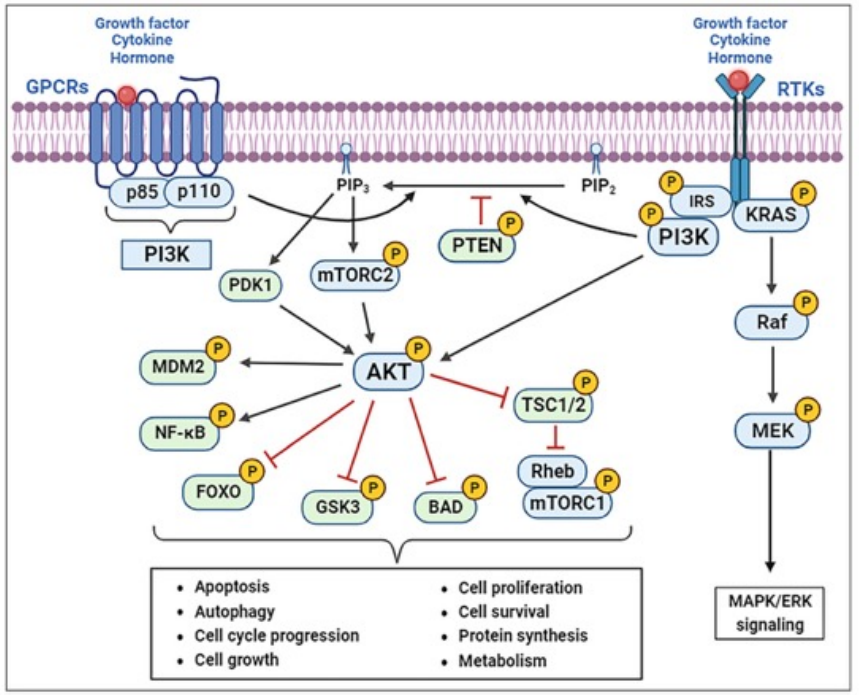

Die **AKT-Kinase**, auch als Proteinkinase B (PKB) bekannt, ist eine Serin-Threonin-Proteinkinase, die an der Signalübertragung in Zellen beteiligt ist und wesentliche Zellprozesse wie Zellwachstum.

COX-2 und die Phosphoinositid 3-Kinase (PI3K) sind zwei verschiedene, aber miteinander verbundene Signalwege, die an Entzündungsprozessen und dem Zellwachstum beteiligt sind. COX-2 ist ein Enzym, das Entzündungen fördert, während die PI3K-Signalwege Funktionen in der Zellteilung und beim Stoffwechsel übernehmen und mit Krebs in Verbindung gebracht werden. Die Hemmung von COX-2, zum Beispiel durch ASS oder Coxibe, kann das Tumorwachstum verringern, und es wird untersucht, wie diese Wege zusammenwirken, etwa bei der Tumorentstehung oder -progression.

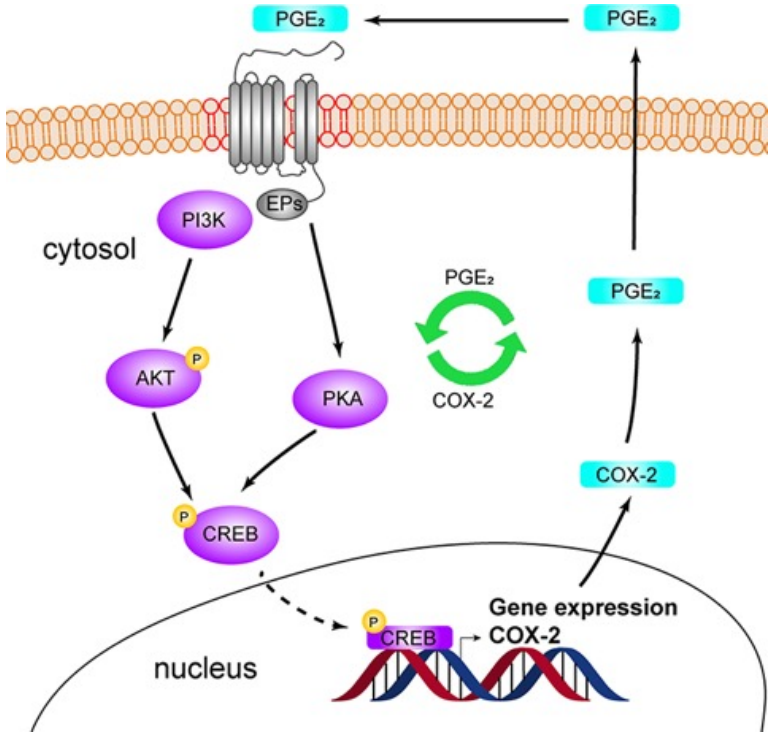

PIK3CA ist ein Gen, das die katalytische Untereinheit (p110α) des Enzyms Phosphatidylinositol-3-Kinase (PI3K) kodiert. Mutationen in diesem Gen, die zur Überaktivität des PI3K-Signalwegs führen, sind mit verschiedenen Krebsarten assoziiert.

Low-Dose Aspirin for PI3K-Altered Localized Colorectal Cancer

Aspirin reduces the incidence of colorectal adenoma and colorectal cancer among high-risk persons. Observational studies suggest that aspirin may also improve disease-free survival after diagnosis, particularly among patients with tumors harboring somatic *PIK3CA* mutations. However, data from randomized trials are lacking.

We conducted a double-blind, randomized, placebo-controlled trial involving patients with stage I, II, or III rectal cancer or stage II or III colon cancer with somatic alterations in PI3K pathway genes. The patients were assigned in a 1:1 ratio to receive 160 mg of aspirin or matched placebo once daily for 3 years. Patients with prespecified *PIK3CA* hotspot mutations in exon 9 or 20 (group A alterations) and those with other moderate- or high-impact somatic variants in *PIK3CA*, *PIK3R1*, or *PTEN* (group B alterations) were eligible for randomization. The primary end point was colorectal cancer recurrence, assessed in a time-to-event analysis, in patients with group A alterations. Secondary end points included colorectal cancer recurrence in patients with group B alterations, disease-free survival, and safety.

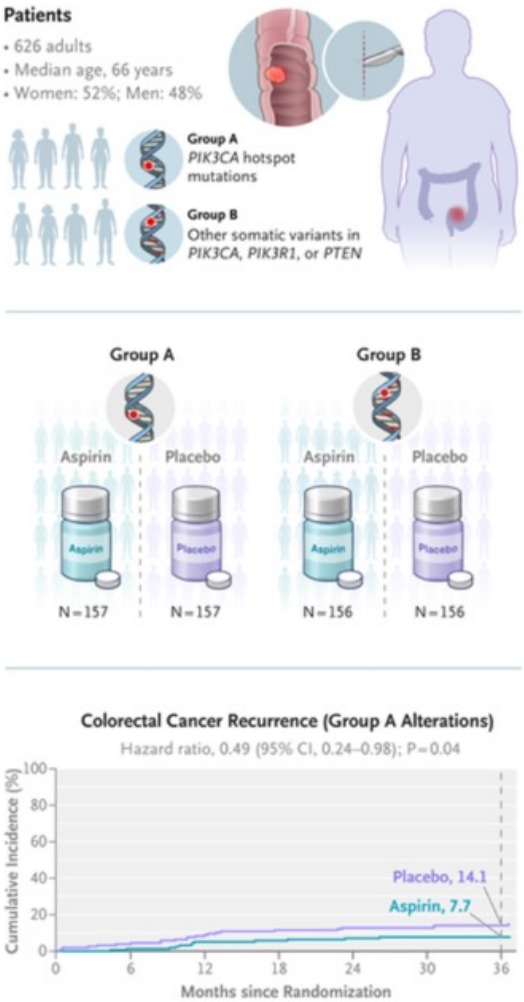

The antineoplastic effects of aspirin are believed to occur primarily through the inhibition of cyclooxygenase-2 (COX-2), an enzyme frequently overexpressed in colorectal cancer. COX-2 promotes tumorigenesis by increasing the production of prostaglandin E2 (PGE2), which subsequently activates the phosphatidylinositol 3-kinase (PI3K)–protein kinase B–mammalian target of rapamycin signaling pathway. Although PI3K signaling has been linked to the upregulation of COX-2 expression, the mechanistic interplay between these pathways remains incompletely understood. The PI3K pathway is genetically altered in approximately one third of colorectal cancers; such alterations most commonly involve mutations in *PIK3CA*, *PIK3R1*, or *PTEN*.

Preclinical and retrospective clinical data suggest that COX-2 may be a critical downstream effector of *PIK3CA*-mutated tumors and a key determinant of aspirin sensitivity and that such effects are potentially mediated by a positive feedback loop between PI3K signaling and COX-2 expression. Several observational studies have shown that aspirin improves survival among patients with *PIK3CA*-mutated tumors but has no benefit in those with wild-type tumors. However, given the variability in existing clinical and experimental findings, further research is warranted to elucidate the basis of the interaction between aspirin and mutations in *PIK3CA*, *PIK3R1*, and *PTEN*. We conducted the ALASCCA (Adjuvant Low-Dose Aspirin in Colorectal Cancer) trial to prospectively evaluate the efficacy of adjuvant aspirin in patients who had resected stage I, II, or III colorectal cancer with a primary tumor harboring somatic alterations in genes involved in the PI3K signaling pathway.

Patients

Patients 18 to 80 years of age with pathological tumor–node–metastasis (pTNM) stage II or III colon cancer or pTNM stage I, II, or III rectal cancer who had undergone radical resection of the primary tumor were prospectively screened for prespecified somatic alterations in *PIK3CA*, *PIK3R1*, and *PTEN*. Cancer stage was assessed according to the criteria in the *AJCC [American Joint Committee on Cancer] Cancer Staging Manual*, 7th edition.

Patients were eligible for inclusion if somatic alterations from group A, group B, or both were present. Group A alterations were prespecified hotspot mutations in exons 9 and 20 of *PIK3CA*. Group B alterations were other moderate- or high-impact somatic variants in *PIK3CA*, *PIK3R1 (encodes a regulated subunit)*, or *PTEN* (encompassing mutations with varying degrees of functional effects on the encoded protein). Patients with group A and group B alterations were included in the cohort with group A alterations.

Trial Design

The trial was conducted in 33 hospitals in Sweden, Norway, Denmark, and Finland. Patients were assigned, in a 1:1 ratio, within 12 weeks after surgery to receive aspirin at a dose of 160 mg or matched placebo once daily for 3 years. Aspirin and placebo were administered alone or with adjuvant chemotherapy chosen by the local investigator in accordance with national guidelines for colorectal cancer treatment in each country.

Characteristics of the Patients at Baseline (Full Analysis Population).

Characteristic	Group A Alterations		Group B Alterations	
	Aspirin (N=157)	Placebo (N=157)	Aspirin (N=156)	Placebo (N=156)
Age — yr				
Median (IQR)	65 (59–72)	66 (59–73)	66 (57–74)	66 (56–71)
Range	31–80	35–80	33–80	31–80
Female sex — no. (%)	81 (51.6)	75 (47.8)	83 (53.2)	85 (54.5)
Time from surgery to randomization — wk				
Median (IQR)	8.0 (6.1–10.1)	8.0 (6.1–10.0)	7.0 (5.6–8.3)	7.9 (5.7–10.0)
Range	1.9–15.9	3.9–21.0	3.9–18.3	1.6–23.3
Tumor location — no. (%)				
Right colon	65 (41.4)	79 (50.3)	72 (46.2)	63 (40.4)
Left colon	44 (28.0)	29 (18.5)	27 (17.3)	37 (23.7)
Colon, not otherwise specified	1 (0.6)	2 (1.3)	0	0
Rectum	47 (29.9)	47 (29.9)	57 (36.5)	56 (35.9)
ASA score — no. (%)†				
1	39 (24.8)	35 (22.3)	36 (23.1)	25 (16.0)
2	101 (64.3)	102 (65.0)	97 (62.2)	113 (72.4)
3 or 4	14 (8.9)	14 (8.9)	19 (12.2)	14 (9.0)
Missing data	3 (1.9)	6 (3.8)	4 (2.6)	4 (2.6)
pTNM stage in colon cancer — no./total no. (%)				
II	60/110 (54.5)	60/110 (54.5)	52/99 (52.5)	51/100 (51.0)
III	50/110 (45.5)	50/110 (45.5)	47/99 (47.5)	49/100 (49.0)
pTNM stage in rectal cancer — no./total no. (%)				
I	11/47 (23.4)	10/47 (21.3)	14/57 (24.6)	14/56 (25.0)
II	21/47 (44.7)	20/47 (42.6)	21/57 (36.8)	22/56 (39.3)
III	15/47 (31.9)	17/47 (36.2)	22/57 (38.6)	20/56 (35.7)
Tumor grade — no. (%)				
Low grade	126 (80.3)	119 (75.8)	113 (72.4)	116 (74.4)
High grade	24 (15.3)	27 (17.2)	31 (19.9)	32 (20.5)
Missing data	7 (4.5)	11 (7.0)	12 (7.7)	8 (5.1)
Neoadjuvant treatment in rectal cancer — no./total no. (%)				
Radiotherapy only	11/47 (23.4)	9/47 (19.1)	21/57 (36.8)	13/56 (23.2)
Chemoradiotherapy	5/47 (10.6)	3/47 (6.4)	3/57 (5.3)	7/56 (12.5)
Total neoadjuvant treatment	9/47 (19.1)	9/47 (19.1)	2/57 (3.5)	12/56 (21.4)
No neoadjuvant treatment	22/47 (46.8)	26/47 (55.3)	31/57 (54.4)	24/56 (42.9)
Adjuvant chemotherapy in colon cancer — no./total no. (%)				
Fluorouracil–capecitabin	19/110 (17.3)	21/110 (19.1)	26/99 (26.3)	16/100 (16.0)
Fluorouracil–capecitabin plus oxaliplatin	31/110 (28.2)	30/110 (27.3)	27/99 (27.3)	41/100 (41.0)
No adjuvant chemotherapy	60/110 (54.5)	58/110 (52.7)	46/99 (46.5)	43/100 (43.0)
Missing data	0/110	1/110 (0.9)	0/99	0/100
Adjuvant chemotherapy in rectal cancer — no./total no. (%)				
Fluorouracil–capecitabin	7/47 (14.9)	3/47 (6.4)	3/57 (5.3)	4/56 (7.1)
Fluorouracil–capecitabin plus oxaliplatin	7/47 (14.9)	7/47 (14.9)	12/57 (21.1)	9/56 (16.1)
No adjuvant chemotherapy	33/47 (70.2)	37/47 (78.7)	42/57 (73.7)	43/56 (76.8)
MSI status — no. (%)				
MSI-high	33 (21.0)	39 (24.8)	38 (24.4)	35 (22.4)
MSS or MSI-low	98 (62.4)	104 (66.2)	94 (60.3)	89 (57.1)
Unknown	26 (16.6)	14 (8.9)	24 (15.4)	32 (20.5)
BRAF V600E mutation status — no. (%)				
Present	32 (20.4)	30 (19.1)	40 (25.6)	38 (24.4)
Absent	110 (70.1)	115 (73.2)	96 (61.5)	91 (58.3)
Unknown	15 (9.6)	12 (7.6)	20 (12.8)	27 (17.3)
KRAS mutation status — no. (%)				
Present	85 (54.1)	87 (55.4)	53 (34.0)	63 (40.4)
Absent	60 (38.2)	65 (41.4)	87 (55.8)	79 (50.6)
Unknown	12 (7.6)	5 (3.2)	16 (10.3)	14 (9.0)
NRAS mutation status — no. (%)				
Present	7 (4.5)	5 (3.2)	12 (7.7)	3 (1.9)
Absent	130 (82.8)	140 (89.2)	120 (76.9)	123 (78.8)
Unknown	20 (12.7)	12 (7.6)	24 (15.4)	30 (19.2)

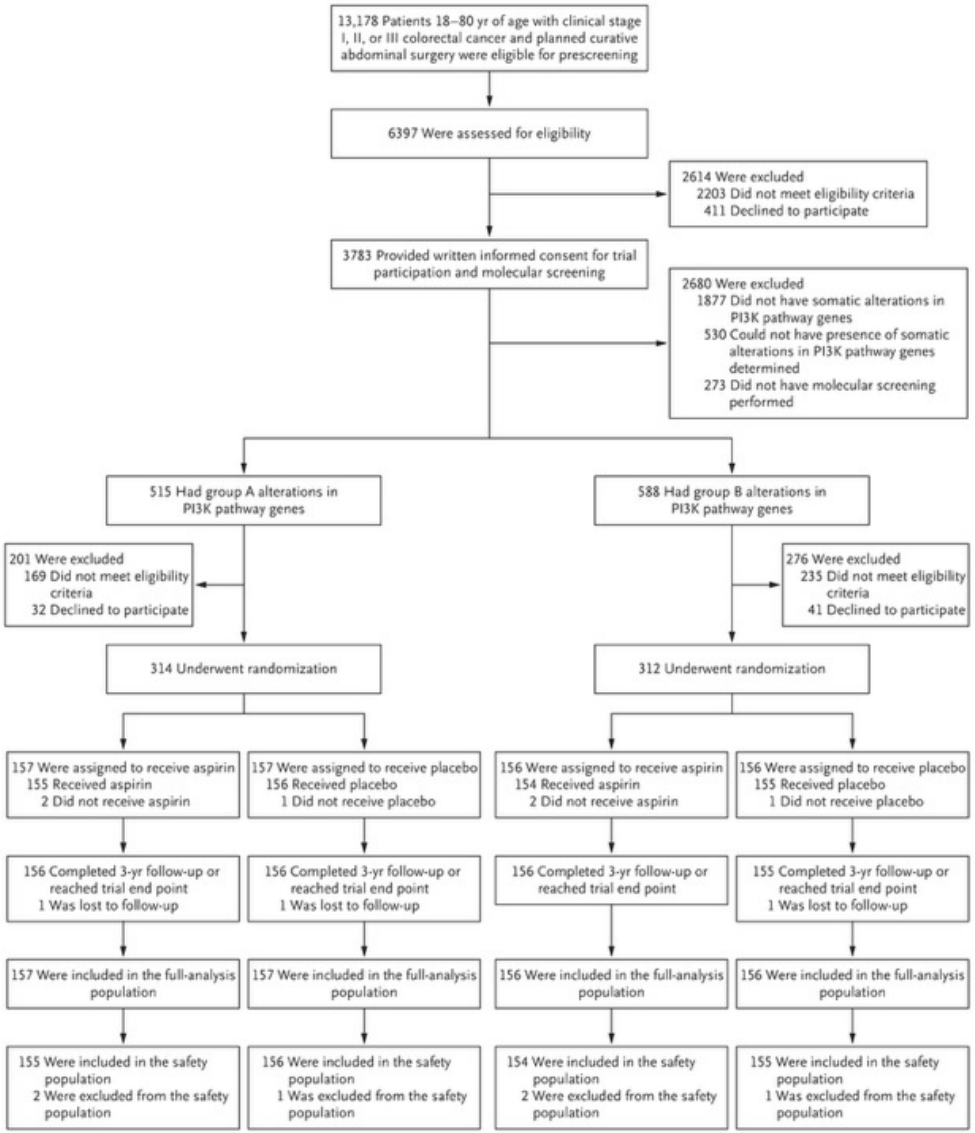

Adverse Events in the Safety Population.

Characteristic	Nonsevere Adverse Events				Severe Adverse Events			
	Aspirin		Placebo		Aspirin		Placebo	
	no. of events	*no. of patients (%)*	*no. of events*	*no. of patients (%)*	*no. of events*	*no. of patients (%)*	*no. of events*	*no. of patients (%)*
Overall	302	134 (43.4)	228	110 (35.4)	56	52 (16.8)	38	36 (11.6)
Type of event†								
Hematologic disorders	70	46 (14.9)	35	29 (9.3)	2	2 (0.6)	0	0
Cardiovascular disorders	14	13 (4.2)	10	10 (3.2)	18	18 (5.8)	13	13 (4.2)
CNS and neurologic disorders	8	8 (2.6)	11	9 (2.9)	4	4 (1.3)	3	3 (1.0)
Dermatologic disorders	17	15 (4.9)	17	16 (5.1)	0	0	0	0
Endocrine disorders	2	2 (0.6)	1	1 (0.3)	0	0	0	0
Eyes, ears, nose, and throat disorders	16	11 (3.6)	6	5 (1.6)	0	0	0	0
Gastrointestinal disorders	56	43 (13.9)	51	43 (13.8)	22	20 (6.5)	13	12 (3.9)
Urogenital disorders	16	12 (3.9)	18	13 (4.2)	2	2 (0.6)	4	4 (1.3)
Immunologic disorders	0	0	2	2 (0.6)	1	1 (0.3)	1	1 (0.3)
Musculoskeletal disorders	14	13 (4.2)	14	12 (3.9)	2	2 (0.6)	3	3 (1.0)
Respiratory disorders	10	8 (2.6)	3	3 (1.0)	0	0	0	0
Other	79	42 (13.6)	60	36 (11.6)	5	5 (1.6)	1	1 (0.3)
Description of event								
Event leading to death	—	—	—	—	3	3 (1.0)	1	1 (0.3)
Life-threatening event	—	—	—	—	2	2 (0.6)	2	2 (0.6)
Other clinically significant medical event	—	—	—	—	15	15 (4.9)	10	10 (3.2)
Event resulting in hospitalization for >24 hr or extended medical care	—	—	—	—	36	33 (10.7)	25	23 (7.4)
Intensity of event								
Mild	189	102 (33.0)	150	84 (27.0)	6	6 (1.9)	9	9 (2.9)
Moderate	102	60 (19.4)	66	47 (15.1)	25	25 (8.1)	18	16 (5.1)
Severe	11	9 (2.9)	12	9 (2.9)	25	23 (7.4)	11	11 (3.5)
Modification of aspirin or placebo use because of event								
No modification	244	104 (33.7)	187	86 (27.7)	17	15 (4.9)	9	8 (2.6)
Discontinuation	10	10 (3.2)	9	9 (2.9)	23	23 (7.4)	14	14 (4.5)
Other modification‡	48	39 (12.6)	32	30 (9.6)	16	15 (4.9)	15	15 (4.8)
Outcome of event								
Patient recovered	117	68 (22.0)	104	68 (21.9)	34	31 (10.0)	23	22 (7.1)
Patient improving	147	95 (30.7)	103	66 (21.2)	16	16 (5.2)	9	9 (2.9)
Patient did not recover, ongoing sequelae	38	23 (7.4)	21	13 (4.2)	3	3 (1.0)	5	5 (1.6)
Death	0	0	0	0	3	3 (1.0)	1	1 (0.3)
Event considered to be potentially related to aspirin or placebo								
As assessed by local investigator								
Yes	—	—	—	—	6	5 (1.6)	2	2 (0.6)
No	—	—	—	—	52	47 (15.2)	36	35 (11.3)
As assessed by principal investigator								
Yes	—	—	—	—	4	4 (1.3)	0	0
No	—	—	—	—	52	48 (15.5)	38	36 (11.6)

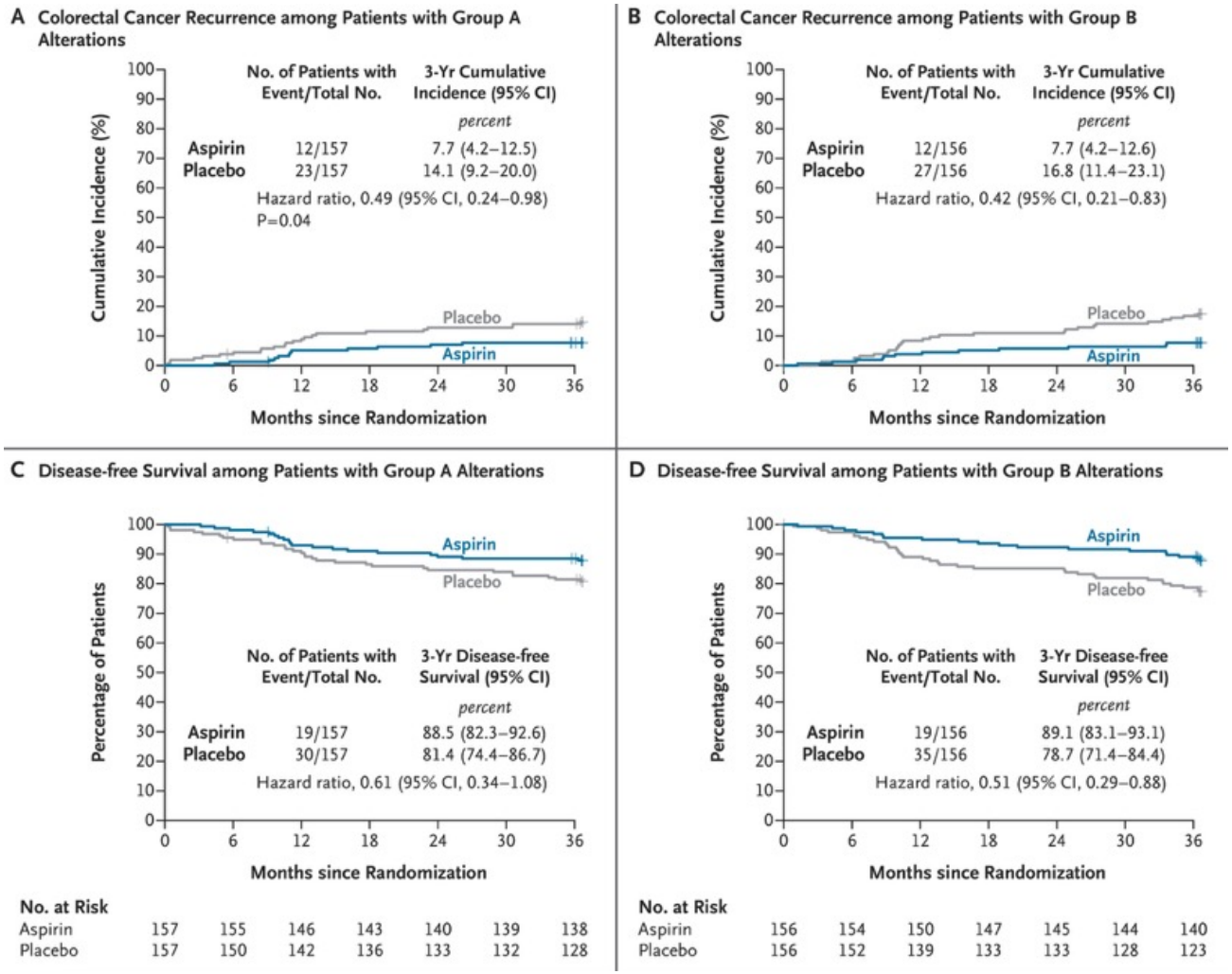

Colorectal Cancer Recurrence and Disease-free Survival.

Aalen–Johansen estimates of the cumulative incidence of colorectal cancer recurrence within 3 years after randomization are shown for patients with group A alterations (Panel A) and those with group B alterations (Panel B) according to trial-group assignment. Colorectal cancer recurrence was defined as locoregional recurrence, distant metastasis, or death from colorectal cancer. Kaplan–Meier estimates of disease-free survival within 3 years after randomization are shown for patients with group A alterations (Panel C) and those with group B alterations (Panel D) according to trial-group assignment. Disease-free survival was defined as the time from randomization to the first occurrence of locoregional recurrence, distant metastasis, any new primary cancer, or death from any cause. CI denotes confidence interval.

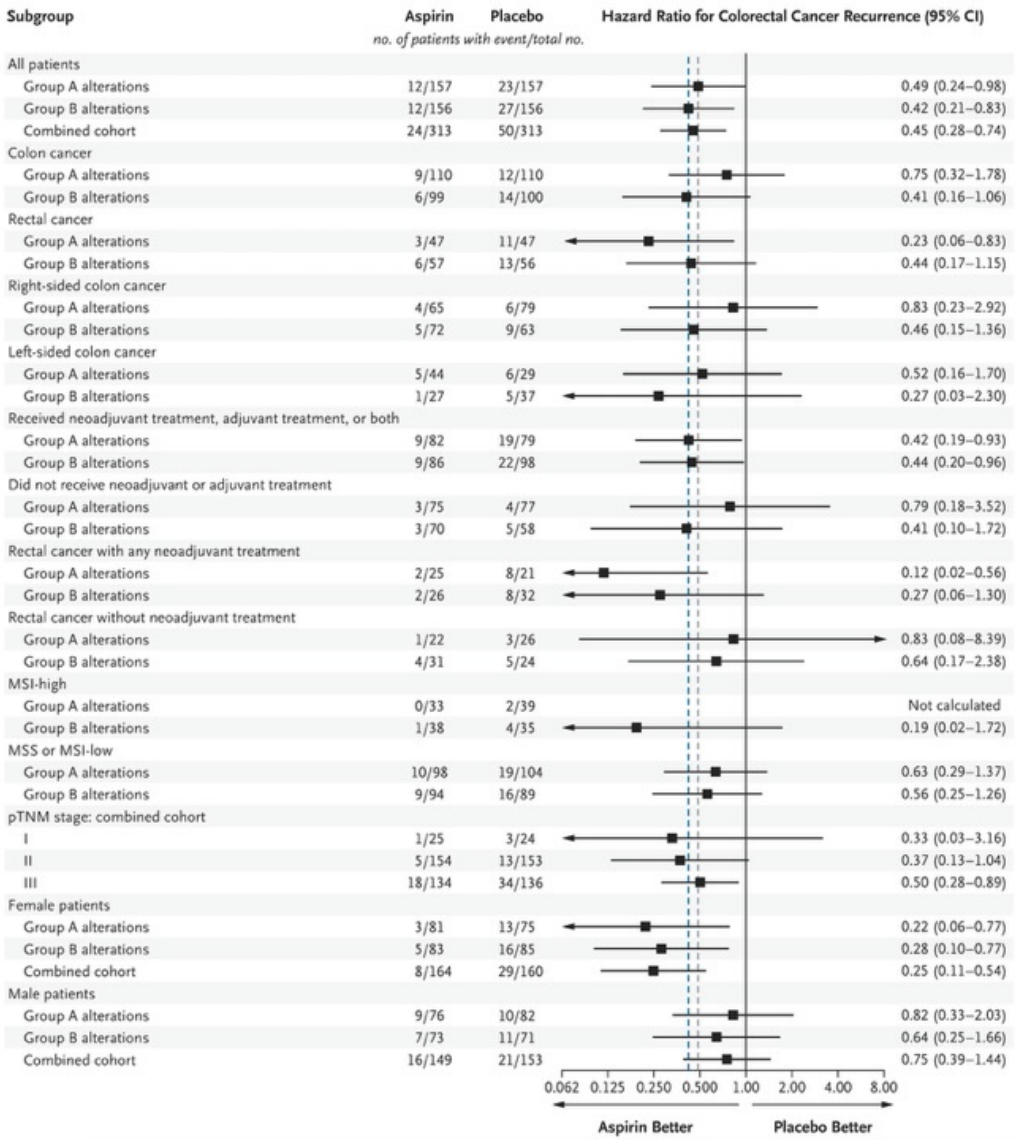

Subgroup Analyses of Colorectal Cancer Recurrence.

Shown are hazard ratios (aspirin vs. placebo) for colorectal cancer recurrence within 3 years after randomization, according to subgroup. The gray dashed line indicates the hazard ratio for recurrence among all patients with group A alterations, and the blue dashed line indicates the hazard ratio for recurrence among all those with group B alterations. The analyses according to sex were post hoc analyses. MSI denotes microsatellite instability, and MSS microsatellite stable.

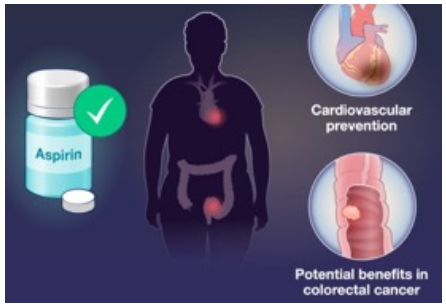
Aspirin
Cardiovascular prevention
Potential benefits in colorectal cancer

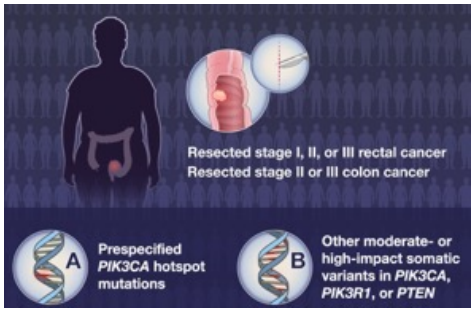
Resected stage I, II, or III rectal cancer
Resected stage II or III colon cancer
A
Prespecified PIK3CA hotspot mutations
B
Other moderate- or high-impact somatic variants in PIK3CA, PIK3R1, or PTEN

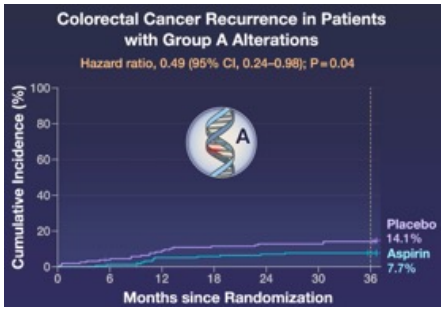
Colorectal Cancer Recurrence in Patients with Group A Alterations
Hazard ratio, 0.49 (95% CI, 0.24–0.98); P=0.04
Cumulative Incidence (%)
Placebo 14.1%
Aspirin 7.7%
Months since Randomization

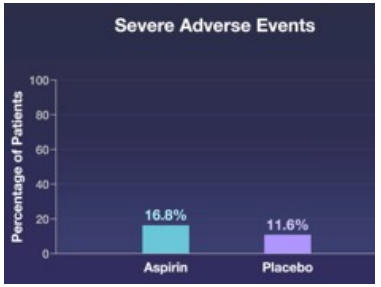
Severe Adverse Events
Percentage of Patients
16.8%
11.6%
Aspirin
Placebo

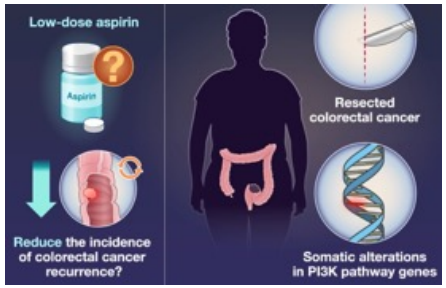
Low-dose aspirin
Reduce the incidence of colorectal cancer recurrence?
Resected colorectal cancer
Somatic alterations in PI3K pathway genes

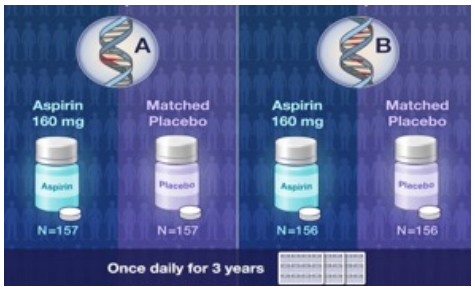
A
Aspirin 160 mg
Matched Placebo
N=157
N=157
B
Aspirin 160 mg
Matched Placebo
N=156
N=156
Once daily for 3 years

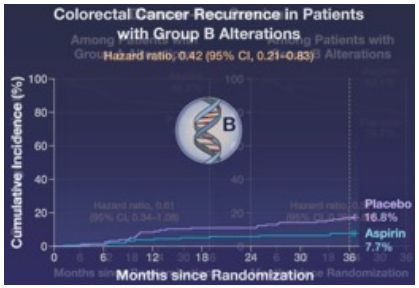
Colorectal Cancer Recurrence in Patients with Group B Alterations
Hazard ratio, 0.42 (95% CI, 0.21–0.83)
Cumulative Incidence (%)
Placebo 16.8%
Aspirin 7.7%
Months since Randomization

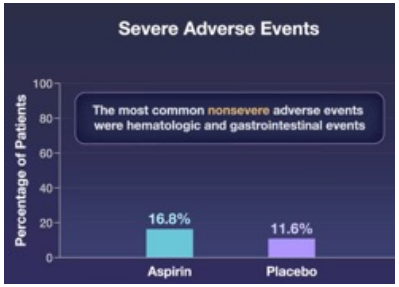
Severe Adverse Events
The most common nonsevere adverse events were hematologic and gastrointestinal events
Percentage of Patients
16.8%
11.6%
Aspirin
Placebo

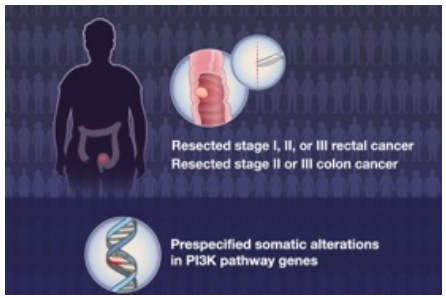
Resected stage I, II, or III rectal cancer
Resected stage II or III colon cancer
Prespecified somatic alterations in PI3K pathway genes

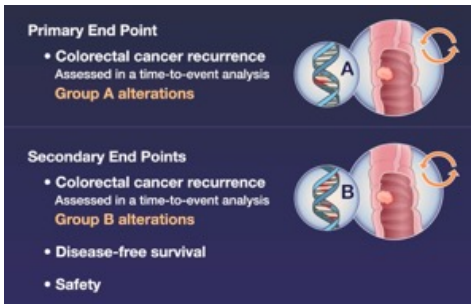
Primary End Point
• Colorectal cancer recurrence
Assessed in a time-to-event analysis
Group A alterations
Secondary End Points
• Colorectal cancer recurrence
Assessed in a time-to-event analysis
Group B alterations
• Disease-free survival
• Safety

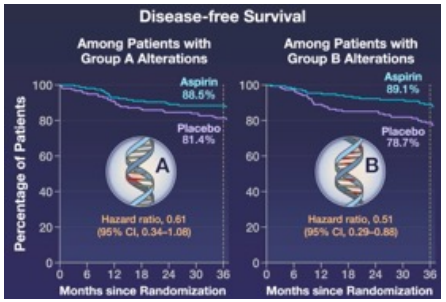
Disease-free Survival
Among Patients with Group A Alterations
Among Patients with Group B Alterations
Percentage of Patients
Aspirin 88.5%
Placebo 81.4%
Hazard ratio, 0.61 (95% CI, 0.34–1.08)
Aspirin 89.1%
Placebo 78.7%
Hazard ratio, 0.51 (95% CI, 0.29–0.88)
Months since Randomization
Months since Randomization

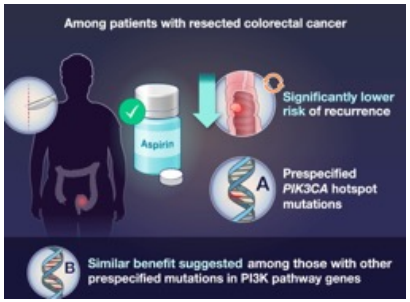
Among patients with resected colorectal cancer
Aspirin
Significantly lower risk of recurrence
Prespecified PIK3CA hotspot mutations
Similar benefit suggested among those with other prespecified mutations in PI3K pathway genes

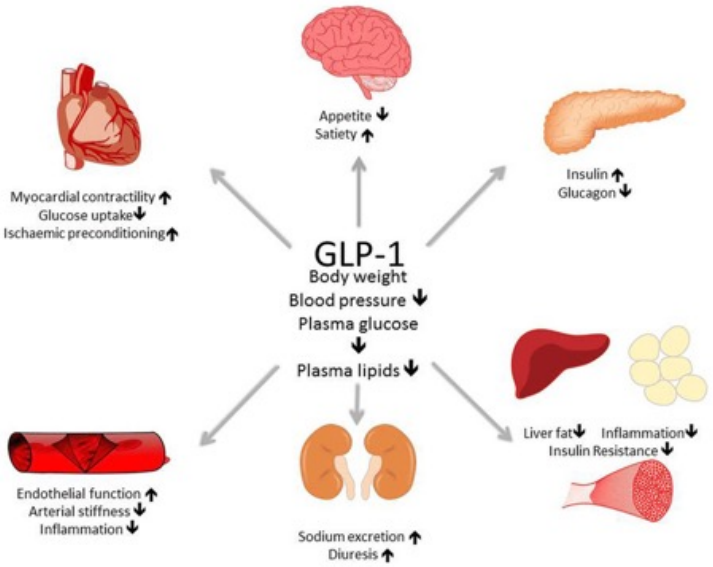

Orforglipron ist eine noch in Entwicklung befindliche, nicht-peptidische orale Tablette von Eli Lilly zur Gewichtsreduktion und Behandlung von Typ-2-Diabetes, die als Alternative zu GLP-1-Injektionen konzipiert ist. Als GLP-1-Rezeptoragonist ahmt es ein körpereigenes Hormon nach, das Appetit und Blutzucker reguliert. Studien zeigen, dass Orforglipron eine signifikante Gewichtsabnahme und eine Verbesserung der Blutzuckerwerte bewirkt, wobei die Ergebnisse denen der Spritzen ähneln, wenn auch etwas geringer sind als bei manchen oralen Alternativen.

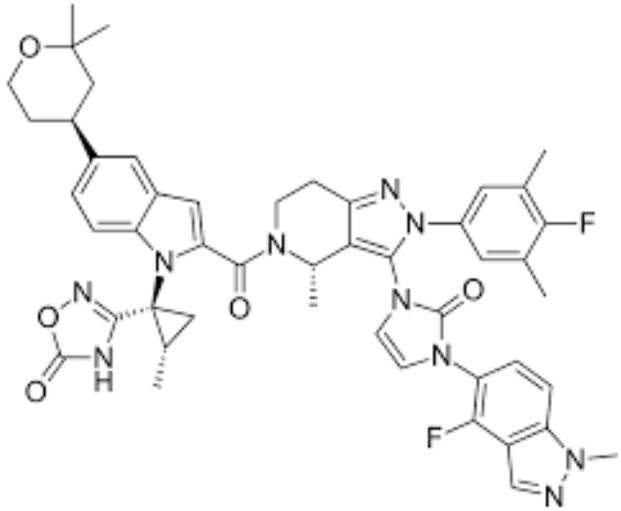

Orforglipron, an Oral Small-Molecule GLP-1 Receptor Agonist, in Early Type 2 Diabetes

Orforglipron is a small-molecule, nonpeptide glucagon-like peptide-1 (GLP-1) receptor agonist in clinical development for type 2 diabetes and weight management. Additional data on the efficacy and safety of orforglipron are needed.
In this phase 3, double-blind, placebo-controlled trial, we randomly assigned participants in a 1:1:1:1 ratio to receive orforglipron at one of three doses (3 mg, 12 mg, or 36 mg) or placebo once daily for 40 weeks. Participants had type 2 diabetes treated only with diet and exercise, a glycated hemoglobin level of at least 7.0% but no more than 9.5%, and a body-mass index (the weight in kilograms divided by the square of the height in meters) of at least 23.0. The primary end point was the change from baseline to week 40 in the glycated hemoglobin level. A key secondary end point was the percent change in body weight from baseline to week 40.

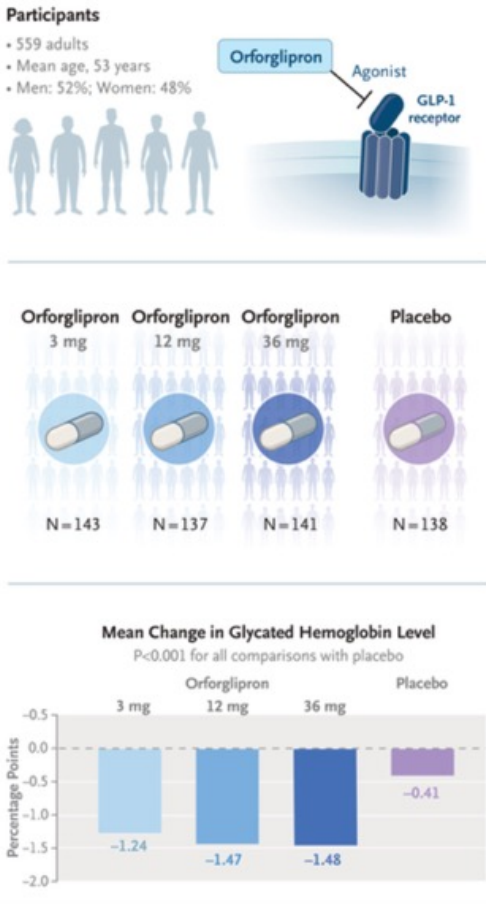

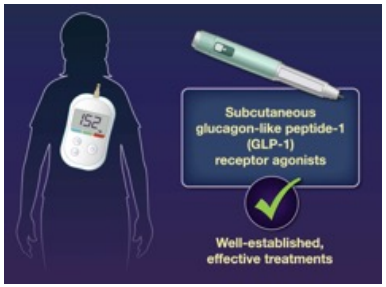
Subcutaneous glucagon-like peptide-1 (GLP-1) receptor agonists
Well-established, effective treatments

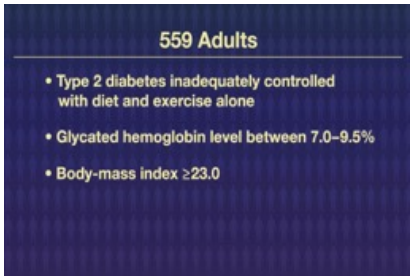
559 Adults
• Type 2 diabetes inadequately controlled with diet and exercise alone
• Glycated hemoglobin level between 7.0–9.5%
• Body-mass index ≥23.0

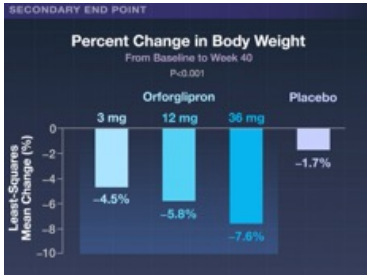
SECONDARY END POINT
Percent Change in Body Weight
From Baseline to Week 40
P<0.001
Orforglipron
Placebo
3 mg
12 mg
36 mg
Least-Squares Mean Change (%)
0
−2
−4
−6
−8
−10
−4.5%
−5.8%
−7.6%
−1.7%


Orforglipron
Lowered the glycated hemoglobin level significantly more than placebo at 40 weeks

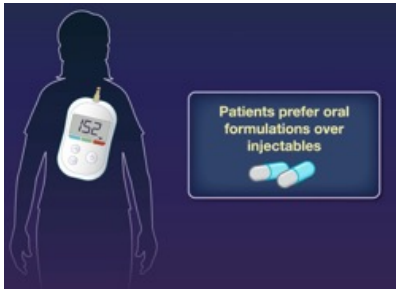
Patients prefer oral formulations over injectables


Orforglipron
Orforglipron
Orforglipron
Placebo
3 mg
N=143
12 mg
N=137
36 mg
N=141
N=138
Once daily for 40 weeks
YEAR

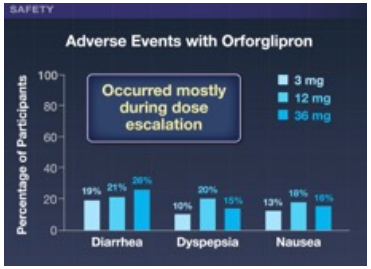
SAFETY
Adverse Events with Orforglipron
Occurred mostly during dose escalation
3 mg
12 mg
36 mg
Percentage of Participants
100
80
60
40
20
0
19%
21%
26%
10%
20%
15%
13%
18%
19%
Diarrhea
Dyspepsia
Nausea

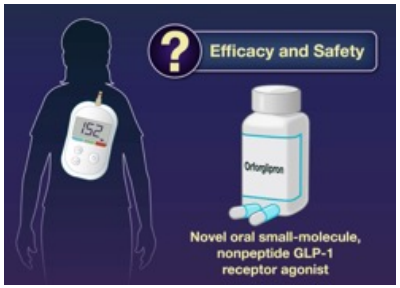
Efficacy and Safety
Orforglipron
Novel oral small-molecule, nonpeptide GLP-1 receptor agonist

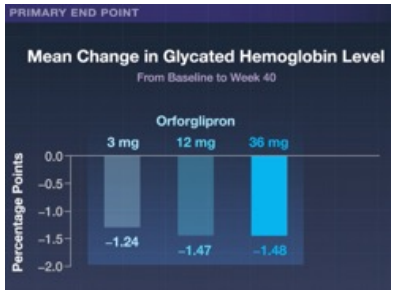
PRIMARY END POINT
Mean Change in Glycated Hemoglobin Level
From Baseline to Week 40
Orforglipron
3 mg
12 mg
36 mg
Percentage Points
0.0
−0.5
−1.0
−1.5
−2.0
−1.24
−1.47
−1.48

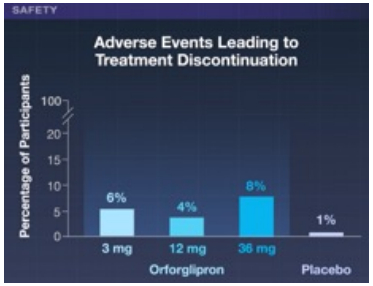
SAFETY
Adverse Events Leading to Treatment Discontinuation
Percentage of Participants
100
20
15
10
5
0
6%
4%
8%
1%
3 mg
12 mg
36 mg
Orforglipron
Placebo

Der Glucagon-like-Peptid-1(GLP-1)-Rezeptoragonist Semaglutid ist bereits seit Februar 2018 zur subkutanen Injektion zugelassen. Die Europäische Kommission hat im April 2020 nun auch die orale Zubereitung des Wirkstoffes zugelassen. Semaglutid ist indiziert zur Therapie von Erwachsenen mit unzureichend kontrolliertem Typ-2-Diabetes. Die Zulassung ist auf der Basis der Ergebnisse des PIONEER-Studienprogramms erfolgt.

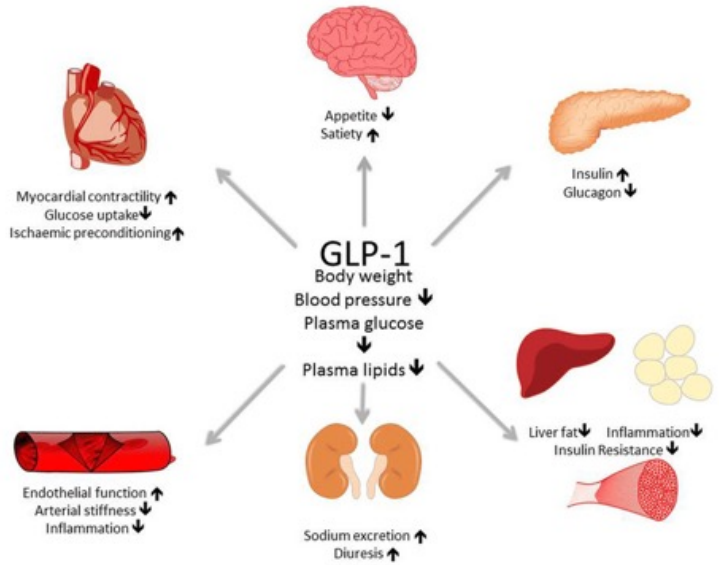

Parameter	
Nüchternglucose gegenüber Placebo	–22 %
Postprandiale Glucose gegenüber Placebo	–29 %
Postprandiale Glucagonkonzentration gegenüber Placebo	–29 %
Frühe postprandiale Magenentleerung	–31 %
Triglyceride nüchtern gegenüber Placebo	–19 %
VLDL nüchtern gegenüber Placebo	–20 %
Triglyceride nach einer fettreichen Mahlzeit	–24 %
VLDL nach einer fettreichen Mahlzeit	–21 %
ApoB48 nüchtern	–25 %
ApoB48 postprandial	–30 %

VLDL: very-low-density lipoproteins

Oral Semaglutide at a Dose of 25 mg in Adults with Overweight or Obesity

Oral semaglutide at a dose of 25 mg may provide an alternative treatment option to injectable semaglutide (2.4 mg) and higher-dose oral semaglutide (50 mg) for persons with overweight or obesity.

In a 71-week, double-blind, randomized, placebo-controlled trial conducted at 22 sites in four countries, we enrolled persons without diabetes who had a body-mass index (BMI; the weight in kilograms divided by the square of the height in meters) of 30 or higher or a BMI of 27 or higher with at least one obesity-related complication. The participants were randomly assigned in a 2:1 ratio to receive oral semaglutide (25 mg) or placebo once daily, plus lifestyle interventions. The coprimary end points at week 64 were the percent change in body weight and a reduction of 5% or more in body weight; confirmatory secondary end points included reductions in body weight of 10% or more, 15% or more, and 20% or more and the change in the Impact of Weight on Quality of Life–Lite Clinical Trials Version (IWQOL-Lite-CT) Physical Function score.

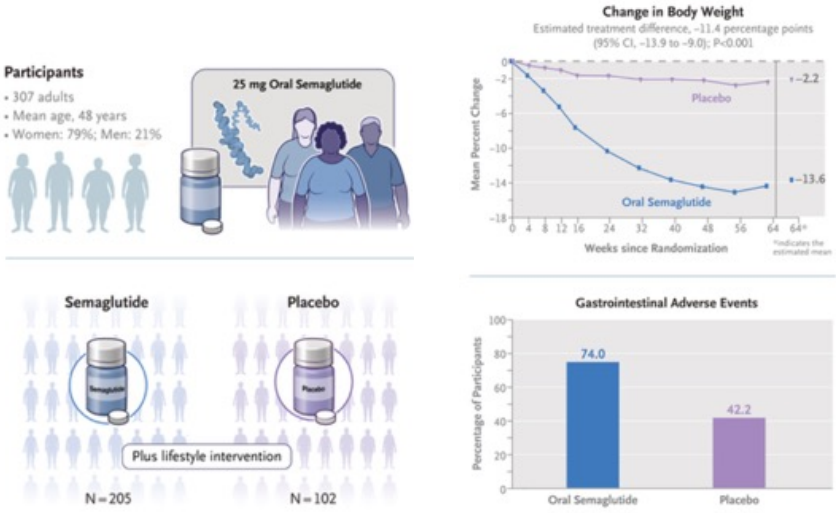

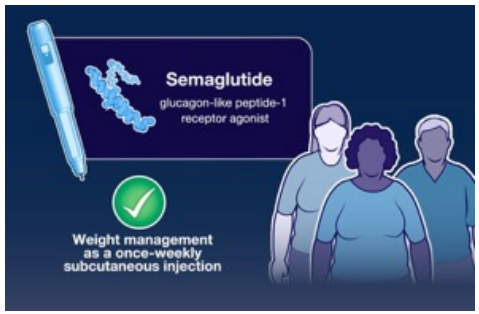
Semaglutide
glucagon-like peptide-1 receptor agonist
Weight management as a once-weekly subcutaneous injection


25 mg once daily
Semaglutide
N=205
Placebo
N=102
Plus lifestyle interventions


COPRIMARY END POINTS
Participants Meeting Weight-Loss Targets at Week 64
Placebo
Oral semaglutide
Percentage of Participants
31.1%
79.2%
14.4%
63.0%
5.6%
50.0%
3.3%
29.7%
≥5
≥10
≥15
≥20
Weight Loss (%)

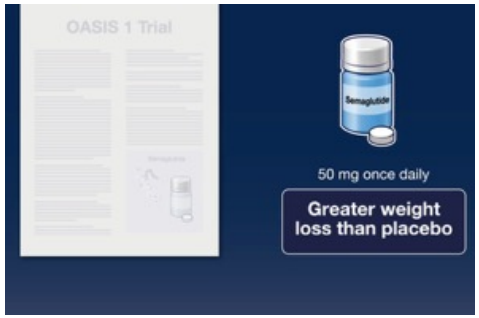
OASIS 1 Trial
Semaglutide
50 mg once daily
Greater weight loss than placebo

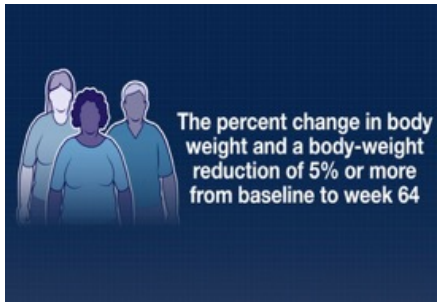
The percent change in body weight and a body-weight reduction of 5% or more from baseline to week 64

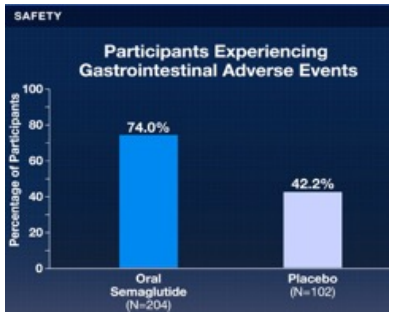
SAFETY
Participants Experiencing Gastrointestinal Adverse Events
Percentage of Participants
74.0%
42.2%
Oral Semaglutide (N=204)
Placebo (N=102)


OASIS 4 Trial
• Phase 3
• Randomized
• Placebo-controlled
BMI ≥30
BMI ≥27 with at least one weight-related complication
Without diabetes

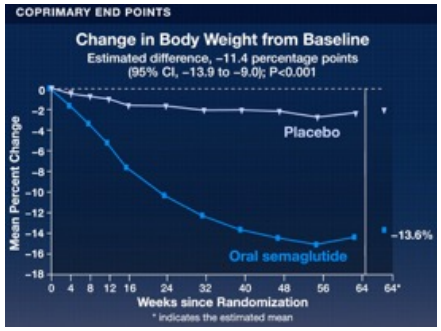
COPRIMARY END POINTS
Change in Body Weight from Baseline
Estimated difference, −11.4 percentage points
(95% CI, −13.9 to −9.0); P<0.001
Mean Percent Change
Placebo
Oral semaglutide
−13.6%
Weeks since Randomization
* indicates the estimated mean


Semaglutide
25 mg once daily
Resulted in significantly greater weight loss than placebo at 64 weeks

Die Proportional Assist Ventilation, kurz PAV, ist eine fortschrittliche Methode der mechanischen Beatmung, die eine dynamische Anpassung der Atemunterstützung an die Eigenleistung des Patienten ermöglicht. Ziel ist es, die Atemarbeit proportional zur Atemanstrengung zu entlasten und eine physiologisch synchronisierte Beatmung zu gewährleisten.

Funktionsprinzip

Die PAV unterscheidet sich grundlegend von herkömmlichen Beatmungsmodi, da sie auf einem proportionalen Feedbacksystem basiert. Die Beatmungsmaschine misst kontinuierlich die Atemanstrengung des Patienten (Inspirationsdruck und Fluss) und liefert eine angepasste Unterstützung. Zwei wesentliche Komponenten dabei sind:

- Elastischer Druckanteil: Kompensation der Kraft, die erforderlich ist, um die Elastizität von Lunge und Thoraxwand zu überwinden (siehe auch: Elastance und Compliance)
- Resistiver Druckanteil: Unterstützung zur Überwindung des Atemwegswiderstandes (Strömungswiderstand)

Die Höhe der Unterstützung wird durch individuell festgelegte Verstärkungsfaktoren (Gain-Faktoren) für beide Komponenten bestimmt. Dies gewährleistet eine kontinuierliche Anpassung an die physiologischen Bedürfnisse des Patienten.

Pressure-support ventilation (PSV)

Proportional-assist ventilation (PAV)

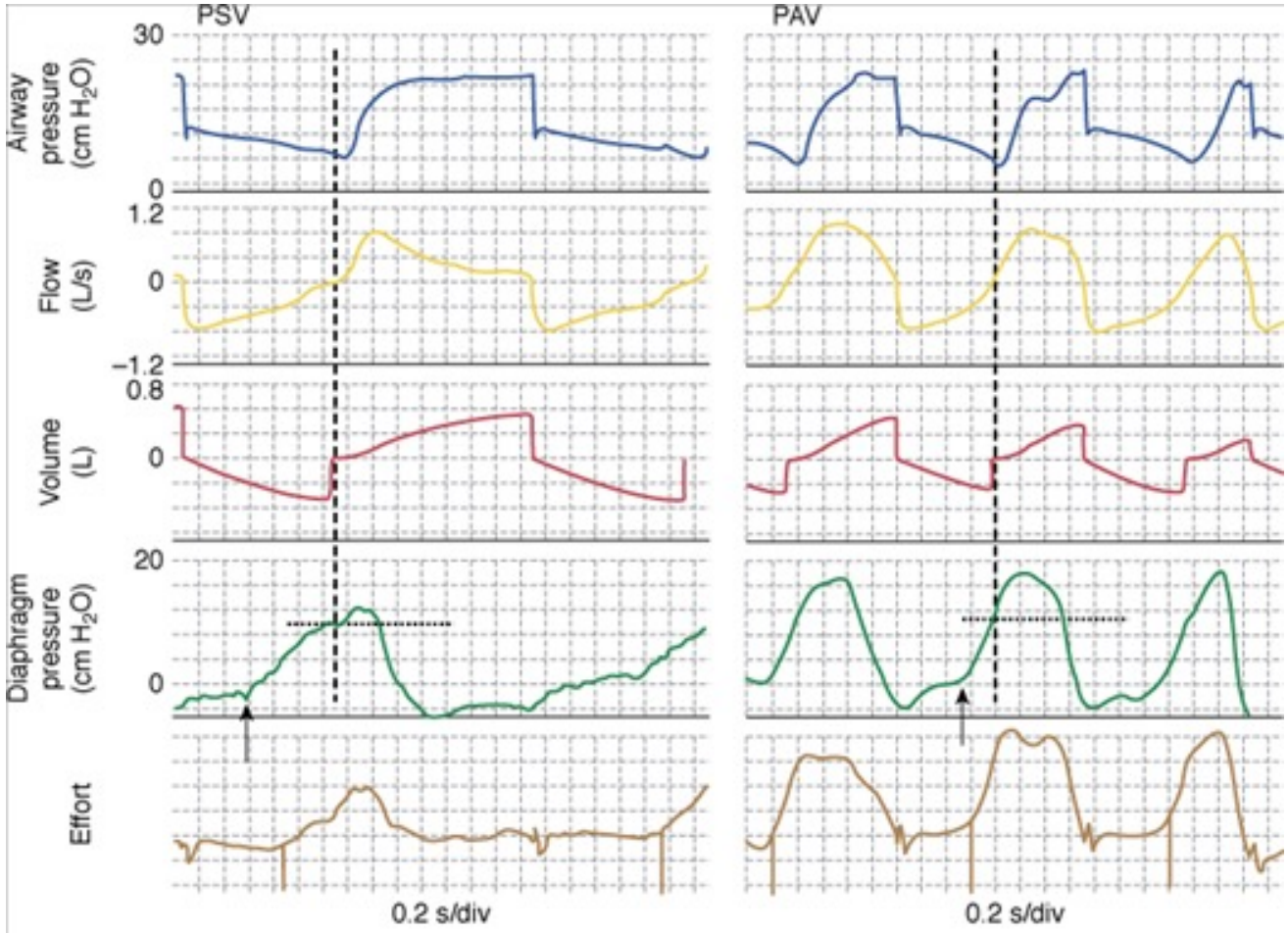

Source: Tobin MJ: *Principles and Practice of Mechanical Ventilation, 3rd Edition:* www.accessanesthesiology.com

Proportional-Assist Ventilation for Minimizing the Duration of Mechanical Ventilation

In critically ill patients, acceleration of liberation from mechanical ventilation is important in order to reduce the risk of complications and to improve long-term outcomes. Whether the use of proportional-assist ventilation with load-adjustable gain factors (PAV+) results in a shorter time to successful liberation from mechanical ventilation than pressure-support ventilation (PSV) is unclear.
In this international clinical trial, we randomly assigned adult patients who had been receiving mechanical ventilation for at least 24 hours and were able to undergo partial ventilatory support with PSV but were not yet ready for liberation from ventilation to undergo PAV+ (which targeted normal work of breathing) or PSV (which targeted a normal respiratory rate and tidal volume). The primary outcome was the time from randomization to successful liberation from mechanical ventilation.

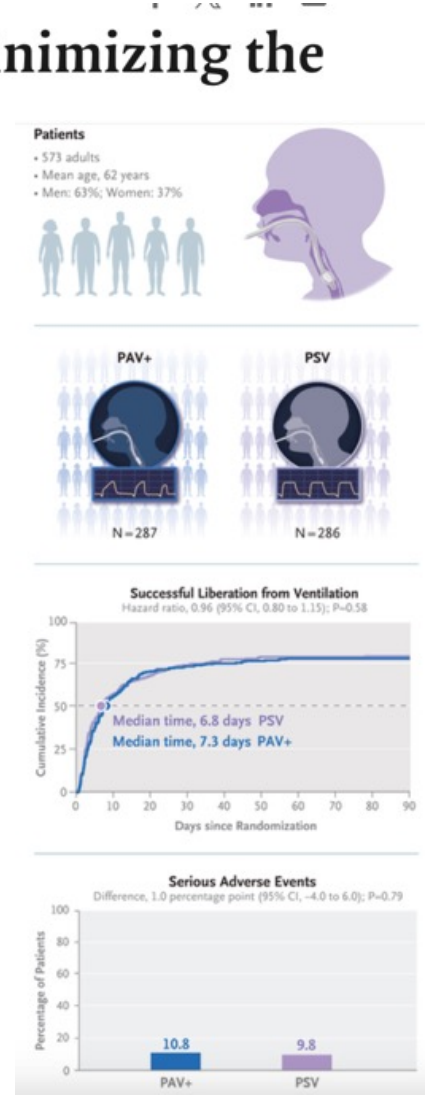

Rapid deconditioning of respiratory muscles during controlled ventilation under sedation has been described, and such deconditioning places patients at risk for prolonged weaning. Early transition to a partial ventilatory support mode, in which the patient triggers every breath, may help to mitigate this risk. Pressure-support ventilation (PSV) is the most common partial ventilatory support mode used after the first few days of full ventilatory support, but this mode has limitations: breathing may become passive after triggering of breathing has begun, and the patient's respiratory muscle activity cannot be evaluated. If not carefully adjusted, PSV may lead to over-assistance, diaphragmatic atrophy, and patient–ventilator dyssynchrony, all of which are associated with prolonged weaning. Alternatively, proportional-assist ventilation with load-adjustable gain factors (PAV+) delivers assistance that is proportional to patients' efforts. Clinicians can adjust the gain (i.e., the proportional assistance) to maintain a normal patient respiratory workload. Previous studies have shown short-term advantages of PAV+ over PSV, including fewer adverse effects associated with ventilation, a decrease in dyspnea, and improved patient–ventilator synchrony and sleep quality.

We hypothesized that PAV+ could improve patient-centered outcomes, potentially by reducing the risk of ventilator-induced diaphragm dysfunction and promoting safe reconditioning of respiratory muscles. The primary objective of the Proportional Assist Ventilation for Minimizing the Duration of Mechanical Ventilation (PROMIZING) trial was to determine whether ventilation with PAV+, instituted early after acute respiratory failure and set to maintain a normal range of breathing workload, would result in a shorter time to successful ventilator liberation than PSV, which was set to maintain a normal tidal volume and breathing frequency.

Patients

We enrolled critically ill patients 18 years of age or older who had been receiving mechanical ventilation for at least 24 hours and were able to undergo PSV for at least 30 minutes but were not yet ready for liberation from ventilation. We used a staged recruitment process, with assessment of inclusion and exclusion criteria at each step, for enrollment and subsequent randomization of eligible patients. Patients who had severe chronic respiratory diseases or severe neurologic disorders were excluded, as were patients in whom withdrawal of life support was anticipated.

Randomization and Interventions

Participating sites underwent a “run-in” training phase with at least one patient undergoing each mode (PSV or PAV+) before being granted permission to randomly assign patients in the trial; details are provided in the protocol. These patients were not included in the analysis.

Outcomes

The primary outcome was the time from randomization to successful liberation from mechanical ventilation, which was defined as the time of extubation or final separation from the ventilator, provided that the patient remained alive and free from invasive ventilation for 7 days.

Variable	Overall (N=573)	PAV+ (N=287)	PSV (N=286)
At the time of ICU admission			
Age — yr	62.1±14.5	62.3±13.8	62.0±15.2
Female sex — no. (%)	211 (36.8)	102 (35.5)	109 (38.1)
Body-mass index†	29.3±7.8	28.8±7.6	29.8±7.9
Median Clinical Frailty Scale score (IQR)‡	3 (2–4)	3 (2–4)	3 (2–4)
Median Charlson Comorbidity Index score (IQR)§	3 (2–6)	4 (2–6)	3 (2–6)
APACHE III score on ICU admission¶	80.26±26.6	81.9±27.2	78.4±25.8
APACHE III diagnosis — no. (%)			
Nonoperative	476 (83.1)	236 (82.2)	240 (83.9)
Operative	96 (16.8)	50 (17.4)	46 (16.1)
Category of diagnostic cause of admission — no. (%)			
Respiratory condition	272 (47.5)	135 (47.0)	137 (47.9)
Cardiovascular condition	91 (15.9)	49 (17.1)	42 (14.7)
Sepsis	69 (12.0)	29 (10.1)	40 (14.0)
Gastrointestinal condition	64 (11.2)	31 (10.8)	33 (11.5)
Neurologic condition	22 (3.8)	14 (4.9)	8 (2.8)
Other condition	54 (9.4)	28 (9.8)	26 (9.1)
From ICU admission to enrollment			
Use of glucocorticoids — no. (%)	278 (48.5)	126 (43.9)	152 (53.1)
Use of neuromuscular blockers — no. (%)	217 (37.9)	100 (34.8)	117 (40.9)
Use of opioid continuous infusion — no. (%)	483 (84.3)	241 (84.0)	242 (84.6)
Use of benzodiazepine continuous infusion — no. (%)	277 (48.3)	135 (47.0)	142 (49.7)
At time of enrollment or randomization			
No. of days in hospital, from hospital admission to randomization	10.8±11.4	10.1±9.4	11.5±13.0
No. of days in ICU, from ICU admission to randomization	7.1±5.6	6.8±5.1	7.5±6.1
Median no. of days of IMV receipt, at time of randomization (IQR)	4.9 (3.1–8.9)	4.8 (3.2–8.4)	5.0 (3.0–9.5)
Mode of IMV at time of enrollment — no. (%)			
PSV	505 (88.1)	253 (88.2)	252 (88.1)
Assist–control	60 (10.5)	31 (10.8)	29 (10.1)
PAV+	7 (1.2)	3 (1.0)	4 (1.4)
Median cumulative fluid balance (IQR) — liters	3.40 (1.44–7.78)	3.12 (1.41–7.42)	3.84 (1.48–8.31)
SOFA score — no. (%)‖	5.9 (3.1)	5.8 (3.2)	5.9 (2.9)
Use of vasopressors — no. (%)	275 (48.0)	132 (46.0)	143 (50.0)
Use of renal replacement therapy — no. (%)	84 (14.7)	37 (12.9)	47 (16.4)
Patient status in successive-step process for randomization — no. (%)**			
Patient did not meet weaning criteria	279 (48.7)	140 (48.8)	139 (48.6)
Patient did not pass CPAP trial for assessment of RSBI	219 (38.2)	109 (38.0)	110 (38.5)
Patient did not pass SBT	74 (12.9)	37 (12.9)	37 (12.9)

Primary and Secondary Outcomes.

ıtcome	PAV+ (N=287)	PSV (N=286)	Hazard Ratio or Relative Risk (95% CI)°	P Value	Absolute Difference (95% CI)††
edian time to event (95% CI) — days‡					
Successful liberation from ventilation: primary outcome	7.3 (6.2 to 9.7)	6.8 (5.4 to 8.8)	0.96 (0.80 to 1.15)	0.58	0.5 (−3.0 to 3.5)
Live ICU discharge	13.0 (10.7 to 15.2)	12.2 (9.9 to 14.1)	0.97 (0.80 to 1.17)	—	0.8 (−2.9 to 4.2)
Live hospital discharge	30.2 (27.0 to 35.5)	29.1 (25.4 to 37.9)	0.91 (0.75 to 1.12)	—	1.1 (−7.3 to 8.0)
edian no. of ventilator-free days (IQR)§					
At day 14	6.7 (0.0 to 10.9)	7.1 (0.0 to 11.3)	—	—	0.4 (−2.9 to 1.5)
At day 21	13.1 (0.0 to 17.9)	13.8 (0.0 to 18.2)	—	—	0.7 (−2.9 to 2.4)
At day 28	19.9 (0.0 to 24.8)	20.5 (0.1 to 25.2)	—	—	0.6 (−3.0 to 2.9)
ath — no./total no. (%)					
In the ICU	55/287 (19.2)	53/286 (18.5)	1.03 (0.74 to 1.46)	—	0.6 (−5.8 to 7.0)
In the hospital	78/287 (27.2)	73/286 (25.5)	1.06 (0.81 to 1.40)	—	1.7 (−5.6 to 8.9)
By day 21	42/287 (14.6)	44/286 (15.4)	0.95 (0.64 to 1.41)	—	−0.8 (−6.6 to 5.1)
By day 28	58/287 (20.2)	54/286 (18.9)	1.07 (0.77 to 1.50)	—	1.3 (−5.2 to 7.8)
By day 90	85/287 (29.6)	76/286 (26.6)	1.13 (0.83 to 1.54)	—	3.0 (−4.3 to 10.4)
eaning progress: median time to event (95% CI) — days					
First SBT	2.7 (2.1 to 3.3)	2.2 (1.9 to 2.7)	0.91 (0.77 to 1.09)	—	0.5 (−0.4 to 1.2)
First successful SBT	4.1 (3.7 to 5.8)	4.1 (3.2 to 5.4)	0.96 (0.80 to 1.15)	—	0.0 (−1.3 to 1.9)
First extubation or disconnection from ventilator	5.2 (4.2 to 6.4)	4.2 (3.3 to 5.4)	0.88 (0.74 to 1.05)	—	1.0 (−0.7 to 2.3)
vel of weaning difficulty — no./total no. (%)¶					
Short weaning	99/260 (38.1)	95/269 (35.3)	—	—	2.8 (−5.5 to 11.0)
Difficult weaning	77/260 (29.6)	83/269 (30.9)	—	—	−1.2 (−9.1 to 6.6)
Prolonged weaning	49/260 (18.8)	52/269 (19.3)	—	—	−0.5 (−7.2 to 6.2)
Unable to wean and still receiving ventilation at day 90	2/260 (0.8)	4/269 (1.5)	—	—	−0.7 (−2.5 to 1.1)
Died before successful liberation	33/260 (12.7)	35/269 (13.0)	—	—	−0.3 (−6.0 to 5.4)
eaning complications — no./total no. (%)					
Noninvasive ventilation initiated after extubation	71/231 (30.7)	69/240 (28.8)	1.10 (0.74 to 1.63)	—	2.0 (−6.3 to 10.2)
Tracheostomy performed after randomization‖	58/277 (20.9)	52/271 (19.2)	1.12 (0.73 to 1.70)	—	1.8 (−5.0 to 8.5)
Ventilation continued >7 days after randomization**	146/278 (52.5)	129/275 (46.9)	1.25 (0.90 to 1.75)	—	5.7 (−2.7 to 13.9)
Ventilation continued >21 days after intubation††	80/259 (30.9)	84/256 (32.8)	0.92 (0.63 to 1.33)	—	−1.9 (−10.0 to 6.1)
Reintubation performed <7 days after planned extubation‡‡	53/239 (22.2)	57/245 (23.3)	0.93 (0.61 to 1.44)	—	−1.1 (−8.6 to 6.4)
rdinal outcome: status of combination of patient disposition and liberation from ventilation at 90 days — no./total no. (%)§§					
Died	85/284 (29.9)	76/286 (26.6)	—	—	3.4 (−4.0 to 10.7)
Still receiving ventilation at any location	2/284 (0.7)	4/286 (1.4)	—	—	−0.7 (−2.4 to 1.0)
Not receiving ventilation but in hospital or ICU	21/284 (7.4)	14/286 (4.9)	—	—	2.5 (−1.4 to 6.4)
Discharged from hospital and no longer receiving ventilation	176/284 (62.0)	192/286 (67.1)	—	—	−5.2 (−13.0 to 2.7)
ncurrent-intervention outcome: delirium — no. of trial days/total no. of trial days (%)¶¶					
Too sedated to assess for delirium	872/2266 (38.5)	782/2235 (35.0)	—	—	3.5 (0.7 to 6.3)
Positive test for delirium	324/1394 (23.2)	384/1453 (26.4)	—	—	−3.2 (−6.4 to 0)
e of assist–control mode					
Use of assist–control mode at least once — no./total no. (%)	169/287 (58.9)	142/286 (49.7)	1.2 (1.0 to 1.4)	—	9.2 (1.1 to 17.4)
Median duration of assist–control use (IQR) — days	0.44 (0.00 to 3.31)	0.00 (0.00 to 1.66)	—	—	0.44 (0.03 to 0.67)
fety — no./total no. (%)‖‖					
Serious adverse event	31/287 (10.8)	28/286 (9.8)	—	0.79	1.0 (−4.0 to 6.0)
Nonsevere self-extubation	14/287 (4.9)	7/286 (2.4)	—	0.19	2.4 (−0.6 to 5.5)

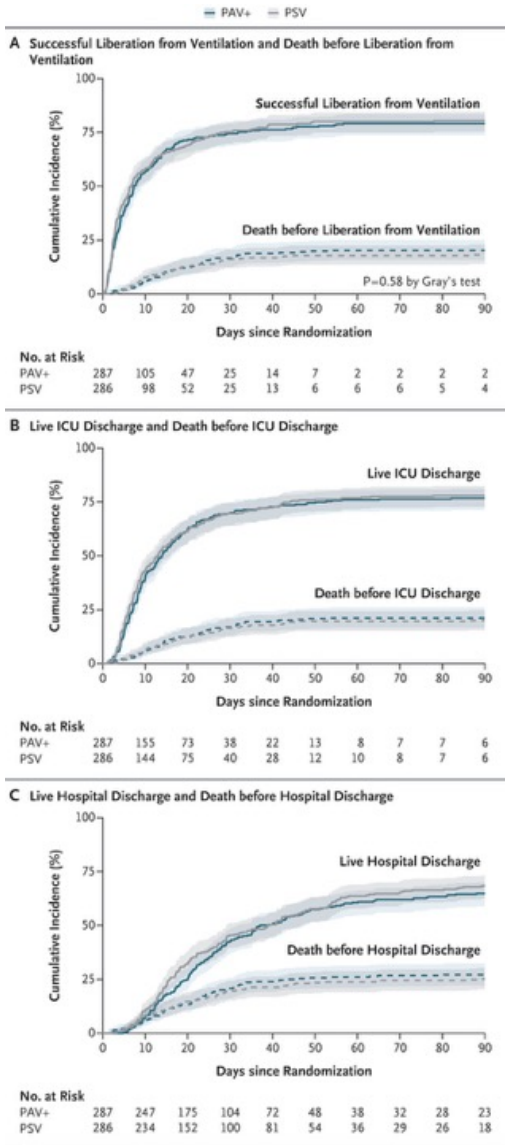

Cumulative Incidence Curves for Successful Liberation from Invasive Mechanical Ventilation, Live ICU Discharge, and Live Hospital Discharge, with Death as a Competing Risk.

Panel A shows the cumulative probability of successful liberation from ventilation and of death before successful liberation. The time of successful liberation was defined as the time of extubation or final disconnection from the ventilator, provided that the patient remained alive and free from invasive ventilation for 7 days. Patients were followed until successful liberation, death, or 90 days after randomization, whichever came first. Panel B shows the cumulative probability of live ICU discharge and of death before live ICU discharge. The time of live ICU discharge was defined as the time that the patient left the ICU after liberation from the ventilator, provided that the patient remained alive and ventilator-free for 7 days and did not return to the ICU for 48 hours. Transfers between ICUs while the patient was still undergoing mechanical ventilation were not considered to be live ICU discharges. Panel C shows the cumulative probability of live hospital discharge and of death before live hospital discharge. The time of live hospital discharge was defined as the time that the patient was discharged from the hospital to a home, long-term care facility, or rehabilitation center. Transfers between hospitals for receipt of ongoing acute care were not considered to be live hospital discharges. The shaded areas indicate 95% confidence intervals.

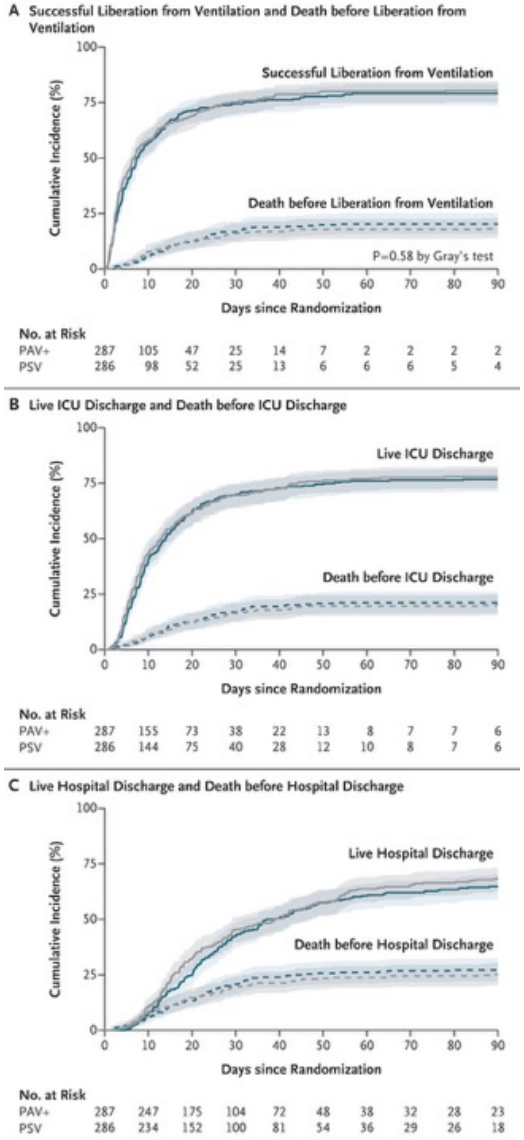

A Successful Liberation from Ventilation and Death before Liberation from Ventilation
Cumulative Incidence (%)
Successful Liberation from Ventilation
Death before Liberation from Ventilation
P=0.58 by Gray's test
Days since Randomization
No. at Risk
PAV+ 287 105 47 25 14 7 2 2 2 2
PSV 286 98 52 25 13 6 6 6 5 4
B Live ICU Discharge and Death before ICU Discharge
Live ICU Discharge
Death before ICU Discharge
No. at Risk
PAV+ 287 155 73 38 22 13 8 7 7 6
PSV 286 144 75 40 28 12 10 8 7 6
C Live Hospital Discharge and Death before Hospital Discharge
Live Hospital Discharge
Death before Hospital Discharge
No. at Risk
PAV+ 287 247 175 104 72 48 38 32 28 23
PSV 286 234 152 100 81 54 36 29 26 18

Cumulative Incidence Curves for Successful Liberation from Invasive Mechanical Ventilation, Live ICU Discharge, and Live Hospital Discharge, with Death as a Competing Risk.

Panel A shows the cumulative probability of successful liberation from ventilation and of death before successful liberation. The time of successful liberation was defined as the time of extubation or final disconnection from the ventilator, provided that the patient remained alive and free from invasive ventilation for 7 days. Patients were followed until successful liberation, death, or 90 days after randomization, whichever came first. Panel B shows the cumulative probability of live ICU discharge and of death before live ICU discharge. The time of live ICU discharge was defined as the time that the patient left the ICU after liberation from the ventilator, provided that the patient remained alive and ventilator-free for 7 days and did not return to the ICU for 48 hours. Transfers between ICUs while the patient was still undergoing mechanical ventilation were not considered to be live ICU discharges. Panel C shows the cumulative probability of live hospital discharge and of death before live hospital discharge. The time of live hospital discharge was defined as the time that the patient was discharged from the hospital to a home, long-term care facility, or rehabilitation center. Transfers between hospitals for receipt of ongoing acute care were not considered to be live hospital discharges. The shaded areas indicate 95% confidence intervals.

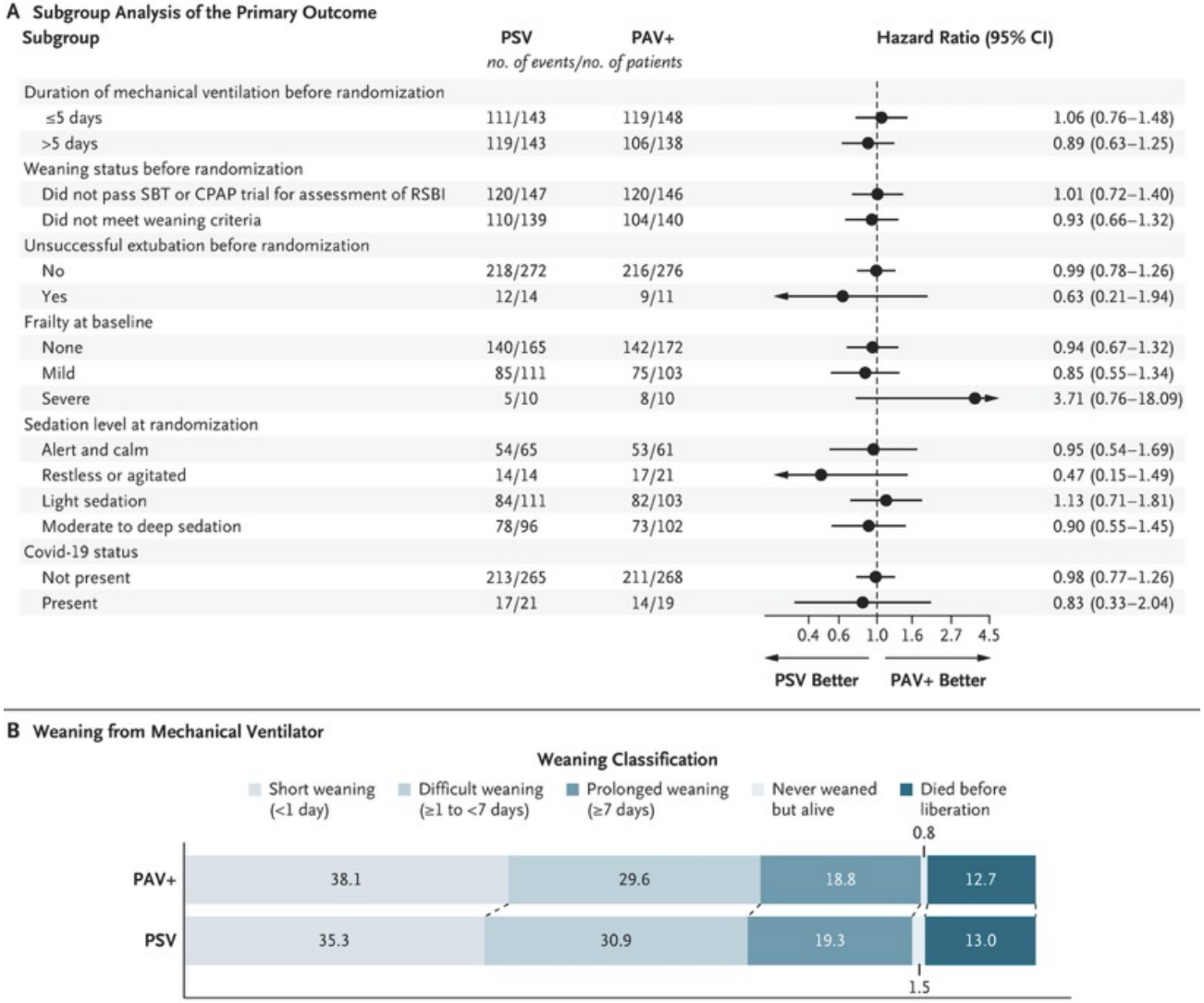

Subgroup Analysis of the Primary Outcome and Weaning Classification.

Panel A shows a forest plot of the hazard ratio for successful liberation from mechanical ventilation in prespecified subgroups. A positive coronavirus disease 2019 (Covid-19) status indicates a positive test for severe acute respiratory syndrome coronavirus 2. The widths of the confidence intervals have not been adjusted for multiplicity and may not be used in place of hypothesis testing. Panel B shows the percentage of patients classified as having short, difficult, or prolonged weaning from the mechanical ventilator; as never having been weaned; or as having died after the first SBT or the first extubation attempt. Patients who died before having a first SBT or a first extubation attempt (41 patients) or who had missing outcome data owing to withdrawal of consent (3 patients) were excluded from this analysis. Of the remaining 529 patients, 36.7% were classified as having short weaning, 30.2% as having difficult weaning, and 19.1% as having prolonged weaning; 1.1% of the patients were alive but still receiving invasive ventilation at day 90; and 12.9% died while still receiving mechanical ventilation. CPAP denotes continuous positive airway pressure, and RSBI rapid shallow-breathing index.

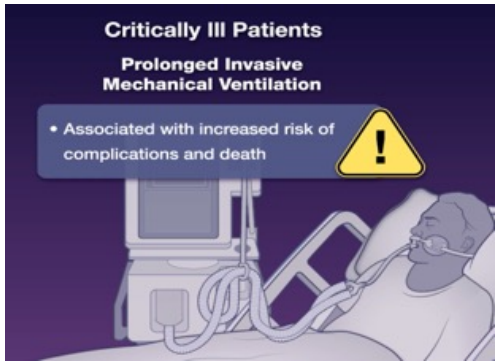
Critically Ill Patients
Prolonged Invasive Mechanical Ventilation
• Associated with increased risk of complications and death

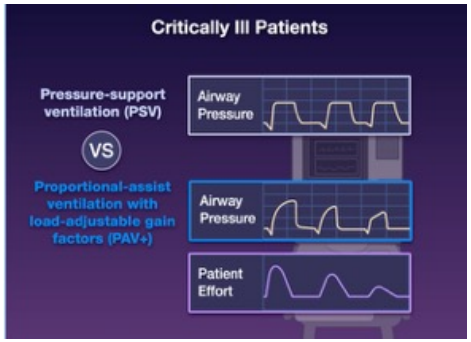
Critically Ill Patients
Pressure-support ventilation (PSV)
Airway Pressure
VS
Proportional-assist ventilation with load-adjustable gain factors (PAV+)
Airway Pressure
Patient Effort

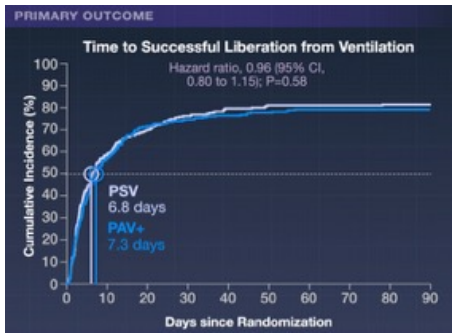
PRIMARY OUTCOME
Time to Successful Liberation from Ventilation
Hazard ratio, 0.96 (95% CI, 0.80 to 1.15); P=0.58
Cumulative Incidence (%)
PSV
6.8 days
PAV+
7.3 days
Days since Randomization

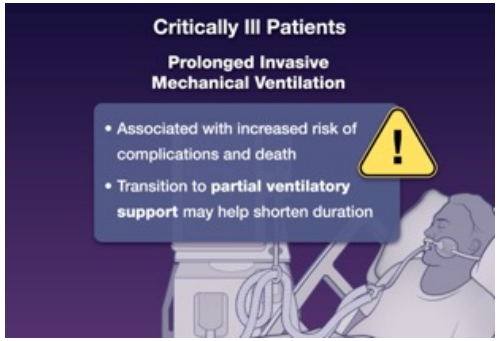
Critically Ill Patients
Prolonged Invasive Mechanical Ventilation
• Associated with increased risk of complications and death
• Transition to partial ventilatory support may help shorten duration

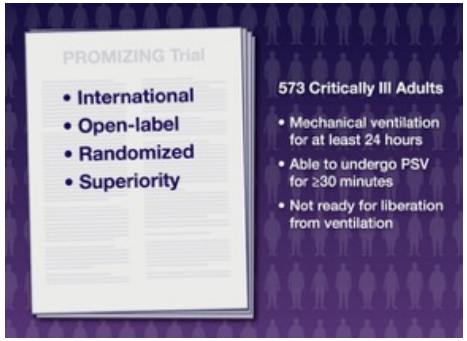
PROMIZING Trial
• International
• Open-label
• Randomized
• Superiority
573 Critically Ill Adults
• Mechanical ventilation for at least 24 hours
• Able to undergo PSV for ≥30 minutes
• Not ready for liberation from ventilation

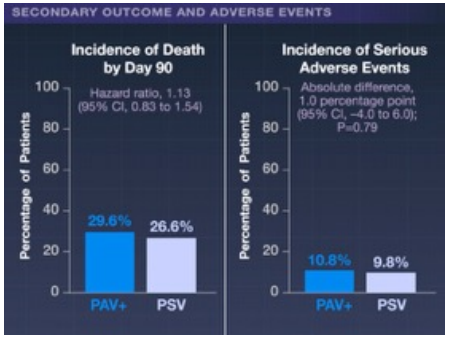
SECONDARY OUTCOME AND ADVERSE EVENTS
Incidence of Death by Day 90
Hazard ratio, 1.13 (95% CI, 0.83 to 1.54)
Percentage of Patients
29.6%
26.6%
PAV+
PSV
Incidence of Serious Adverse Events
Absolute difference, 1.0 percentage point (95% CI, −4.0 to 6.0); P=0.79
Percentage of Patients
10.8%
9.8%
PAV+
PSV

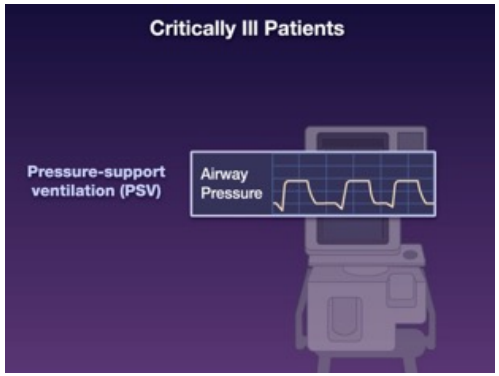
Critically Ill Patients
Pressure-support ventilation (PSV)
Airway Pressure

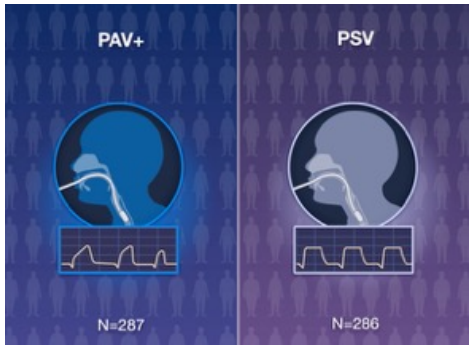
PAV+
PSV
N=287
N=286

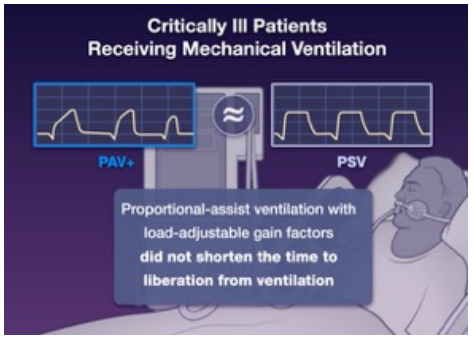
Critically Ill Patients Receiving Mechanical Ventilation
PAV+
PSV
Proportional-assist ventilation with load-adjustable gain factors did not shorten the time to liberation from ventilation

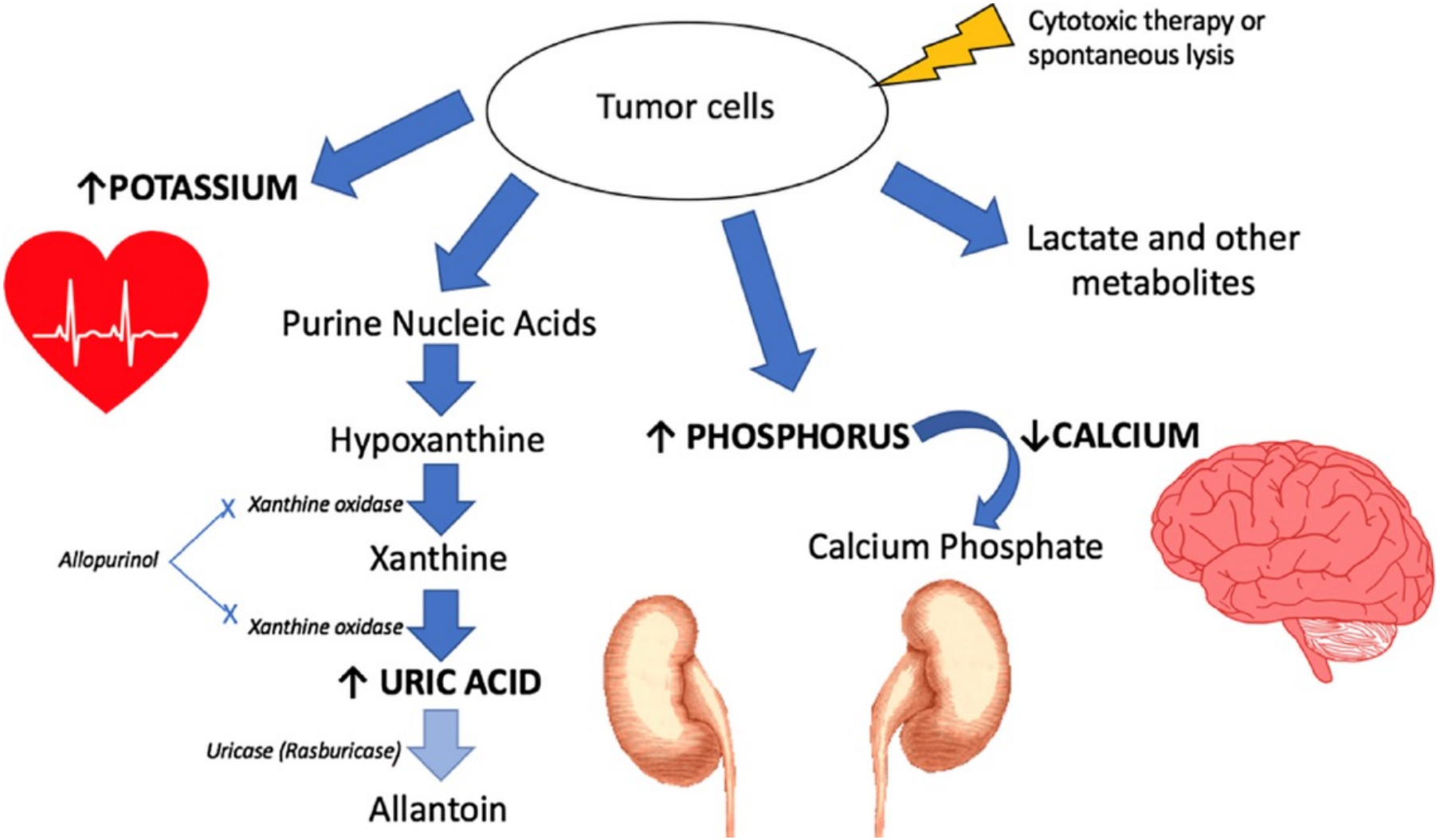
Cytotoxic therapy or spontaneous lysis
Tumor cells
↑POTASSIUM
Lactate and other metabolites
Purine Nucleic Acids
Hypoxanthine
↑ PHOSPHORUS
↓CALCIUM
Xanthine oxidase
Allopurinol
Xanthine
Calcium Phosphate
Xanthine oxidase
↑ URIC ACID
Uricase (Rasburicase)
Allantoin

Tumor Lysis Syndrome

Tumor lysis syndrome is a pathophysiological state that occurs when the ability of the body to maintain electrolyte–uric acid homeostasis is overwhelmed as a result of the destruction of malignant cells and the attendant massive release of cellular contents, including nucleic acids. This disorder was first described more than 100 years ago, and its consequences, as well as prophylaxis, treatment, and prognosis, were first reported in the 1960s. As recently as 1975, some physicians considered hyperphosphatemia–hypocalcemia to be a previously unrecognized complication of tumor lysis. The continuous development of antineoplastic therapies has rendered tumor lysis syndrome a less predictable and increasingly important aspect of the care of patients with cancer. In this article, we review the epidemiology and pathophysiology of tumor lysis syndrome; risk factors, prophylaxis, and treatment; and the evolution of the syndrome that has coincided with a continually expanding list of new therapies.

KEY POINTS

Tumor Lysis Syndrome

- The epidemiology of tumor lysis syndrome is evolving with the introduction of newer therapies.
- The occurrence of tumor lysis syndrome has become a less predictable but increasingly important aspect of the care of patients with cancer.
- With the availability of rasburicase, hyperphosphatemia has replaced hyperuricemia as the main cause of nephrotoxic effects in tumor lysis.
- Careful attention to fluid management and prevention of volume overload may diminish the risk of in-hospital death.
- In patients with acute leukemias or aggressive lymphomas, cytoreduction before the initiation of disease-specific induction therapy may reduce the incidence and severity of subsequent tumor lysis.

Cancers and Therapies Most Commonly Associated with Tumor Lysis Syndrome.

Cancer	Therapy	Evidence
Acute myeloid leukemia	Intensive induction chemotherapy (e.g., cytarabine- or anthracycline-based regimens)	Razis et al.,[5] Mato et al.[6]
Acute lymphoblastic leukemia or lymphoma	Anthracycline-based induction chemotherapy	Rios-Olais et al.[7]
Burkitt's lymphoma	Intensive induction therapy (e.g., CODOX-M or IVAC)*	Wössmann et al.,[4] Barnes et al.[8]
Advanced-stage, aggressive lymphomas (e.g., diffuse large B-cell lymphoma)	Intensive induction therapy	Calvache et al.[11]
Chronic lymphocytic leukemia with nodal masses of ≥10 cm or nodal masses of ≥5 cm and peripheral lymphocytosis (lymphocyte count of ≥25,000/μl)	Venetoclax	Roberts et al.,[21] AbbVie[22]

Diagnostic Criteria for Tumor Lysis Syndrome.

Laboratory Criteria	Clinical Criteria
Uric acid level of ≥8.0 mg/dl (476 μmol/liter) in adults or above the ULN in children or a 25% increase from baseline	Acute kidney injury defined by a creatinine level ≥1.5 times the ULN, an increase in the creatinine level of ≥0.3 mg/dl (26.5 μmol/liter), or urine output of <0.5 ml/kg/hr for 6 hr or more
Inorganic phosphorus level of ≥4.5 mg/dl (1.5 mmol/liter) in adults or ≥6.5 mg/dl (2.1 mmol/liter) in children or a 25% increase from baseline	Cardiac dysrhythmia or sudden death probably or definitely caused by hyperphosphatemia
Potassium level of ≥6.0 mmol/liter	Cardiac dysrhythmia or sudden death probably or definitely caused by hyperkalemia
Corrected calcium level of <7.0 mg/dl (1.75 mmol/liter) or ionized calcium level of <4.5 mg/dl (1.12 mmol/liter)†	Cardiac dysrhythmia, sudden death, seizure, neuromuscular irritability, hypotension, or heart failure probably or definitely caused by hypocalcemia

Cairo–Bishop Grading Classification of Tumor Lysis Syndrome.

Clinical or Laboratory Finding	Grade 0	Grade I	Grade II	Grade III	Grade IV	Grade V
Laboratory criteria for tumor lysis syndrome	Absent	Present	Present	Present	Present	Present
Creatinine	<1.5 times the ULN	1.5 times the ULN	>1.5–3.0 times the ULN	>3.0 to 6.0 times the ULN	>6.0 times the ULN	NA†
Cardiac arrhythmia	None	Intervention not indicated	Nonurgent medical intervention indicated	Symptomatic and incompletely controlled or controlled with a device (e.g., defibrillator)	Life-threatening (e.g., arrhythmia associated with heart failure, hypotension, syncope, or shock)	NA†
Seizure	None	None	One brief generalized seizure, one or more seizures well controlled by anticonvulsants, or infrequent focal motor seizures not interfering with activities of daily living	Seizure with altered consciousness or seizure disorder with breakthrough generalized seizures despite medical intervention	Seizures of any kind that are prolonged, repetitive, or difficult to control (e.g., status epilepticus or intractable epilepsy)	NA†

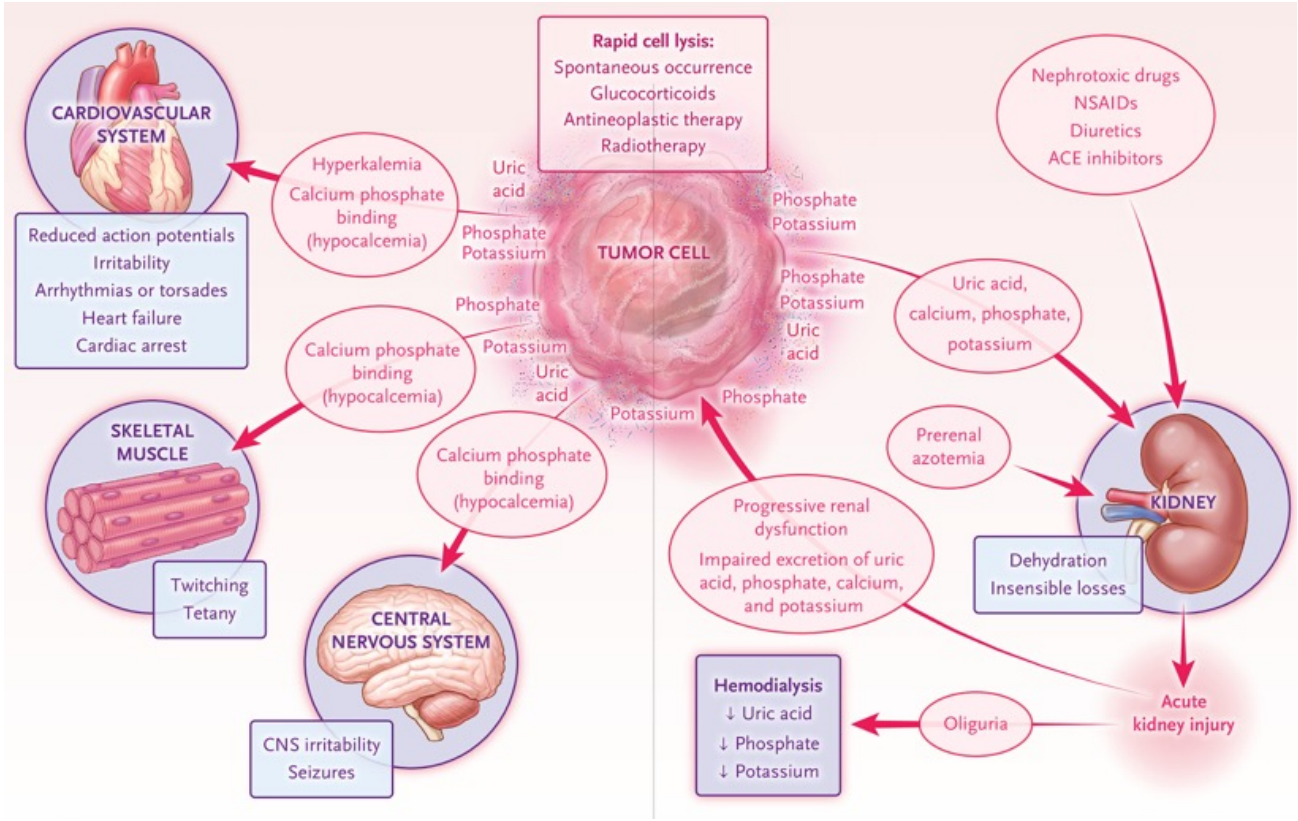

Pathophysiology of Tumor Lysis Syndrome.

Rapid lysis of cells leads to the release of intracellular substances (principally uric acid, potassium, and phosphorus) into the serum, with effects on the cardiovascular system, skeletal muscles, central nervous system, and kidneys. The effects on the kidney may be exacerbated by the presence of prerenal azotemia plus concurrent treatment with nephrotoxic medications. Acute kidney injury may lead to oliguria, which impairs the ability to manage fluid and electrolyte balance. Progressive renal injury or the inability to rapidly clear potassium, phosphorus, and uric acid may lead to an indication for renal replacement therapy. ACE denotes angiotensin-converting enzyme, CNS central nervous system, and NSAIDs nonsteroidal antiinflammatory drugs.

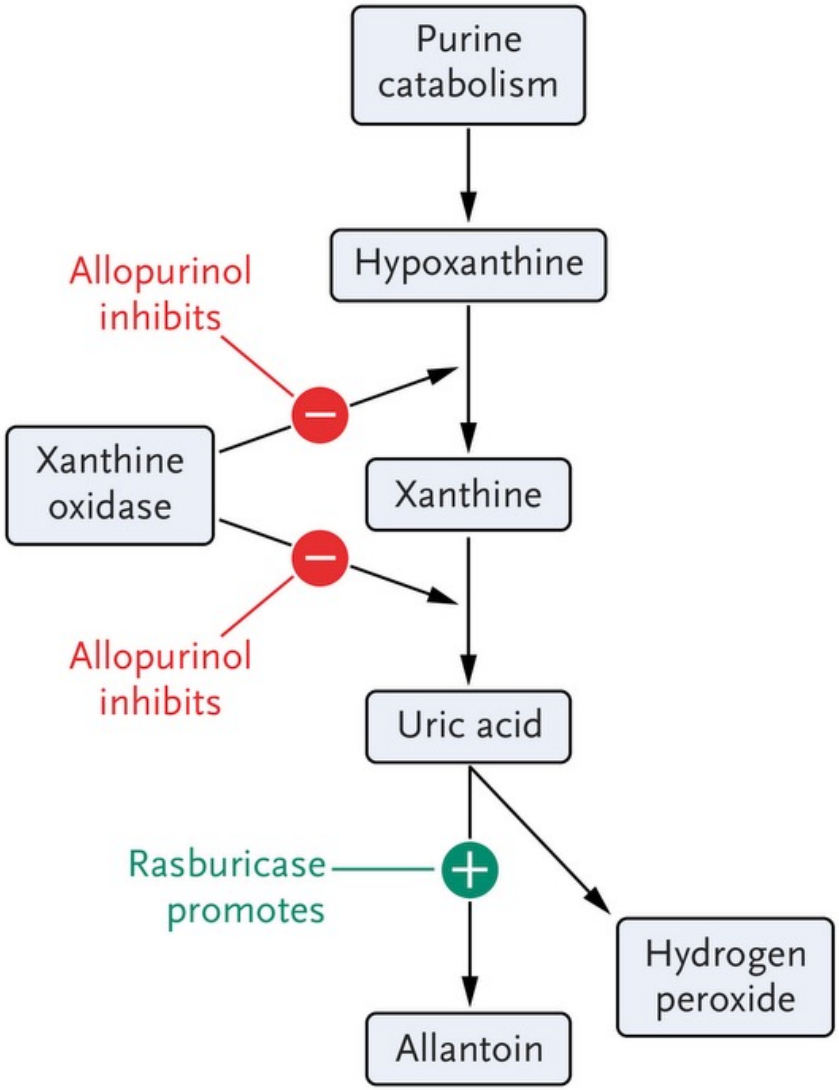

Purine Metabolism Pathway.

Purine nucleic acids are normally metabolized at physiologic rates to hypoxanthine, xanthine, uric acid, and allantoin. Xanthine oxidase inhibitors (allopurinol and febuxostat) decrease uric acid levels by inhibiting the metabolism of hypoxanthine and xanthine to uric acid. Rasburicase promotes the conversion of uric acid to allantoin, a much more soluble metabolite.

Special Management Considerations

Venetoclax

Venetoclax, currently the only B-cell lymphoma 2 inhibitor approved by the Food and Drug Administration (FDA), deserves special emphasis in the management of tumor lysis syndrome. In an early-phase trial, administration of high doses of venetoclax in patients with chronic lymphocytic leukemia (CLL) led to tumor lysis syndrome in 18% of participants (one of whom died) during dose escalation.

Pseudohyperkalemia Confounding Assessment

In patients with lymphoid cancers and extreme leukocytosis (e.g., >100,000 leukocytes per microliter), the laboratory artifact of pseudohyperkalemia may be observed. Pseudohyperkalemia, which is seen most commonly in patients with CLL, probably results from ex vivo lysis of fragile or senescent tumor cells due to the mechanical stress of collection into a vacuum tube, agitation of the tube during transport, or analysis of serum or plasma after cellular stress associated with centrifugation of the sample.

Additional New or Targeted Therapies

Management of tumor lysis syndrome may be a challenge in patients with multiple myeloma because of clinically significant renal dysfunction at baseline. Bortezomib, daratumumab, bispecific antibodies, and chimeric antigen receptor T-cell therapies have all been associated with tumor lysis syndrome in retrospective and pharmacovigilance studies.

Conclusions

The scope of tumor lysis syndrome has changed considerably over the past two decades. Historically high-risk cancers are often treated with lower-intensity induction regimens today, which may mitigate the incidence and severity of tumor lysis. Aggressive cytoreductive management of hyperleukocytosis in patients with acute myelogenous leukemia may also be reducing the risk, as compared with that in previous decades. However, the introduction of targeted therapies, particularly venetoclax in patients with CLL, has made tumor lysis relatively more common among patients with traditionally low-risk tumors. Electronic health records, which provide virtually instantaneous laboratory and supportive information, can be used to discern trends over time and manage tumor lysis in a more nuanced and timely way, particularly during the period of highest risk. Given that the complexity of medicine and the availability of modern therapeutics can be expected to increase, health care professionals need to practice with an enhanced degree of vigilance for situations in which tumor lysis may occur and must recognize the subtle early metabolic disturbances that may herald its onset.

Subcutaneous Panniculitis-like T-Cell Lymphoma

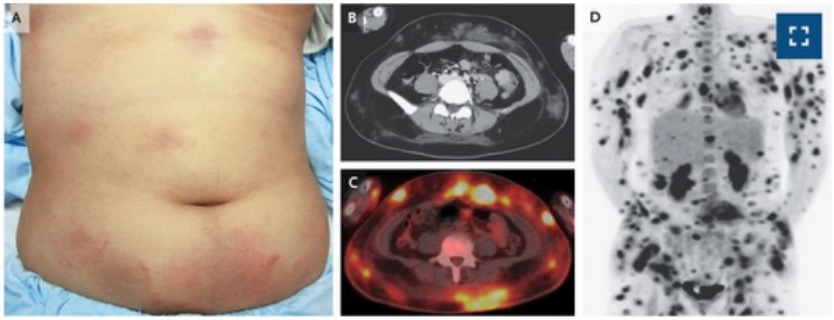

A previously healthy 30-year-old woman was admitted to the hospital with a 10-week history of painful skin nodules and a 6-week history of fevers and night sweats. A nodule biopsy performed 3 weeks before admission had shown only panniculitis. Physical examination was notable for palpable subcutaneous nodules with overlying erythema on the trunk (Panel A), arms, and legs. Computed tomography (CT) of the abdomen showed multiple areas of increased density in subcutaneous fat (Panel B). Splenomegaly was noted, but no lymphadenopathy was seen. Positron-emission tomography–CT (PET-CT) of the whole body showed uptake in the subcutaneous fat lesions (Panel C, fused PET-CT image; Panel D, maximum intensity projection image). Histopathological analysis of a repeat biopsy specimen showed infiltration of inflammatory cells into subcutaneous fat tissue. Adipocytes rimmed by atypical lymphocytes (positive for CD3, CD8, and perforin 1 and negative for CD4 and Epstein–Barr virus–encoded RNA) were also seen. Clonal T-cell receptor–β gene rearrangement was identified. A diagnosis of subcutaneous panniculitis-like T-cell lymphoma — a typically indolent primary cutaneous T-cell lymphoma characterized by adipotropism — was made. Results of laboratory testing did not fulfill the clinical criteria for a diagnosis of hemophagocytic lymphohistiocytosis, which is associated with this lymphoma in some cases. Treatment with chemotherapy was given owing to the rapid progression of the lymphoma. The patient had complete remission that was maintained as of a 2-year follow-up visit.

Primary Varicella Infection

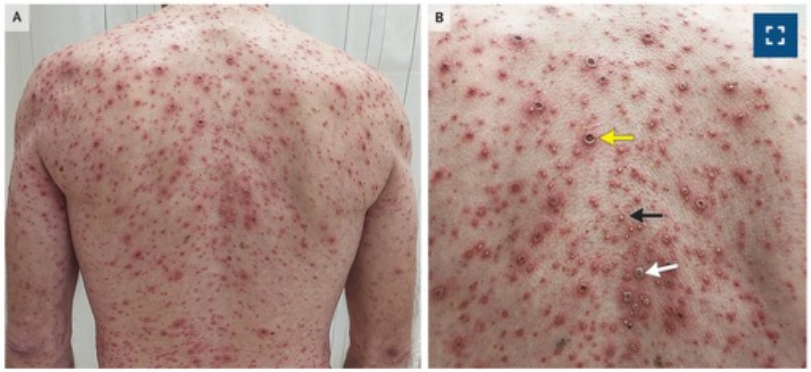

A previously healthy 44-year-old man presented to the dermatology clinic with a 4-day history of an itchy rash and a 2-day history of fever and malaise. The rash had first appeared on the scalp and then spread across the body within 24 hours. The patient reported no history of chicken pox or varicella vaccination. Physical examination was notable for widespread erythematous papules and pustules on the back (Panel A), chest, arms, legs, face, and scalp. The eruption was pleomorphic, with lesions of different sizes and stages of evolution (Panel B), including umbilicated lesions with central necrosis (yellow arrow), pustules (black arrow), and vesicles (white arrow). Laboratory testing was notable for mild elevations in aminotransferase levels. A polymerase-chain-reaction assay of fluid from a vesicle was positive for varicella–zoster virus. A diagnosis of primary varicella infection — or chicken pox — was made. Primary varicella infection in adults is often more severe than in children, which highlights the importance of childhood vaccination. Adults with varicella infection — even immunocompetent ones, such as this patient — have an increased risk of complications, such as pneumonia and encephalitis. Treatment with oral valacyclovir was administered. The illness abated without complications, and only residual hyperpigmentation from the rash remained at the 4-week follow-up.

Case 26-2025: An 11-Year-Old Girl with Chest Pain and Bone and Liver Lesions

An 11-year-old girl was transferred to the pediatric service of this hospital because of chest pain, arm pain, and multiple bone and liver lesions seen on imaging.

The patient had been in her usual state of health until 7 days before this presentation, when nausea, vomiting, and colicky abdominal pain developed, along with atraumatic pain in the right forearm, elbow, upper arm, and shoulder and in the sternal chest. Swelling of the right elbow was present; she had no fever or rigors. During the next few days, the nausea, vomiting, and abdominal pain abated, but the pain in the right arm and chest progressed, and she had discomfort when she took deep breaths. The patient's mother took her to the emergency department of another hospital for evaluation.

On presentation to the other hospital, the oral temperature was 37°C, the blood pressure 109/53 mm Hg, the heart rate 97 beats per minute, the respiratory rate 26 breaths per minute, and the oxygen saturation 100% while the patient was breathing ambient air. No axillary, inguinal, or cervical lymphadenopathy was noted on palpation. Cardiopulmonary auscultation was unremarkable. The abdomen was nontender, and there was no hepatosplenomegaly. The right arm and shoulder were tender on palpation but otherwise unremarkable, without visible joint effusions. No rash was present. Neurologic examination showed no motor or sensory deficits.

Initial Imaging Studies of the Right Shoulder and Liver.

A radiograph of the right shoulder is normal (Panel A). An ultrasound image of the liver shows a subcentimeter hypoechoic lesion in the peripheral right hepatic lobe (Panel B, arrow).

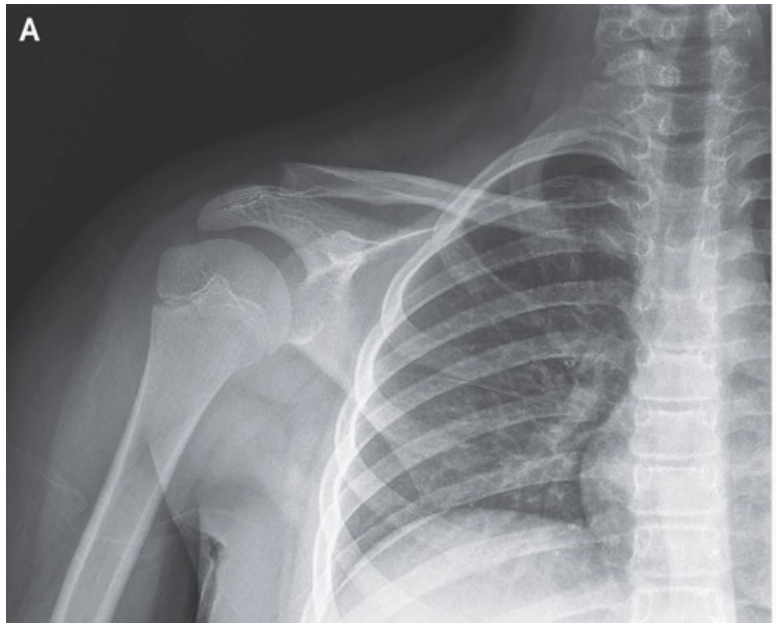

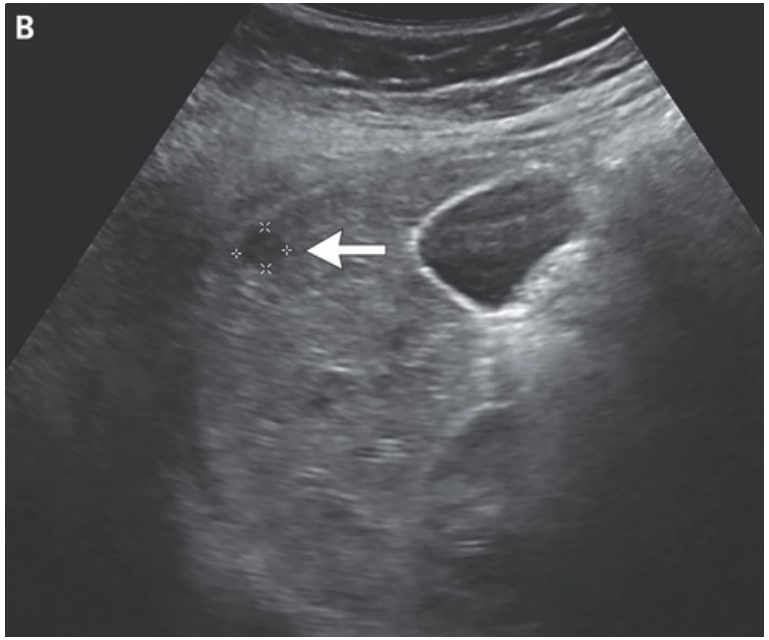

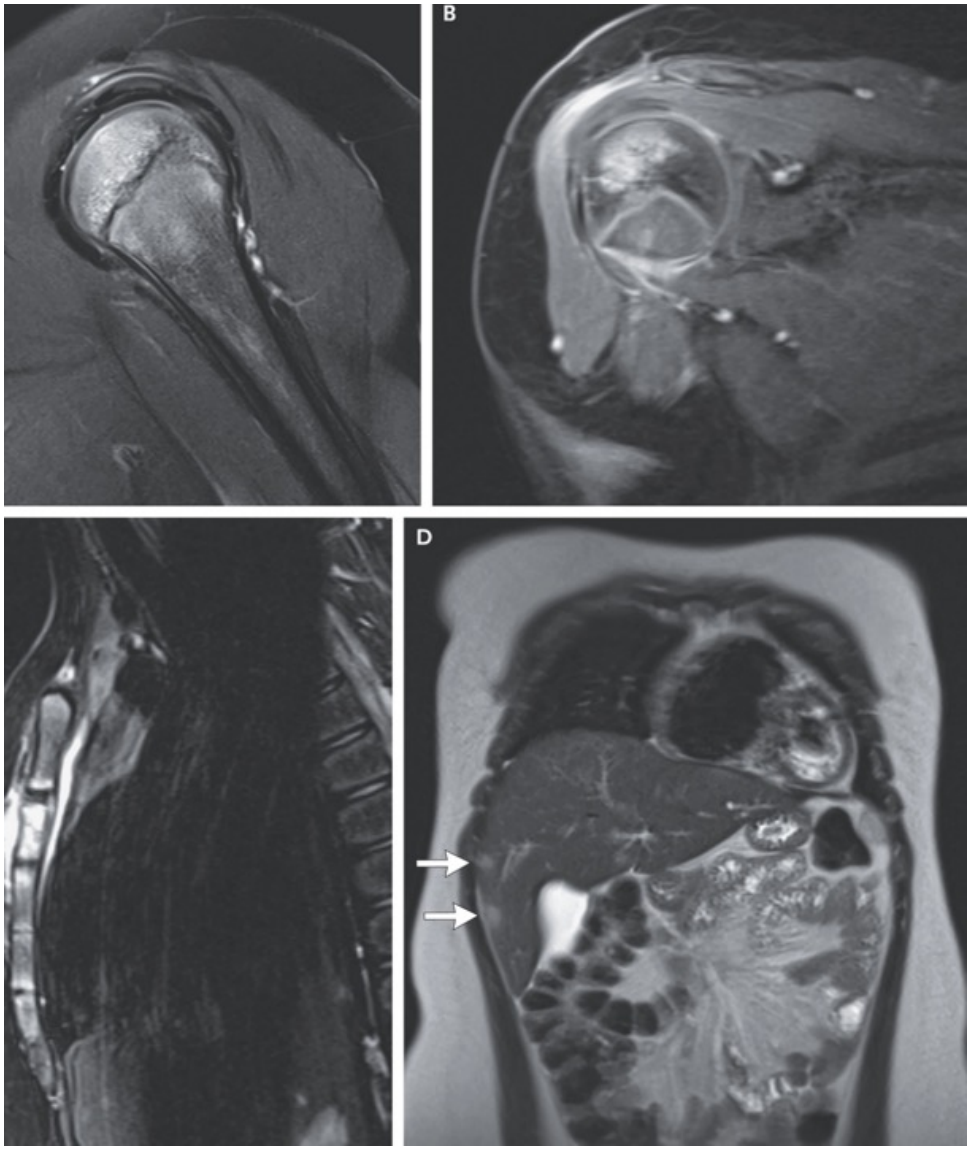

Initial MRI.

MRI of the right shoulder was performed. A fat-suppressed T2-weighted image (Panel A) shows a hyperintense lesion in the right humeral head. A fat-suppressed T1-weighted image, obtained after the administration of intravenous contrast material (Panel B), shows abnormal enhancement. MRI of the chest was also performed. A fat-suppressed T2-weighted image in a midsagittal plane (Panel C) shows an abnormal signal in the bone marrow, centered over the second sternal element, with surrounding soft-tissue involvement. Subsequent whole-body MRI was performed. A non–fat-suppressed T2-weighted image from half-Fourier single-shot turbo spin–echo imaging in a coronal plane (Panel D) shows two hyperintense lesions in the right hepatic lobe (arrows), with the most superior lesion corresponding to the lesion detected on ultrasonography. No other lesions were seen.

On arrival at this hospital, the patient reported no further pain. She had normal vital signs with no fever; the remainder of the physical examination was normal. She did not report easy bruising or bleeding, night sweats, weight loss, anorexia, or rash. Her medical history was notable for eczema, as well as recurrent skin and soft-tissue infections due to methicillin-resistant *Staphylococcus aureus* (MRSA), for which she had most recently been treated with trimethoprim–sulfamethoxazole 2 months before this presentation. She took no medications and was up to date with all routine childhood immunizations. There were no known adverse reactions to medications. She lived in a suburb in Massachusetts with her mother and grandmother. She reported no recent travel or recent changes in dietary habits. She had not consumed raw, undercooked, or unpasteurized foods. The family had recently gotten a kitten; there were no other pets in the home.

Variable	Reference Range, Children†	On Presentation, This Hospital
Hemoglobin (g/dl)	11.2–14.5	10.3
Hematocrit (%)	34.3–43.0	32.0
Mean corpuscular volume (fl)	78.3–87.7	71.4
White-cell count (per μl)	4000–10,000	9720
Differential count (per μl)		
Neutrophils	1960–5690	3370
Lymphocytes	1790–3730	1960
Monocytes	350–780	410
Eosinophils	50–410	450
Basophils	20–60	30
Platelet count (per μl)	205,000–376,000	467,000
Sodium (mmol/liter)	135–145	135
Potassium (mmol/liter)	3.4–5.0	3.8
Chloride (mmol/liter)	98–108	98
Carbon dioxide (mmol/liter)	23–32	23
Urea nitrogen (mg/dl)	9–23	11
Creatinine (mg/dl)	0.50–1.30	0.53
Calcium (mg/dl)	8.5–10.5	9.1
Aspartate aminotransferase (U/liter)	6–40	22
Alanine aminotransferase (U/liter)	10–49	17
Alkaline phosphatase (U/liter)	56–285	174
Total bilirubin (mg/dl)	0.0–1.2	0.2
Albumin (g/dl)	3.3–5.0	2.4
Globulin (g/dl)	1.9–4.1	4.3
Creatine kinase (U/liter)	33–211	106
High-sensitivity troponin T (ng/liter)	0–9	<6
Erythrocyte sedimentation rate (mm/hr)	45–115	>130
C-reactive protein (mg/liter)	0.0–8.0	40.1
Iron (μg/dl)	50–170	50
Transferrin saturation (%)	13–45	15
Total iron-binding capacity (μg/dl)	250–450	280
Ferritin (μg/liter)	Variable	320

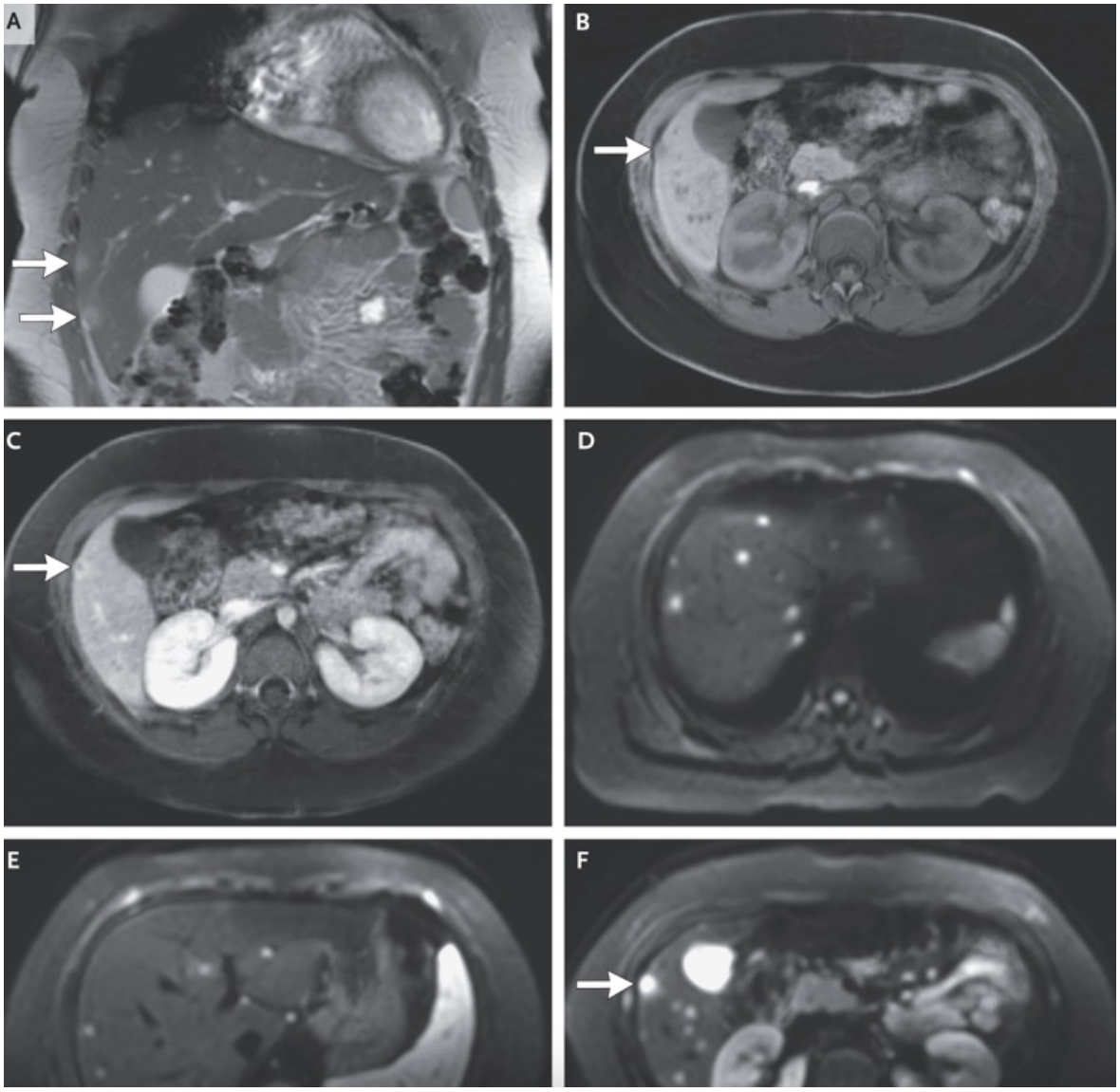

MRI of the Liver.

A coronal T2-weighted image from true fast imaging with steady-state precession (Panel A) confirms the presence of two hyperintense liver lesions (arrows). Axial fat-suppressed T1-weighted images of the most superior lesion, obtained before and after the administration of intravenous contrast material (Panels B and C, respectively), show peripheral (rim) enhancement of the hypointense lesion (arrows). Axial diffusion-weighted images of the liver (Panels D, E, and F) show numerous subcentimeter hyperintense lesions throughout the liver; the largest of these lesions, which corresponds to the sonographic abnormality, is identified with an arrow.

Differential Diagnosis

This 11-year-old, well-appearing girl with a history of eczema and MRSA skin infections presented with pain in the right arm and sternum that had lasted for 7 days. The patient's examination was unremarkable except for tenderness in the right arm and shoulder. Laboratory test results were notable for elevated levels of inflammatory markers, microcytic anemia, and hypoalbuminemia. Imaging revealed multifocal bone involvement without bone destruction, as well as epitrochlear lymphadenopathy and a rim-enhancing liver lesion. She had no fever, murmur, arthritis, joint effusion, systemic lymphadenopathy, organomegaly, or leukocytosis. On the basis of these findings, I will develop a differential diagnosis focusing on cancer, inflammatory disorders, and infection as the possible causes of this patient's bone and liver lesions and regional lymph-node involvement.

Cancer

This patient presented with disease involvement at multiple sites, including bone, liver, and possibly lymph nodes, prompting consideration of various childhood cancers that could explain these findings. The most common bone tumors in children are Ewing's sarcoma and osteosarcoma.

Infection

In an otherwise healthy child, an acute illness such as that seen in this case is most often caused by infection. Bone involvement suggests the possibility of bacterial osteomyelitis. Her history of eczema and MRSA infections increases the probability of hematogenous spread of *S. aureus* to both bone and liver that resulted in hematogenous osteomyelitis and multifocal liver abscesses. However, children with acute hematogenous staphylococcal osteomyelitis typically present with fevers, leukocytosis, and an ill appearance. Despite the absence of pulmonary involvement and epidemiologic risk factors, granulomatous infections due to tuberculous or nontuberculous mycobacteria or due to an endemic mycosis are worth considering in this case.

Given the features of this patient's presentation and recent exposure to a kitten, infection with *Bartonella henselae* (cat scratch disease) is the most likely diagnosis in this case. More than 90% of kittens younger than 1 year of age have antibody reactivity to *B. henselae*. The typical portal of entry for bartonella is inoculation through a kitten scratch, kitten bite, or flea bite. After infection, regional lymphadenopathy develops at the site of inoculation within 1 to 3 weeks. Cat scratch disease is usually a self-limited illness, and up to 50% of patients are afebrile.

Given the patient's well appearance and a desire not to put her through unnecessary invasive testing such as bone biopsy, I would perform serologic testing for bartonella infection to obtain a diagnosis. I would begin empirical antimicrobial therapy while waiting for the test results.

Pathological Discussion

Immunofluorescence antibody assays for *B. henselae* and *B. quintana* were performed at a reference laboratory. *B. henselae* IgM and IgG isotypes were detected at a titer of greater than 1:20 (reference value, negative) and 1:4096 (reference value, negative), respectively; *B. quintana* IgM and IgG isotypes were not detected.

B. henselae is a fastidious gram-negative bacterium that infects red cells and endothelial cells in humans. Its primary vector is *Ctenocephalides felis* (cat flea), and cats serve as the predominant reservoir. Humans are incidental hosts, with the infection occurring as a result of a bite or scratch from an infected cat; human-to-human transmission of bartonella is not typical.

The most common manifestation of *B. henselae* infection is cat scratch disease, which is characterized by the development of a lesion at the site of inoculation, followed by regional lymphadenopathy and systemic symptoms. Atypical manifestations occur in 5 to 20% of patients and can include ocular, neurologic, hepatosplenic, or musculoskeletal involvement.

Serologic testing remains the cornerstone of the diagnosis of cat scratch disease; in this case, the IgM titer of greater than 1:20 and the IgG titer of greater than 1:180 were suggestive of active bartonella infection. In general, an increase in serial IgG titers by a factor of 4 is also supportive of the diagnosis. Direct detection of the pathogen with molecular methods such as polymerase-chain-reaction (PCR) testing is also available in most reference laboratories.

Bartonellose ist eine Gruppe bakterieller Infektionskrankheiten, die durch Bakterien der Gattung Bartonella verursacht werden, welche durch Insekten oder Flöhe auf den Menschen übertragen werden. Bekannte Formen sind die Katzenkratzkrankheit (B. henselae), das Fünftagefieber und die Verruga peruana (B. bacilliformis) sowie durch B. quintana verursachte Krankheiten. Symptome variieren je nach Erreger und können von Lymphknotenschwellungen (Katzenkratzkrankheit) bis zu Fieber und Hautveränderungen reichen. Bartonella gehört zu der Familie Bartonellaceae, welche früher zusammen mit den Rickettsiaceae (Rickettsien) zur Ordnung Rickettsiales gestellt wurde.

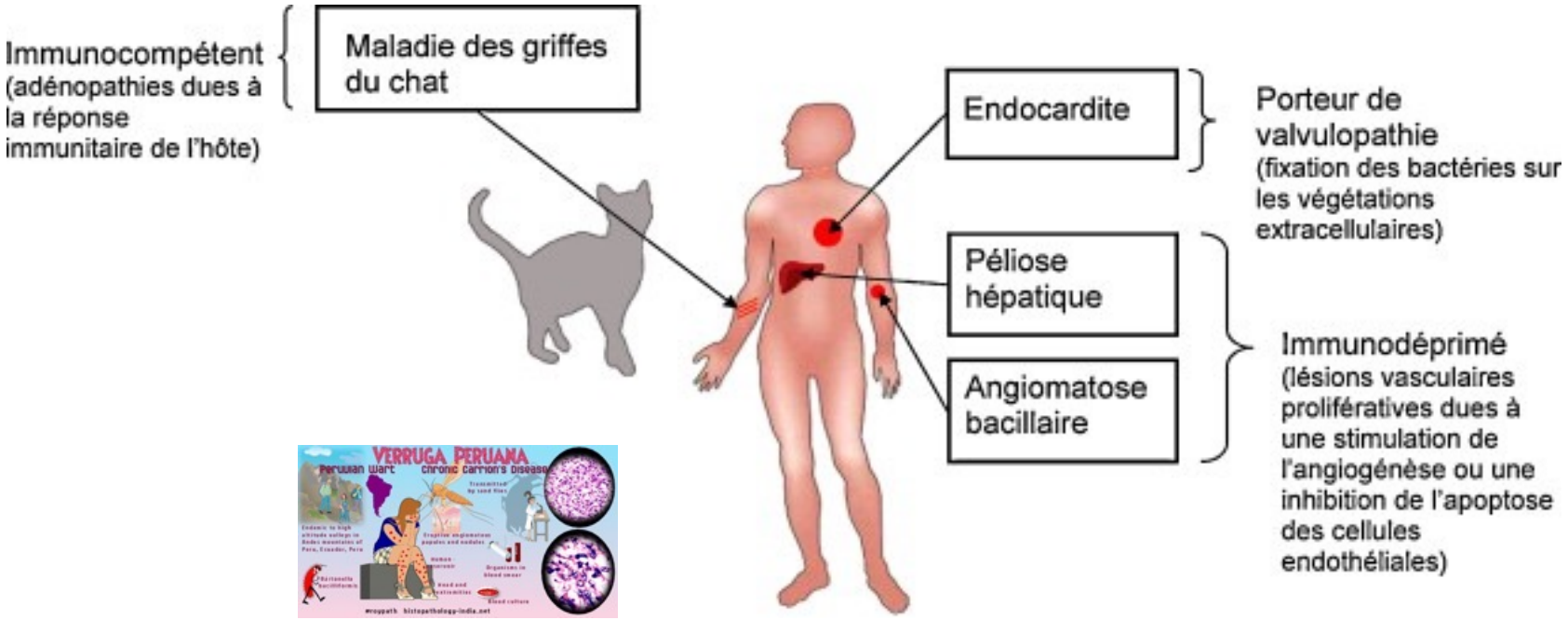

Als Verruga peruana wird die eruptive Spätmanifestation der Bartonellose bezeichnet.
siehe auch: Oroya-Fieber

In 1871, a major outbreak of febrile hemolytic anemia occurred among workers in the Rimac Valley in Lima who were constructing a railway line in the Andes mountains to the mining town of La Oroya, in the highlands of Peru; this outbreak resulted in the death of more than 4000 workers and was referred to as Oroya fever. Less than 15 years later, in 1885, Daniel Alcides Carrión, a Peruvian medical student, demonstrated that verruga peruana and Oroya fever are caused by the same organism; this discovery resulted from a heroic experiment in which he injected himself with infectious skin lesion material from a patient with verruga peruana and soon thereafter developed a fatal infection with fever and severe hemolytic anemia. As a tribute to him, both manifestations of this disease were thereafter known as Carrion's disease.

In 1905, Alberto Barton observed bacteria within red blood cells when examining peripheral blood smears in patients with Oroya fever, and later, the causative organism, Bartonella bacilliformis, was named after him

Daniel Alcides Carrión

PCSK9 ist ein Protein, das maßgeblich an der Regulierung des Cholesterinstoffwechsels beteiligt ist. PCSK9-Hemmer sind Medikamente, die dieses Protein blockieren, um die Menge an LDL-Cholesterin (dem „schlechten“ Cholesterin) im Blut zu senken. Sie sind eine wichtige Therapieoption für Patienten mit extrem hohem Cholesterinspiegel, die selbst mit anderen Medikamenten und Lebensstiländerungen nicht ausreichend kontrolliert werden kann, um Folgeerkrankungen wie Herzinfarkt oder Schlaganfall vorzubeugen.

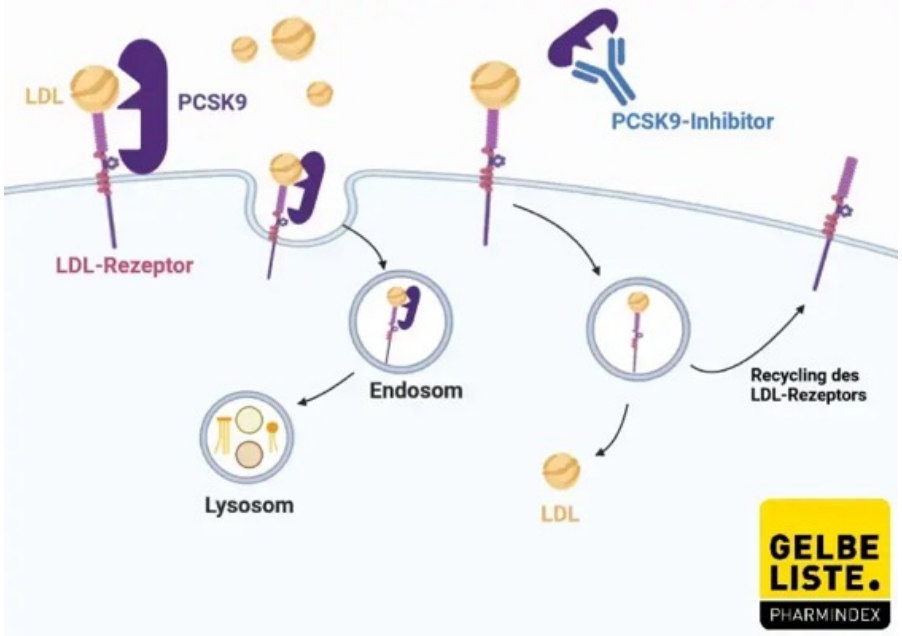

A saphenous vein graft is a length of the patient's own great saphenous vein, a healthy blood vessel from the leg, that is surgically removed and used in coronary artery bypass graft (CABG) surgery to bypass a blocked section of a coronary artery. The graft allows blood to flow freely to the heart muscle, rerouting it around the blockage. While commonly used, saphenous vein grafts are prone to accelerated atherosclerosis and intimal hyperplasia, leading to reduced long-term patency compared to arterial grafts.

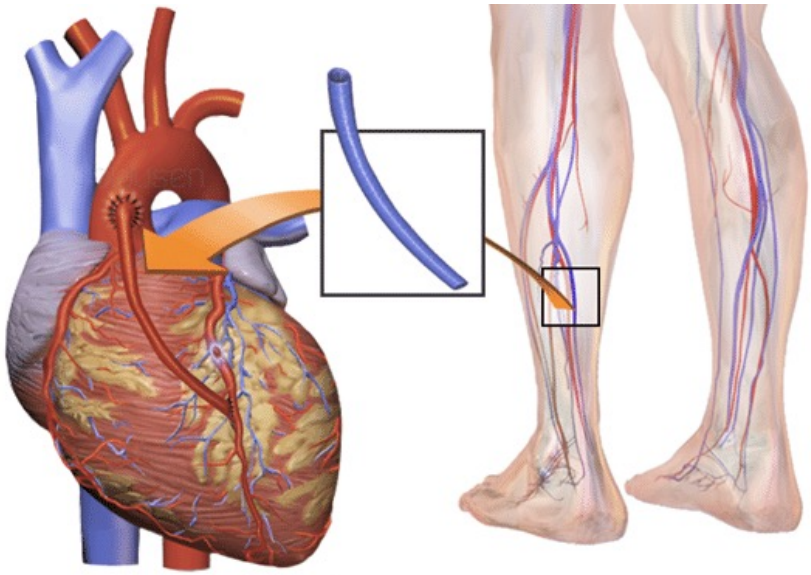

Effect of evolocumab on saphenous vein graft patency after coronary artery bypass surgery (NEWTON-CABG CardioLink-5): an international, randomised, double-blind, placebo-controlled trial

Summary

Background Saphenous vein graft (SVG) failure remains a substantial challenge after coronary artery bypass graft (CABG). LDL cholesterol (LDL-C) is a causal risk factor for atherosclerosis, but its role in SVG failure is not well established. We evaluated whether early initiation of intensive LDL-C lowering with evolocumab could reduce SVG failure.

Methods NEWTON-CABG CardioLink-5 was a multicentre, double-blind, randomised, placebo-controlled trial conducted at 23 sites in Canada, the USA, Australia, and Hungary. Eligible participants were adults (age ≥18 years) who underwent CABG with at least two SVGs and were being treated with statin therapy of moderate or high intensity. Participants were randomly allocated (1:1; variable block size) within 21 days of CABG to subcutaneous evolocumab 140 mg or placebo every 2 weeks. The primary endpoint was the 24-month vein graft disease rate (VGDR; the proportion of SVGs with ≥50% occlusion on coronary CT angiography or clinically indicated invasive angiography) in the modified intention-to-treat population. This trial is registered with ClinicalTrials.gov, NCT03900026, and is completed.

Findings Between June 17, 2019, and Nov 10, 2022, 782 individuals were randomly assigned (389 to evolocumab and 393 to placebo). At baseline, among the 554 participants with primary outcome data available, the median age was 66 years (IQR 60–72), 471 (85%) of 554 participants were male and 83 (15%) were female, and the median LDL-C was 1·85 mmol/L (IQR 1·25–2·84) in the evolocumab group and 1·86 mmol/L (1·20–2·76) in the placebo group. Evolocumab resulted in a mean 48·4% placebo-adjusted reduction in LDL-C at 24 months (–52·4% *vs* –4·0%). The 24-month VGDR was 21·7% (149 of 686 grafts) in the evolocumab group and 19·7% (127 of 644 grafts) in the placebo group (difference 2·0% [95% CI –3·1 to 7·1]; p=0·44). Treatment was well tolerated, with similar adverse event profiles between the groups.

Interpretation Among patients who underwent CABG, evolocumab did not reduce SVG disease at 24 months following the index surgery despite substantial LDL-C lowering. Further LDL-C lowering does not appear to meaningfully affect the pathophysiological mechanisms responsible for early SVG failure.

Funding Amgen Canada.

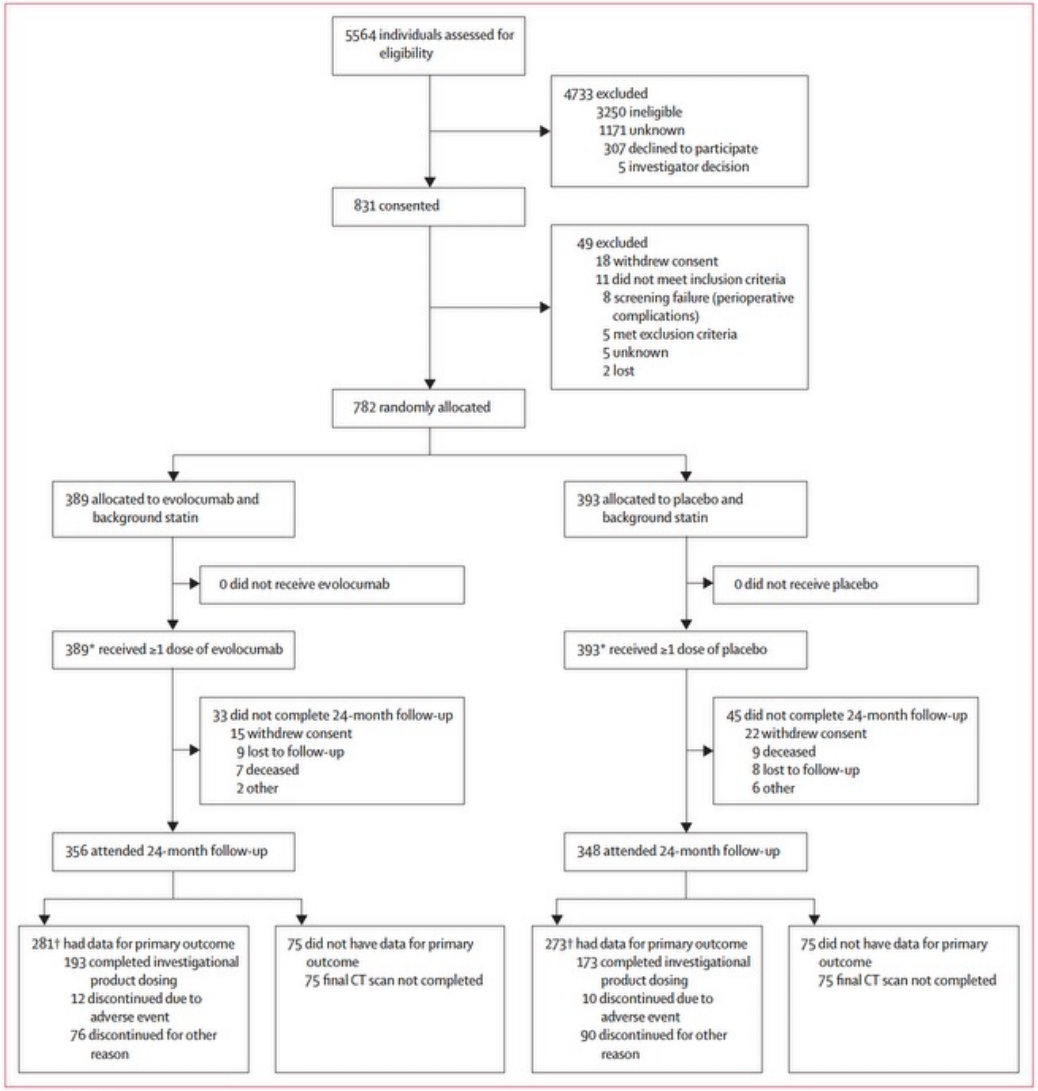

Figure 1: **Trial profile**

*Safety population. †Modified intention-to-treat population.

	Evolocumab group (n=281)	Placebo group (n=273)
Age, years	66 (60-72)	67 (61-73)
Sex		
Female	40 (14%)	43 (16%)
Male	241 (86%)	230 (84%)
Race or ethnicity		
White	201 (72%)	183 (67%)
South Asian	56 (20%)	66 (24%)
East Asian	10 (4%)	19 (7%)
African descent	4 (1%)	2 (1%)
Other	10 (4%)	3 (1%)
BMI, kg/m²	28·5 (25·4-30·9)	27·7 (25·0-31·2)
Blood pressure, mm Hg		
Systolic	123 (111-134)	122 (114-135)
Diastolic	74 (68-81)	74 (68-80)
History of major cardiovascular events		
Myocardial infarction	114 (41%)	125 (46%)
Percutaneous coronary intervention	49 (17%)	44 (16%)
Peripheral artery disease	10 (4%)	9 (3%)
Stroke	6 (2%)	5 (2%)
New York Heart Association class III or IV heart failure	12 (4%)	11 (4%)
Cardiovascular risk factors		
Hypertension	238 (85%)	212 (78%)
Diabetes	116 (41%)	116 (42%)
Never smoker	126 (45%)	143 (52%)
Former smoker (>12 months)	88 (31%)	87 (32%)
Recent smoker (≤12 months)	67 (24%)	43 (16%)
Medications		
Statin	277 (99%)	271 (99%)
Aspirin	273 (97%)	265 (97%)
$P2Y_{12}$ inhibitor	93 (33%)	79 (29%)
Aspirin and $P2Y_{12}$ inhibitor	91 (32%)	78 (29%)
β blocker	262 (93%)	252 (92%)
Angiotensin-converting enzyme inhibitor	88 (31%)	82 (30%)
Angiotensin receptor blocker	28 (10%)	37 (14%)
Calcium channel blocker	51 (18%)	39 (14%)
Diuretic	109 (39%)	105 (38%)
Other antihypertensive	4 (1%)	6 (2%)
Anti-arrhythmic or amiodarone	52 (19%)	44 (16%)
Lipids, mmol/L		
Total cholesterol	3·70 (2·87-4·83)	3·70 (2·80-4·72)
LDL cholesterol	1·85 (1·25-2·84)	1·86 (1·20-2·76)
HDL cholesterol	0·97 (0·79-1·19)	1·00 (0·81-1·22)
Non-HDL cholesterol	2·61 (1·90-3·67)	2·44 (1·88-3·45)
Triglycerides	1·56 (1·13-2·18)	1·54 (1·07-2·09)
Haemoglobin A_{1c}, %	6·2% (5·7-7·1)	6·2% (5·6-7·0)
Haemoglobin A_{1c} for participants living with diabetes, %	7·3% (6·5-8·4)	7·0% (6·4-8·0)
Time from surgery to randomisation, days	13 (6-17)	12 (6-16)
Status of index CABG procedure		
Elective procedure	199 (71%)	187 (68%)
Urgent procedure	76 (27%)	77 (28%)
Emergency procedure	6 (2%)	9 (3%)

(Table 1 continues on next page)

	Evolocumab group (n=281)	Placebo group (n=273)
(Continued from previous page)		
CABG performed with cardiopulmonary bypass	261 (93%)	262 (96%)
Duration of cardiopulmonary bypass among those who were operated on, min	85 (66–104)	86 (69–103)
Cross-clamp time, min	69 (58–87)	71 (57–89)
Off-pump CABG	20 (7%)	11 (4%)
SVG harvesting method		
Open	87 (31%)	89 (33%)
Endoscopic	193 (69%)	182 (67%)
Not recorded	1 (<1%)	2 (1%)
Grafts per participant (SVG or arterial)	3 (3–4)	3 (3–4)
Patients receiving at least 3 grafts (SVG or arterial)	276 (98%)	259 (95%)
SVGs per participant	2 (2–3)	2 (2–3)
Patients receiving left internal mammary artery	267 (95%)	253 (93%)
Patients receiving radial artery	21 (7%)	23 (8%)

Data are median (IQR) or n (%). Percentages may not total 100% because of rounding. CABG=coronary artery bypass graft. SVG=saphenous vein graft.

***Table 1*: Baseline and procedural characteristics in the modified intention-to-treat population**

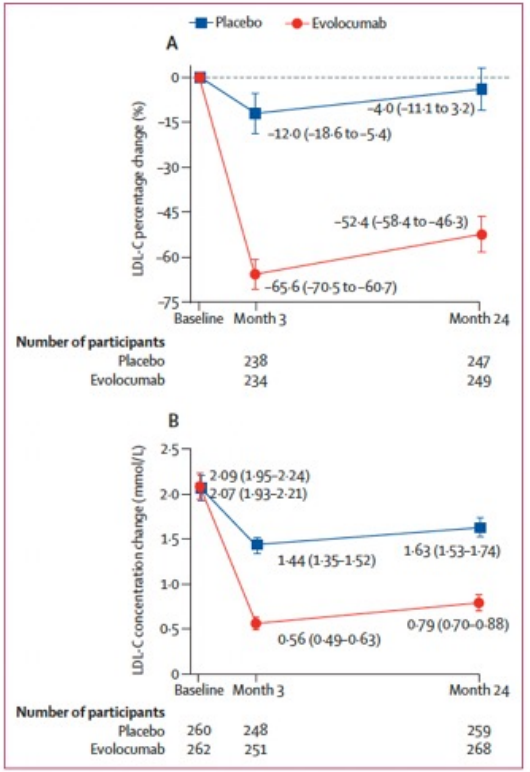

***Figure 2*: LDL-C variation during the trial**
Percentage changes (A) and concentration changes (B) in LDL-C during the trial. Filled symbols correspond to means and error bars correspond to 95% CIs. LDL-C=LDL cholesterol.

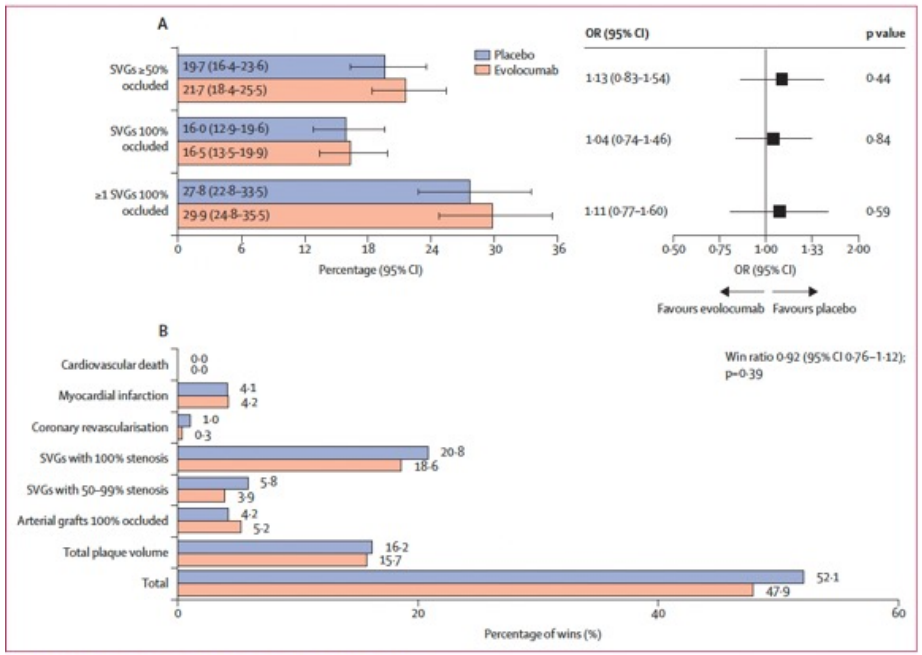

Figure 3: **Key saphenous vein graft and clinical outcomes at 24 months**
SVG outcomes (A) and win ratio and its components in hierarchical order (B). No randomly allocated participants with end-of-study graft assessments (ie, the modified intention-to-treat population) died during the study, and therefore none had the cardiovascular death component of the win ratio. OR=odds ratio. SVG=saphenous vein graft.

	Evolocumab group	Placebo group	Odds ratio	p value
Number of patients included in the modified intention-to-treat analysis	281	273	..	..
Vein graft disease rate*	149/686 (22% [18–25])	127/644 (20% [16–24])	1·13 (0·83–1·54)	0·44
SVGs completely occluded*	113/686 (16% [14–20])	103/644 (16% [13–20])	1·04 (0·74–1·46)	0·84
Participants with ≥1 SVG completely occluded	84/281 (30% [25–36])	76/273 (28% [23–33])	1·11 (0·77–1·60)	0·59
SVG total plaque volume,† mm³	18·1 (12·1–23·7)	17·0 (13·1–22·3)	..	0·69
All grafts total plaque volume,† mm³	20·7 (15·2–27·1)	20·7 (15·6–26·7)	..	0·91
Number of patients included in the safety analysis	389	393	..	..
Composite of myocardial infarction (non-fatal and fatal), stroke (fatal and non-fatal), cardiovascular death, and repeat coronary revascularisation	25/389 (6%)	21/393 (5%)	1·22 (0·67–2·21)	0·52
Myocardial infarction (fatal and non-fatal)	15/389 (4%)	16/393 (4%)	0·95 (0·46–1·94)	0·88
Stroke (fatal and non-fatal)	3/389 (1%)	0	Not estimable	Not applicable
Cardiovascular death	6/389 (2%)	4/393 (1%)	1·52 (0·43–5·44)	0·52
Repeat coronary revascularisation	5/389 (1%)	1/393 (<1%)	5·10 (0·59–43·89)	0·14
All-cause mortality	7/389 (2%)	9/393 (2%)	0·78 (0·29–2·12)	0·63

Data are n/N (% [95% CI]), or median (IQR), unless otherwise specified. SVG=saphenous vein graft. *Graft-level analyses (denominators show the total number of SVGs assessed for the primary outcome in each group [evolocumab: 686 SVGs; placebo: 644 SVGs]). Analyses account for clustering of grafts within patients; intraclass correlation coefficient=0·23. †Data normalised by lengths.

Table 2: **Primary, secondary, and safety outcomes at 24 months**

Research in context

Evidence before this study

Coronary artery bypass graft (CABG) remains one of the most commonly performed cardiac surgical procedures worldwide, and saphenous vein grafts (SVGs) are used in almost all of these procedures. However, SVG failure remains a persistent clinical problem. We searched PubMed, Embase, and the Cochrane Library for articles published from database inception to June 30, 2025, using the terms "saphenous vein OR SVG", "coronary artery bypass OR CABG", "paten* OR fail*", "low-density lipoprotein cholesterol OR LDL-C OR LDL cholesterol OR LDL", "randomi* OR RCT OR trial", and "statin". We included observational studies, randomised controlled trials, and meta-analyses that reported on SVG patency or failure, LDL cholesterol (LDL-C) levels, or lipid-lowering therapies in post-CABG populations. We restricted the search to those in humans and published in English. The available evidence suggested that 20–30% of SVGs fail within the first year and nearly half are occluded within 10 years after surgery. Although LDL-C is a recognised causal factor in arterial atherosclerosis and cardiovascular risk, evidence linking LDL-C levels or LDL-C lowering therapies to SVG patency is sparse and inconsistent. No randomised trials have specifically evaluated the effect of intensive LDL-C lowering with PCSK9 inhibition, in addition to background statin therapy, on early SVG patency in contemporary post-CABG populations; the quality of the available evidence is limited by heterogeneity in study design, small sample sizes, and risk of bias in observational studies.

Added value of this study

To the best of our knowledge, NEWTON-CABG is the first randomised, placebo-controlled trial to assess the effect of early initiation of a PCSK9 inhibitor on SVG disease after CABG, on a background of statin therapy of moderate to high intensity. Regardless of LDL-C entry levels, evolocumab substantially lowered LDL-C concentrations, but did not reduce SVG disease rates at 24 months compared with placebo. These findings suggest that further LDL-C lowering does not meaningfully affect the pathophysiological mechanisms responsible for early SVG failure, which are likely to be dominated by thrombotic and remodelling processes rather than conventional atherosclerosis mechanisms.

Implications of all the available evidence

Although intensive LDL-C lowering with PCSK9 inhibition reduces cardiovascular events in high-risk populations, including those who have undergone CABG, this strategy does not appear to have a major impact on early SVG patency. These findings further support the notion that early SVG failure is mechanistically distinct from native coronary atherosclerosis and might require novel therapeutic approaches targeting vein graft remodelling, thrombosis, or inflammation. Nevertheless, the long-term cardiovascular benefits of LDL-C reduction with PCSK9 inhibitors remain well established and these agents should continue to be an important part of secondary prevention strategies in this population.

Childhood obesity is a complex health issue where children have excess body fat, increasing risks for serious health problems like type 2 diabetes, heart disease, and depression. It is diagnosed by a healthcare professional using a BMI-for-age chart, with obesity defined as a BMI at or above the 95th percentile for a child's age and sex. Factors contributing to childhood obesity include genetics, environment, diet, lack of physical activity, and socioeconomic factors, while management focuses on promoting healthy lifestyle changes, and in some cases, medication or surgery.

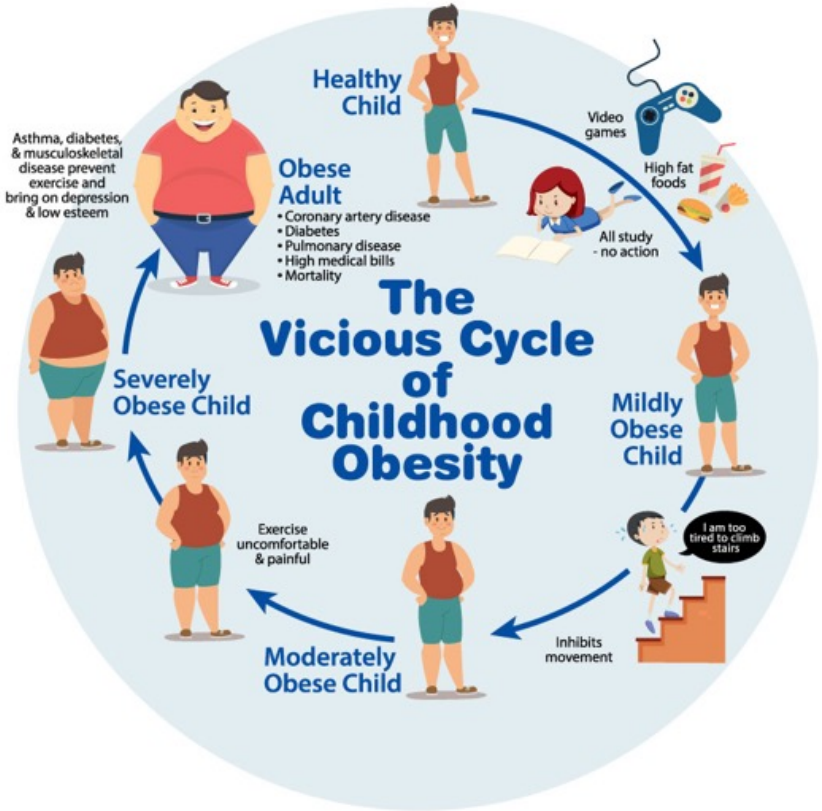

Useless ▶ # Parent-focused behavioural interventions for the prevention of early childhood obesity (TOPCHILD): a systematic review and individual participant data meta-analysis

Summary

Background Childhood obesity is a global public health issue, which has prompted governments to invest in prevention programmes. We aimed to investigate the effectiveness of parent-focused early childhood obesity prevention interventions globally.

Methods We did a systematic review and individual participant data meta-analysis. We searched databases and trial registries (MEDLINE, Embase, CENTRAL, CINAHL, PsycInfo, ClinicalTrials.gov, and WHO International Clinical Trials Registry Platform) from inception until Sept 30, 2024, for randomised controlled trials commencing before 12 months of age examining parent-focused behavioural interventions to prevent obesity in children, compared with usual care, no intervention, or attention control. Individual participant data were checked, harmonised, and assessed for integrity and risk of bias. We excluded trials that were quasi-randomised, investigated pregnancy-only interventions, or did not collect any child weight-related outcomes. The primary outcome was BMI Z score at age 24 months (±6 months). We did an intention-to-treat, two-stage, random effects meta-analysis to examine effects overall and for prespecified subgroups. We assessed certainty of evidence using Grading of Recommendations Assessment, Development, and Evaluation. This study is registered with PROSPERO, CRD42020177408.

Findings Of 19 990 identified records, 47 (0·24%) trials were completed and eligible. Of these, 18 (38%) assessed our primary outcome, BMI Z score. We obtained individual participant data for 17 (94%; n=9128) of these 18 trials (n=9383), representing 97% of eligible participants. Of these 9128 participants, 4549 (50%) were boys, 4415 (48%) were girls, and 164 (2%) had unknown sex. We found no evidence of an effect of interventions on BMI Z score at age 24 months (±6 months; mean difference –0·01 [95% CI –0·08 to 0·05]; high certainty evidence, τ^2=0·01; n=6505; 2623 missing). Findings were robust to prespecified sensitivity analyses (eg, different analysis methods and missing data), and we found no evidence of differential intervention effects for prespecified subgroups including priority populations and trial-level factors.

Useless ▶

Interpretation These findings indicate that examined parent-focused behavioural interventions are insufficient to prevent obesity at age 24 months (±6 months). This evidence highlights a need to re-think childhood obesity prevention approaches.

Funding Australian National Health and Medical Research Council.

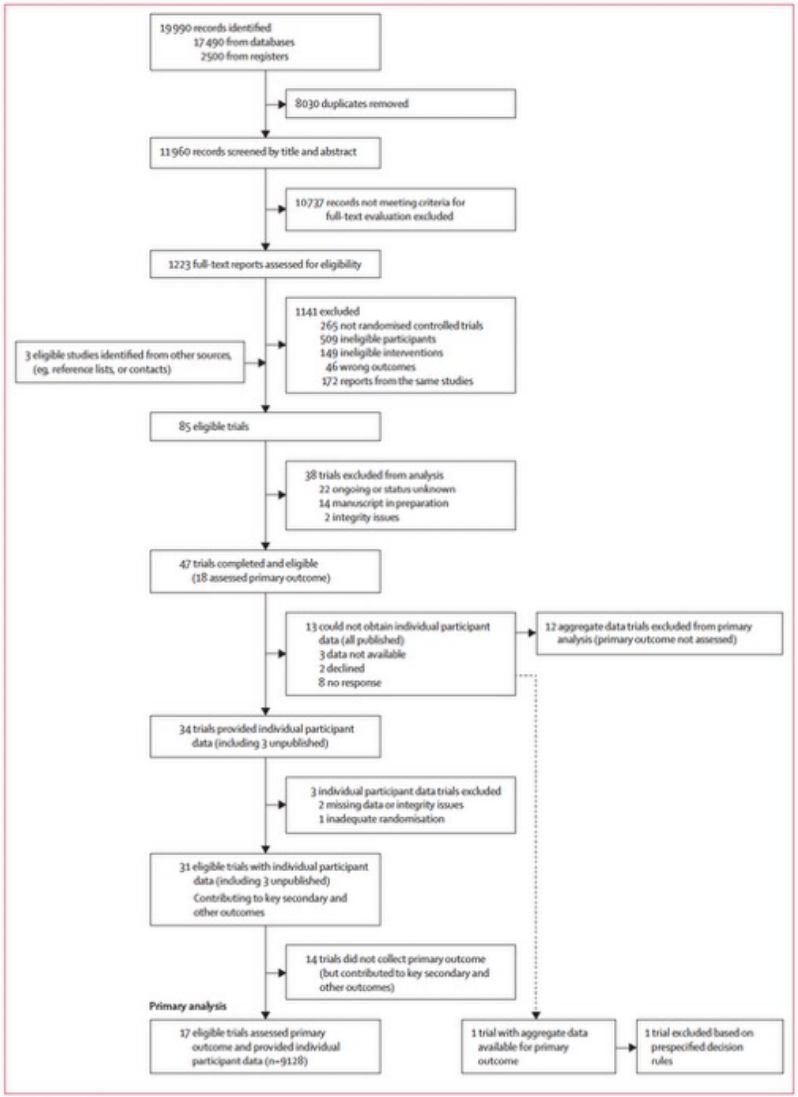

Figure 1: Study profile

	Dates	Sample size*	Unit of randomisation	Participants	Intervention period	Intervention	Control	Primary outcome
Trials contributing to primary outcome analysis, with or without secondary outcome analysis (n=17)								
Australia (Campbell et al 2013)[30]	2008-10	Randomly assigned: 542 Eligible: 542	Cluster	First-time parents regularly attending first-time parent group Parent groups were eligible if ≥8 parents were enrolled, or ≥6 parents were enrolled in areas of low socioeconomic position	Began within the first 6 months; ended by age 24 months	Six 2 h sessions delivered within pre-existing mothers' groups (age 3, 6, 9, 12, 15, and 18 months) Behaviours targeted: food provision and parent feeding practices and movement practices (n=271)	Usual care plus quarterly newsletter on general child health messages excluding sleep, food, and activity (n=271)	Dietary intake
Australia (Campbell et al 2016)[31]	2011-201	Randomly assigned: 514 Eligible: 514	Cluster	First-time parents with infants aged 3–4 months regularly attending a parent group in disadvantaged areas	Began within the first 6 months; ended by age 36 months	Six 1·5 h group sessions (age 3, 6, 9, 12, 15, and 18 months), then six quarterly newsletters (21, 24, 27, 30, 33, and 36 months) Behaviours targeted: food provision and parent feeding practices and movement practices (n=263)	Usual care plus quarterly generic child health newsletters (n=251)	Anthropometry: height, bodyweight, waist circumference, and BMI Z score at age 18 months and 36 months
Australia (Daniels et al 2013)[32]	2008-10	Randomly assigned: 698 Eligible: 698	Individual	First-time mothers of healthy term infants	Began at age 4–7 months; ended by age 16 months	Two education peer support modules (six fortnightly sessions each) at age 4–7 months and 13–16 months at community health venues Behaviours targeted: food provision and parent feeding practices and movement practices (n=346)	Usual care plus quarterly newsletter on general child health messages excluding sleep, food, and activity (n=352)	Food intake, food preferences, and feeding behaviour
Australia (Wen et al 2012)[33]	2007-10	Randomly assigned: 667 Eligible: 667	Individual	Women aged 16 or over, expecting their first child, in 24–34 weeks' pregnancy	Began during pregnancy; ended by age 24 months	Eight home visits providing maternal advice (antenatal and at age 1, 3, 5, 9, 12, 18, and 24 months) Behaviours targeted: infant feeding practices, food provision and parent feeding practices, and movement practices (n=337)	Usual care plus written home safety and tobacco prevention information sent by post at 6 months and 12 months (n=330)	BMI at age 2 years
Australia (Wen et al 2022)[34]	2017-20	Randomly assigned: 1155 Eligible: 1155	Individual	Women aged ≥16 years in their third trimester that can communicate in English, Chinese, or Arabic	Began during pregnancy; ended by age 24 months	Group 1 (telephone support): nine staged intervention booklets (posted) and nine 30–60 min telephone support sessions to mothers by Child & Family Health Nurses (third trimester, and at age 1, 3, 5, 7, 10, 12–15, 15–18, and 18–24 months; n=386) Group 2 (SMS): nine staged SMS interventions after posting intervention booklets Behaviours targeted: infant feeding practices, food provision and parent feeding practices, and movement practices (n=384)	Usual care comprising at least one nurse visit for general support at home and possible multiple home visits for vulnerable families from the local health districts (n=385)	BMI, breastfeeding duration, and timing of introduction of solids
Italy (Morandi et al 2019)[35]	2014-17	Randomly assigned: 529 Eligible: 529	Cluster (paediatrician)	Healthy term newborn babies	Began in the first 6 months; ended by age 24 months	Intensive education: at each well visit until child age 2 years, parents provided with oral and written information on obesity-protective behaviours for their children Behaviours targeted: infant feeding practices, food provision and parent feeding practices, and movement practices (n=278)	Usual education about nutrition and lifestyle, during their child's first 2 years of life (n=251)	BMI at age 2 years

(Table 1 continues on next page)

	Dates	Sample size*	Unit of randomisation	Participants	Intervention period	Intervention	Control	Primary outcome
(Continued from previous page)								
Netherlands (Kaissen et al 2021)[36]	2018-19†	Randomly assigned: 357 Eligible: 270	Individual	Parents with low or medium educational attainment with an infant aged 5-15 months	Began at age 5-15 months; ended after 12 months	Mobile application parenting programme, *Samen Happie!*, teaching parents about healthy parenting practices and general healthy authoritarian parenting style Behaviours targeted: food provision and parent feeding practices, movement practices, and sleep health practices (n=137)	Waiting list control (n=133)	BMI at 6 months and 12 months post baseline
New Zealand (Taylor et al 2017a)[37]	2009-17	Randomly assigned: 802 Eligible: 802	Individual	Women aged >16 years before 34 weeks' gestation; preterm infants born before 36·5 weeks excluded	Began during pregnancy; ended by age 24 months	Group 1 (food, activity and breastfeeding): mix of seven home visits and group-based sessions promoting breastfeeding, healthy eating, and physical activity (1 week, and age 3, 4, 7, 9, 12, and 18 months; n=214) Group 2 (sleep): two home visits (antenatal and 3 weeks) targeting prevention of sleep problems, as well as a sleep treatment programme if requested (age 6-24 months; n=209) Group 3: (food, activity and breastfeeding, and sleep) Behaviours targeted: infant feeding practices, food provision and parent feeding practices, movement practices, and sleep health practices (n=210)	Usual care: first 4-week midwife home visits Well Child (Plunkett) nurse: eight visits in 5 years (n=214)	Bodyweight at age 6, 12, and 24 months and BMI at age 24 months
New Zealand (Taylor et al 2017b)[38]	2012-16	Randomly assigned: 206 Eligible: 206	Individual	Pregnant women aged ≥16 years, before 34 weeks' gestation, who could communicate in English or Te Reo Maori; preterm infants excluded	Began during pregnancy; ended by age 12 months	Baby-led introduction to solids: lactation consultant support (three face-to-face sessions and two telephone sessions; 10-60 min each) up to age 6 months and three personalised face-to-face contacts (age 5·5, 7, and 9 months) Behaviours targeted: infant feeding practices, food provision, and parent feeding practices (n=105)	Usual Well Child care, usually 6-7 home or clinic visits (from age 6 weeks to 2 years) from a trained health professional (n=101)	BMI at age 12 months
Norway (Helle et al 2019)[39]	2015-21	Randomly assigned: 533 Eligible: 533	Individual	Parents and their child aged 3-5 months	Began at age 6 months; ended by age 12 months	eHealth intervention: access to website with seven monthly short video clips (3-5 min) addressing infant feeding topics and age-appropriate baby food recipes Behaviours targeted: food provision and parent feeding practices (n=269)	Usual care from the local child health clinic with consultations at child age 6, 8, 10, and 12 months (n=264)	Child eating behaviour, food intake, mealtime routines, and maternal feeding practices
Norway (Øverby et al 2017)[40]	2012-15	Randomly assigned: 110 Eligible: 110	Individual	Parents and their 4-6-month-old infants attending selected public health clinics	Began in the first 6 months; ended by age 6 months	Two 4-h course days providing parent groups with nutritional information and instruction to prepare nutritious and varied dishes, delivered by home economics teacher and Masters student Behaviours targeted: food provision and parent feeding practices (n=56)	Parents received a booklet containing recipes for homemade foods for infants (n=54)	Food intake at age 6, 15, and 24 months
Norway (Rød et al 2021)[41]	2015-22	Randomly assigned: 298 Eligible: 237	Individual	Infants close to age 12 months and one of their parents	Began in the first 12 months; ended by age 24 months	Food4toddlers eHealth intervention: website with seven modules (2-4 lessons approximately 10 min each) promoting healthy food and eating environments, recipes, discussion forum, information about food and beverages, plus 20 weekly emails with link to new lessons Behaviours targeted: food provision and parent feeding practices (n=148)	Usual care at the community child health centres (n=150)	Child diet quality and food variety, assessed at age 18 months and 24 months

(Table 1 continues on next page)

	Dates	Sample size*	Unit of randomisation	Participants	Intervention period	Intervention	Control	Primary outcome
(Continued from previous page)								
Sweden (Döring et al 2016)[50]	2008-15	Randomly assigned: 1369 Eligible: 1148	Cluster (child health-care centres)	First-time mothers and their children (aged 9-10 months) recruited at child health-care centres	Began in the first 12 months; ended by age 48 months	Nine sessions: one group (11 months), six individual (age 8-9 months, and 1, 1·5, 2, 3, and 4 years), two individual telephone sessions (age 2·5 years and 3·5 years) delivered by nurse focusing on healthy food habits and physical activity Behaviours targeted: food provision and parent feeding practices and movement practices (n=601)	Usual care: regular age-related health checkups of Swedish child health services (n=768)	BMI and waist circumference of children at age 4 years and their mothers
UK (Bryant et al 2021)[51]	2017-19	Randomly assigned: 117 Eligible: 28	Cluster (children's centres)	Parents or other carers and at least one child aged 6 months to 5 years	Began within the first 6 months to 5 years; ended after 8 weeks	8-week Health, Exercise, Nutrition for the Really Young programme, including eight weekly 2·5 h sessions delivered in children centres to groups of 8-10 parents Behaviours targeted: food provision and parent feeding practices and movement practices (n=47)	Waiting list control (n=70)	Feasibility and child BMI Z score
USA (Messito et al 2020)[56]	2012-20	Randomly assigned: 533 Eligible: 533	Individual	Latina mothers with a singleton uncomplicated pregnancy, fluent in English or Spanish	Began during pregnancy; ended by age 36 months	Starting Early Program: 15 sessions, two individual (third trimester and postpartum) and 13 group (age 1, 2, 4, 6, 9, 12, 15, 18, 21, 24, 27, 30, and 33 months), providing nutrition counselling and support Behaviours targeted: infant feeding practices and movement practices (n=266)	Usual care: one prenatal nutrition consultation, one childbirth or breastfeeding class, as-needed lactation support, and paediatric visits as per American Academy of Pediatrics guidelines (n=267)	Infant feeding practices and material infant feeding knowledge
USA (Paul et al 2018)[55]	2012-23	Randomly assigned: 291 Eligible: 291	Individual	Full-term singleton infants born to primiparous mothers	Began within the first 6 months; ended by age 36 months	Responsive parenting: four home visits by research nurses (age 3, 16, 28, and 40 weeks) and annual research centre visits until age 3 years, focused on feeding, sleep, interactive play, and emotion regulation Behaviours targeted: infant feeding practices, food provision and parent feeding practices, movement practices, and sleep health practices (n=145)	Home safety intervention (n=146)	BMI Z score at age 3 years
USA (Sanders et al 2021)[36]	2010-14	Randomly assigned: 865 Eligible: 865	Cluster (trial sites)	Infants presenting for 2-month well-child check-up, whose caregiver could speak Spanish or English	Began at age 2 months; ended by age 18 months	Greenlight toolkit: low literacy booklets that reviewed dietary, physical activity, sleep, and screentime advice for parents and education for providers on health communication Behaviours targeted: infant feeding practices, food provision and parent feeding practices, movement practices, and sleep health practices (n=459)	Attention placebo: injury prevention counselling according to The Injury Prevention Program by the American Academy of Pediatrics (n=406)	Percentage of children with overweight or obesity at age 2 years
Other trials contributing to secondary outcomes only (n=14)								
Belarus (Kramer et al 2001)[57]	1996-98	Randomly assigned: 17 046 Eligible: 17 046	Cluster (hospital and associated outpatient clinic)	Full-term singleton infants weighing at least 2500 g and their healthy mothers who intended to breastfeed	Began at birth; ended by age 12 months	Breastfeeding promotion and support according to the WHO's Baby Friendly Hospital Initiative at hospital and follow-up visits Behaviours targeted: infant feeding practices (n=8865)	Usual care (n=8181)	Breastfeeding (any and duration), gastrointestinal infection, respiratory tract infection, and atopic eczema during the first 12 months of life

(Table 1 continues on next page)

	Dates	Sample size*	Unit of randomisation	Participants	Intervention period	Intervention	Control	Primary outcome
(Continued from previous page)								
Brazil (Sangalli et al 2021)[68]	2008–10	Randomly assigned: 715 Eligible: 715	Cluster (health-care centre)	Pregnant women in their third trimester attending health centres predominantly serving low-income families	Began during pregnancy; ended by age 24 months	Breastfeeding promotion, introduction of foods, healthy eating and healthy eating habits, based on the Ten Steps for Healthy Feeding guideline Behaviours targeted: infant feeding practices, food provision and parent feeding practices (n=373)	Usual care (n=363)	Exclusive breastfeeding at age 4 months
UK (Lakshman et al 2018)[26]	2011–15	Randomly assigned: 669 Eligible: 669	Individual	Parents (mainly mothers) and their infants (aged 2–14 weeks) who were formula-fed	Began within the first 6 months; ended by age 6 months	Baby Milk programme supported mothers feeding their babies according to the WHO recommendations for energy requirements: three 30–45 min face-to-face contacts (at age 2, 4, and 6 months) and two 15–20-min telephone calls (at age 3 months and 5 months) and leaflets (at age 2 months and 4 months); involved components on motivation, setting goals and actions, and overcoming barriers Behaviours targeted: infant feeding practices (n=340)	Usual care group had the same number of contacts but received general information about formula-milk feeding and infant health (n=329)	The change in infant bodyweight SD score from birth to age 12 months
UK (McEachan et al 2016)[70]	2012–14	Randomly assigned: 120 Eligible: 120	Individual	Pregnant women with overweight or obesity (BMI ≥25 kg/m²) at 10–12 weeks' gestation and infants from birth	Began during pregnancy; ended by age 12 months	Healthy and Active Parenting Programme for Early Years aimed to promote breastfeeding, promote healthy eating and habits, and promote physical activity: delivered through 12 group sessions (six antenatal and six postnatal); the intervention was developed to be culturally appropriate for key groups (White British and South Asian origin women) Behaviours targeted: infant feeding practices, food provision and parent feeding practices, and movement practices (n=59)	Usual care (n=61)	Child bodyweight at age 12 months
USA (de la Haye et al 2019)[71]	2018–19	Randomly assigned: 50 Eligible: 50	Individual	Mother–child dyads enrolled in home visitation programmes—included mothers facing poverty, housing instability, lack of social and material support, lack of transportation, and limited education and literacy	Began after birth; ended after 6 months	Home visitation programme core curriculum with nutrition and physical activity enhancement: home visits (weekly for 6 months) Behaviours targeted: food provision and parent feeding practices and movement practices (n=30)	Healthy families America Home visitation programme: home visits (weekly, up to age 2–5 years)—a culturally sensitive programme to strengthen parent–child relationships, promote child development, and link to community resources (n=20)	Bodyweight of mothers, rate of weight gain of infants, and waist circumference of mother
USA (Fiks et al 2017)[31]	2014–15	Randomly assigned: 87 Eligible: 85	Individual	Pregnant women with overweight or obesity (BMI ≥25 kg/m²), Medicaid insured, and who owned a smartphone	Began during pregnancy; ended by age 12 months	Grow2Gether for healthy infant growth and behaviour: two in-person meetings (at enrolment and age 4 months) and 11 online group activities (two prenatally, and until age 9 months) Behaviours targeted: infant feeding practices, food provision and parent feeding practices, movement practices, and sleep health practices (n=43)	Parents received text message reminders to schedule recommended primary care visits for their infant, and to attend appointments scheduled in Children's Hospital of Philadelphia Care Network (n=42)	Feasibility

(Table 1 continues on next page)

	Dates	Sample size*	Unit of randomisation	Participants	Intervention period	Intervention	Control	Primary outcome
(Continued from previous page)								
USA (Linares et al 2019)[73]	2016–18	Randomly assigned: 39 Eligible: 39	Individual	Immigrant Hispanic pregnant women who intended to breastfeed their infants	Began during pregnancy; ended by age 6 months	Early Childhood Obesity Risk-Reduction Program in Hispanics culturally acceptable and linguistically diverse promotion of exclusive breastfeeding: prenatal sessions (40 min), prenatal calls (10 min), hospital visit (30 min), postpartum home visit (40 min), and postpartum calls (monthly, 10 min) Behaviours targeted: feeding practices (n=20)	Usual care provided by the Special Supplemental Nutritional for Women, Infants, and Children programme (n=19)	Exclusive breastfeeding from birth to age 6 months
USA (Palacios et al 2018)[74]	2016–16	Randomly assigned: 202 Eligible: 202	Block	Caregivers of healthy term infants aged 0–2 months participating in the WIC Program in Puerto Rico and Hawaii	Began within the first 2 months; ended after 4 months	Weekly text messages (for 4 months) reinforcing the feeding messages provided by WIC Behaviours targeted: infant feeding practices and food provision and parent feeding practices (n=102)	Control text messages were sent, relating to general infant's health (n=100)	Infant weight-for-length percentile
USA (Paul et al 2011)[75]	2006–09	Randomly assigned: 160 Eligible: 160	Individual	Mother-newborn baby dyads, primiparous, singleton, and gestational age ≥34 weeks	Began 2–3 weeks after birth; ended by age 6 months	SLIMTIME Nurse home visits (2–3 weeks after birth and at age 4–6 months) Group 1 (introduction to solids): instruction on delay of complementary foods and importance of repeat exposure to foods Behaviours targeted: infant feeding practices and food provision and parent feeding practices (n=38) Group 2 (soothe/sleep): parents were taught alternate strategies to feeding as an indiscriminate first response to infant distress Behaviours targeted: infant feeding practices and sleep health practices (n=39) Group 3 (soothe/sleep and introduction to solids): both Group 1 and Group 2 interventions Behaviours targeted: infant feeding practices, food provision and parent feeding practices, and sleep health practices (n=42)	Usual care (n=41)	Weight-for-length percentile at age 1 year
USA (Rybak et al 2023)[76]	2021–22	Randomly assigned: 65 Eligible: 65	Individual	Mothers of singleton infants born >2500 g, at 37–42 weeks' gestation, English-speaking, and attending a primary care practice primarily serving minority groups and low-income populations	Began at 1 month well-child visit; ended at 6-month well-child visit	A strengths-based responsive parenting intervention, teaching healthy responsive parenting during infancy to promote vital growth and regulation, delivered via Integrated Behavioral Health at well-child visits (at age 1, 2, 4, and 6 months) that helps caregivers recognise and respond to infant cues for hunger, fullness, and distress, emphasising non-feeding soothing strategies, responsive feeding practices, and sleep-promoting behaviours Behaviours targeted: infant feeding practices, food provision and parent feeding practices, and sleep health practices=33)	A socioemotional development and positive parenting intervention matched for time, attention, and level of provider, but without the specific active ingredients of the THRIVE intervention related to infant feeding, sleep, and regulation (n=32)	Feasibility (enrolment) and acceptability (retention and adherence)

(Table 1 continues on next page)

	Dates	Sample size*	Unit of randomisation	Participants	Intervention period	Intervention	Control	Primary outcome
(Continued from previous page)								
USA (Stough et al 2018; NCT03597061)	2018-20†	Randomly assigned: 34 Eligible: 32	Individual	Parents and infants born at >38 weeks' gestation, above 10th percentile of length-for-weight, and aged 2–3 months	Began at age 4 months; ended by age 9 months	Healthy Start to Feeding has three individual sessions providing parent education and skills training on responsive feeding approach to introduction of healthy foods Behaviours targeted: infant feeding practices and food provision and parent feeding practices (n=16)	Participants and their parents completed pre-treatment and post-treatment period study visits to assess study outcomes; they received no intervention (n=16)	Weight-for-length percentile, appetite regulation, and fruit and vegetable variety at age 3 months and 9 months
USA (Thomson et al 2018)[17]	2013-16	Randomly assigned: 82 Eligible: 54	Individual	Pregnant women at least 18 years of age, <19 weeks pregnant and their infant from birth, residing in a rural region with high rates of infants with low birthweight, preterm infants, child poverty, and childhood overweight/obesity	Began during pregnancy; ended by age 12 months	Parents as Teachers Experimental-group received the enhanced nutrition and physical activity lessons and materials, which follow the family wellbeing Parents as Teachers curriculum; the added maternal weight management and early childhood obesity prevention components are based on social cognitive theory and behaviour change; monthly lessons at in-home visits from gestational month 4 to age 12 months Behaviours targeted: infant feeding practices, food provision and parent feeding practices, movement practices, and sleep health practices (n=24)	Parents as Teachers curriculum, home visits, optional group sessions (monthly), developmental screenings, and resource network for families, which aimed to increase parental knowledge of child development, improve parenting, early detection of developmental delay, prevent abuse, and increase child reading (n=30)	Maternal outcomes: gestational bodyweight gain, bodyweight retention, dietary intake, and physical activity Infant outcomes: dietary at age 12 months
USA (Trak-Fellermeier et al 2019)[18]	2013-15	Randomly assigned: 31 Eligible: 31	Individual	Women with overweight/obesity, singleton pregnancy <16 weeks' gestation and their infant from birth, residing in Puerto Rico	Began during pregnancy; ended 6 days after birth	Health empowerment programme: individual visits, two visits (prenatal at around 16 weeks' and 27 weeks' gestation); group sessions, six 2 h sessions (starting 1–2 weeks after randomisation, occurring every 2 weeks); and telephone calls, six 30 min calls (monthly) Behaviours targeted: infant feeding practices, food provision and parent feeding practices, movement practices, and sleep health practices (n=15)	Group sessions with health advice about dental care and child safety (n=16)	Gestational bodyweight gain
USA (Wasser et al 2020)[19]	2013-17	Randomly assigned: 430 Eligible: 429	Individual (stratified)	Primiparous and multiparous non-Hispanic Black mothers enrolled at 28 weeks' pregnancy	Began during pregnancy; ended by age 12 months	Home visits: six visits by peer educators (prenatal <28 weeks' gestation and antenatal at age 1, 3, 6, 9, and 12 months); and maternal and study partner advice Behaviours targeted: infant feeding practices, food provision and parent feeding practices, movement practices, and sleep health practices (n=215)	Attention-control received maternal advice on injury prevention (n=214)	Infants' mean weight-for-length Z score at age 15 months

Allocation ratio was 1:1 for all trials. WIC=Women, Infants, and Children (a programme that supports high-risk, low-income populations). *Randomly assigned sample size represents the total number of participants randomly assigned in the trial. Eligible sample size represents the total number of participants randomised in the trial that met eligibility criteria for TOPCHILD (eg, Bryant and colleagues[16] randomly assigned 117 children aged 6 months to 5 years. Of these, 28 participants were randomly assigned before age 12 months and thus were eligible for TOPCHILD). †Main results unpublished at time of analysis.

Table 1: Characteristics of included studies (n=31)

	Trials	Participants	Intervention*	Control*†	Effect estimate (95% CI)	Heterogeneity, τ^2 (95% PI)	GRADE
Primary outcome							
BMI Z score at age 24 months (±6 months)	17	6505	0·71 (1·08)	0·72 (1·05)	Mean difference −0·01 (−0·08 to 0·05)	0·01 (−0·17 to 0·14)	High
Key secondary outcomes							
Duration of exclusive breastfeeding assessed at age 6 months (±2 months), weeks	5	1653	12·22 (9·32); 13 (10 to 13)‡	10·69 (8·86); 12 (8·69 to 13)‡	Hazard ratio 0·86 (0·74 to 1·00)	0·01 (0·65 to 1·14)	Moderate
Vegetable intake per day at age 24 months (±6 months), g	12	4616	117·18 (90·06)	107·48 (84·09)	Mean difference 3·11 (−0·64 to 6·85)	0·00 (−0·64 to 6·85)	Moderate
Screen time per day at age 24 months (±6 months), min	9	3650	59·58 (69·98)	72·36 (69·98)	Mean difference −9·60 (−13·72 to −5·47)	0·00 (−13·72 to −5·47)	Moderate
Physical activity per day at age 24 months (±6 months), min	1	314	252·59 (137·46)	276·60 (150·13)	Mean difference −24·14 (−57·17 to 8·90)	NA	Very low
Combined sleep duration per night and day at age 24 months (±6 months), h	10	3839	12·68 (1·53)	12·69 (1·57)	Mean difference 0·06 (−0·02 to 0·15)	0·002 (−0·06 to 0·18)	Moderate
Parent feeding practices, control (restriction) score ≥3 at age 24 months (±6 months)§	2	545	81/269 (30%)	91/276 (33%)	Risk ratio 0·90 (0·72 to 1·13)	0·00 (0·72 to 1·13)	Low

Data are n, n/N (%), mean (SD), or median (IQR), unless otherwise specified. GRADE=Grading of Recommendations Assessment, Development, and Evaluation. NA=not applicable. PI=prediction interval. *Means are crude estimates not adjusting for clustering by trial or centre. †For multi-arm trials, the approximate adjustment method was used to avoid unit-of-analysis errors that can be introduced when using the same control group for two different comparisons.[82] ‡Survival analysis performed for this outcome, thus survival median with 95% CI is reported. §Event defined as regular use of feeding practice—ie, domain score of at least 3.[82]

Table 2: **Primary and key secondary outcomes**

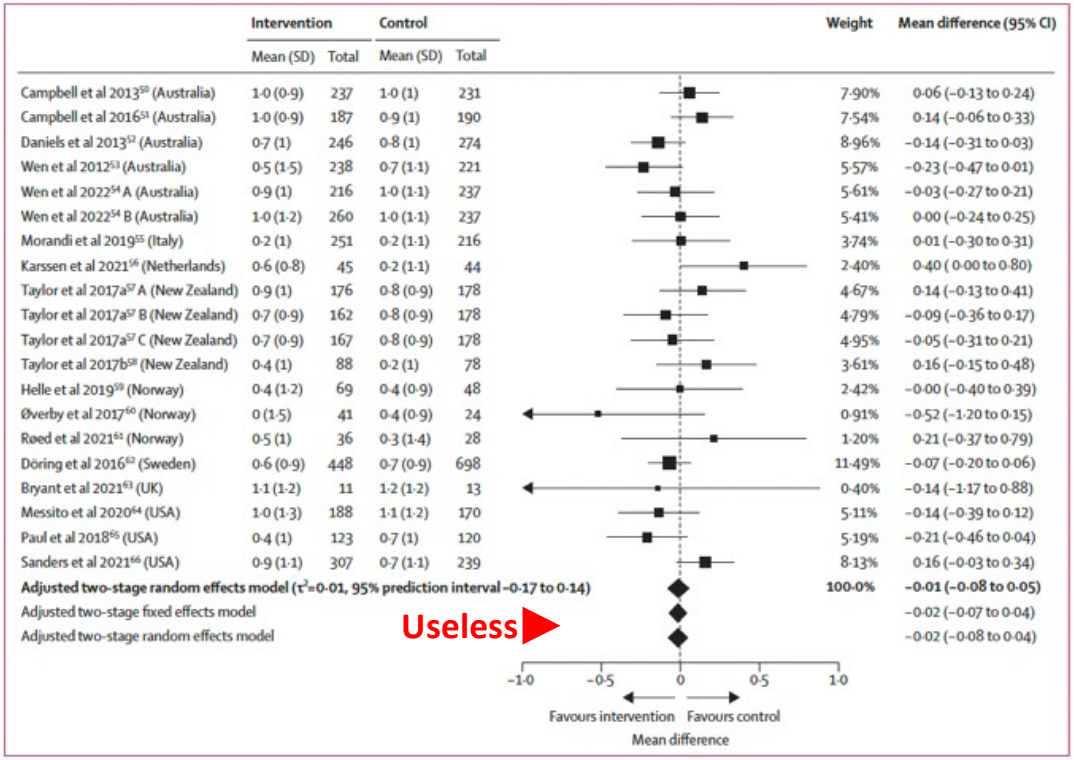

Figure 2: **Forest plot for the primary outcome of BMI Z score at age 24 months (or within 6 months either side)**
There are two multi-arm trials: Wen and colleagues[54] (2022) and Taylor and colleagues[57] (2017). Each group is indicated by A, B, or C after the study name. The black squares capture the intervention effect estimate. The 95% CIs around this estimate are represented by the black line. Lines with arrows indicate CIs that extend beyond the scale of the plot. The adjusted two-stage random effects model (bolded) presents the primary analysis. τ^2 is the variance of the between-study effects. The prediction interval represents the range within which the treatment effect in a future trial from a similar population is expected to fall. The adjusted two-stage fixed effects model and the adjusted one-stage random effects model are sensitivity analyses.

	Studies	Participants	Pooled interaction effect (95% CI)
Birthweight, 100 g	16	6222	0·01 (0·00 to 0·02)
Gestational age at birth, weeks	7	3751	0·02 (−0·01 to 0·06)
Maternal BMI, kg/m²	15	6025	−0·00 (−0·02 to 0·01)
Weighted standardised household income*	6	2301	0·14 (−0·07 to 0·36)

Data are n, unless otherwise indicated. For continuous subgroups, the pooled interaction effect is the difference in intervention effect after a one-unit increase in the covariate, assuming a linear relationship between the intervention and BMI Z score across all levels of the covariate (eg, the intervention increases BMI Z score by 0.01 for every 100-g increase in birthweight). A result is statistically significant if the 95% CI of the pooled interaction effect does not include 0. For each participant, weighted standardised household income was calculated as the difference between total household income per year at baseline and annual median country and year specific household income, divided by annual median country and year specific household income (appendix p 60). *0 indicates earning the median, greater than 0 indicates earning more than the median, and below 0 indicates earning less than the median.

Table 3: **Subgroup analyses by individual-level characteristics for the primary outcome of BMI Z score at age 24 months (or within 6 months either side), continuous individual-level factors**

	Studies	Participants	Floating subgroup-specific intervention effect (95% CI)	Pooled interaction effect (95% CI)
Any formal childcare attendance at age 0–12 months	4	1335		
No	4	1156	−0·05 (−0·20 to 0·09)	(reference)
Yes	4	179	0·08 (−0·48 to 0·64)	0·14 (−0·48 to 0·75)
Any formal childcare attendance at age 12–24 months	4	1025		
No	4	266	−0·02 (−0·37 to 0·34)	(reference)
Yes	4	759	−0·08 (−0·24 to 0·07)	−0·07 (−0·43 to 0·29)
Partner status	13	4714		
In a partnership (married, de facto, or living with partner)	13	4418	−0·01 (−0·08 to 0·07)	(reference)
Single (single, divorced, or widowed)	12	296	−0·20 (−0·48 to 0·07)	−0·19 (−0·48 to 0·09)
Parity or first-time parent	12	5330		
First-time parent	12	4221	−0·05 (−0·13 to 0·03)	(reference)
Already has at least one other child	8	1109	0·06 (−0·10 to 0·22)	0·11 (−0·07 to 0·30)
Parent or carer immigration status	7	3636		
Primary parent or carer born in trial country	7	2512	0·01 (−0·11 to 0·13)	(reference)
Primary parent or carer born outside trial country	7	1124	−0·02 (−0·21 to 0·18)	−0·03 (−0·30 to 0·25)
Infant sex	17	6505		
Male	17	3287	0·01 (−0·07 to 0·10)	(reference)
Female	17	3218	−0·04 (−0·12 to 0·04)	−0·05 (−0·16 to 0·05)
Ambiguous or other	0	0	..	..
Carer education	12	4848		
Low education	9	414	0·09 (−0·26 to 0·44)	0·11 (−0·24 to 0·46)
High-school graduate	12	994	0·02 (−0·12 to 0·16)	0·03 (−0·13 to 0·20)
Non-university tertiary education or incomplete university	10	776	−0·04 (−0·18 to 0·11)	−0·02 (−0·19 to 0·16)
University graduate or postgraduate	12	2664	−0·02 (−0·10 to 0·06)	(reference)
Carer employment	15	5598		
Any employment (including paid leave)	15	2738	0·03 (−0·07 to 0·12)	(reference)
Unemployed (includes retired, student without employment, unpaid leave, home duties, or charity work)	15	2860	−0·04 (−0·13 to 0·06)	−0·06 (−0·19 to 0·06)

For categorical subgroups, the pooled interaction is the difference in intervention effect between the comparator and reference subgroup (eg, the intervention reduces BMI Z score by 0·19 for those without a partner compared with those who do have a partner). A result is statistically significant if the 95% CI of the pooled interaction effect does not include zero. Floating subgroup-specific intervention effects can be interpreted as the intervention effect that is specific to their respective subgroup (eg, the intervention reduces BMI Z score by 0·01 for those with a partner and by 0·20 for those without a partner. If the pooled interaction effect is not significant, the subgroup-specific intervention effects are not interpreted as statistically different.

Table 4: **Subgroup analyses by individual-level characteristics for the primary outcome of BMI Z score at age 24 months (±6 months), categorical individual-level subgroups**

	Studies	Participants	Test of subgroup differences, χ^2	p value
Setting (home, community, or combination)	17	6505	0·57	0·75
In-person delivery (yes or no)	17	6505	0·96	0·33
Intervention mode (individual, group, or both)	17	6505	3·47	0·18
Intervention onset (antenatal or postnatal)	17	6505	0·32	0·57

Data are n, unless otherwise indicated.

Table 5: **Subgroup analyses of trial-level characteristics for the primary outcome of BMI Z score at age 24 months (or within 6 months either side), categorical trial-level characteristics**

	Studies	Participants	Meta-regression slope estimate (95% CI)
Intervention duration, h	15	6263	−0·010 (−0·023 to 0·004)
Development of country, human development index	17	6505	−0·70 (−6·43 to 5·04)
Intervention end, months	15	6239	0·0005 (−0·0056 to 0·0066)

Data are n, unless otherwise indicated.

Table 6: **Subgroup analyses of trial-level characteristics for the primary outcome of BMI Z score at age 24 months (±6 months), continuous trial-level characteristics**

Research in context

Evidence before this study

Although there have been several reviews of trials of childhood obesity prevention, few have focused on infancy, and many are narrative. A Cochrane review of obesity prevention interventions in children aged 0–18 years found that combined diet and physical activity interventions led to a small reduction in BMI Z score in children aged 0–5 years (mean difference −0·07 [95% CI −0·14 to −0·01]). However, this review was limited by reliance on published aggregate data, precluding outcome harmonisation and in-depth subgroup analyses. Updates to this review only examined interventions in age groups older than 2 years. The Early Prevention of Obesity in Children (EPOCH) Collaboration did an individual participant data prospective meta-analysis of four Australian and New Zealand randomised controlled trials. The authors found that parent-focused behavioural interventions for the prevention of early childhood obesity resulted in a small reduction in BMI Z score at age 18–24 months, compared with usual care (−0·12 SDs [95% CI −0·22 to −0·02]). However, this difference was no longer statistically significant when accounting for missing data, and there was insufficient power for subgroup analyses. More studies in a global context were needed to confirm this finding and explore differential effects across key subgroups, including priority populations susceptible to obesity (eg, individuals with lower education or income levels and immigrants), with sufficient statistical power.
We searched databases and trial registries (MEDLINE, Embase, CENTRAL, CINAHL, PsycInfo, ClinicalTrials.gov, and WHO International Clinical Trials Registry Platform) from inception up to Sept 30, 2024, without language restrictions, to identify randomised controlled trials investigating the effectiveness of obesity prevention interventions commencing antenatally or during infancy. The search strategy included terms related to weight (eg, "obes*", "overweight", "body mass index", and "adiposity"); behavioural interventions (eg, "behavio?r*", "diet*", "physical activity", "sleep", and "feeding"); children, parents, and families (eg, "child", "infan*", "pregnan*", "prenatal", and "parent$"); and study design (eg, "randomi#ed").

Added value of this study

This is the largest systematic review with an individual participant data meta-analysis in the field to date, including 31 trials set across ten countries with 28 825 participants. Of 18 eligible completed trials that assessed our primary outcome (BMI Z score at age 24 months [±6 months]), we obtained individual participant data for 17 (94%), including 9128 participants (97% of 9383 eligible participants). We used rigorous data checking, harmonisation, and integrity and risk-of-bias assessments enhanced by the availability of individual participant data and collaboration with trial representatives to create a global dataset. Access to original data enhanced statistical power and enabled advanced and complex analyses, including examination of important obesity-susceptible subgroups. The resulting high-quality TOPCHILD dataset provided robust evidence to address our research questions. Here we report findings for the primary outcome, BMI Z score, and for 33 prespecified secondary anthropometric and behavioural outcomes.

Useless

Implications of all the available evidence

This large individual participant data meta-analysis provides evidence that existing approaches to parent-focused behavioural interventions delivered up to 12 months of age are insufficient to affect BMI Z score at age 24 months (or within 6 months either side) or key obesity-related behavioural outcomes covering diet, feeding, physical activity, sleep, and parenting. These findings underscore the need to rethink current behavioural approaches to prevent obesity in early childhood.

Noncommunicable diseases (NCDs) are illnesses that are not transmissible from person to person, typically characterized by long-term health consequences and often linked to lifestyle and environmental factors. The leading NCDs worldwide include cardiovascular diseases, cancers, chronic respiratory diseases, and diabetes, which collectively cause the majority of global deaths. Key risk factors for NCDs are tobacco use, unhealthy diets, physical inactivity, harmful alcohol use, and air pollution, and many NCDs, like heart disease and type 2 diabetes, can be prevented

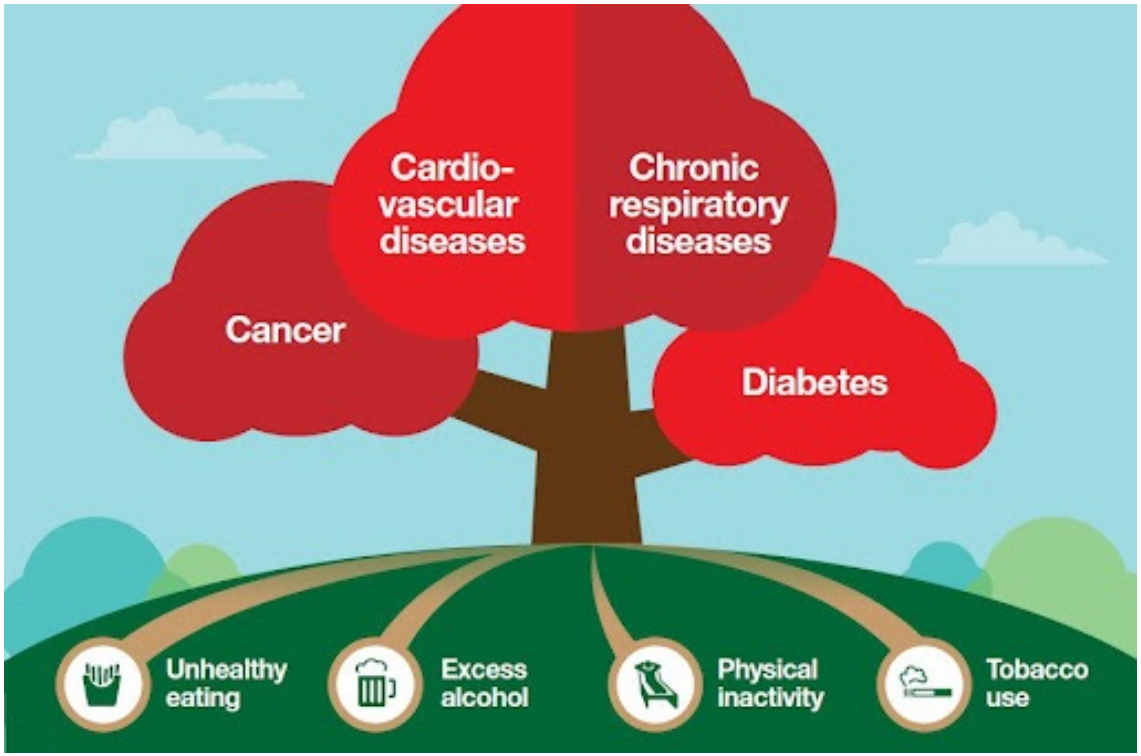

Benchmarking progress in non-communicable diseases: a global analysis of cause-specific mortality from 2001 to 2019

Summary

Background Non-communicable diseases (NCDs) have received substantial policy attention globally and in most countries. Our aim was to quantify how much NCD mortality changed from 2010 to 2019 in different countries, especially compared with the preceding decade and with the best-performing country in each region, and the specific NCD causes of death that contributed to change.

Methods We used data on NCD mortality by sex, age group, and underlying cause of death for 185 countries and territories from the 2021 WHO Global Health Estimates. Our primary outcome was the probability of dying from an NCD between birth and age 80 years in the absence of competing causes of death, and was calculated using age-specific death rates from NCDs and lifetable methods. We calculated change in the probability of death as the difference between values in the final and first year of each period (2001–10 and 2010–19). For 51 countries with high-quality mortality data and 12 countries with large populations within their region, we used the Horiuchi method of decomposition to calculate how much specific causes of death and 5-year age groups contributed towards: (1) increases or decreases in NCD mortality from 2010 to 2019; (2) improvements or deteriorations compared with the preceding decade (2001–10); and (3) differences from the country that had the largest reduction in each region.

Findings From 2010 to 2019, the probability of dying from an NCD between birth and age 80 years decreased in 152 (82%) of 185 countries for females and in 147 (79%) countries for males; it increased in the remaining 33 (18%) countries for females and 38 (21%) countries for males. The countries where NCD mortality declined for females accounted for 72% of the world female population in 2019, and those where NCD mortality declined for males accounted for 73% of the world male population. NCD mortality declined in all high-income western countries, with Denmark experiencing the largest decline for both sexes and the USA experiencing the smallest decline. Among the largest countries in other regions, NCD mortality declined for both sexes in China, Egypt, Nigeria, Russia, and Brazil, and increased for both sexes in India and Papua New Guinea. On average, females in countries in the central Asia, Middle East and north Africa region had the greatest reduction in NCD mortality followed by those in central and eastern Europe. For males, the largest reduction was among countries in central and eastern Europe, followed by those in central Asia, Middle East and north Africa. The smallest declines were those in the Pacific Island nations. Circulatory diseases were the greatest contributors to declines in NCD mortality from 2010 to 2019 in most countries, with some cancers (eg, stomach and colorectal cancers for both sexes, cervical and breast cancers for females, and lung and prostate cancers for males) also contributing towards lower NCD mortality in 2019 than in 2010 in many countries. Neuropsychiatric conditions and pancreatic and liver cancers contributed towards higher NCD mortality from 2010 to 2019 in most countries. In some countries, NCD mortality in working and older (≥65 years) ages changed in the same direction leading to large overall declines or increases; in others, it changed in opposite directions, diminishing the magnitude of the overall change. In 75 (41%) of 185 countries for females and in 73 (39%) countries for males, the change in NCD mortality from 2010 to 2019 was an improvement (ie, larger decline, smaller increase, or reversal of an increase) compared with the change from 2001 to 2010. These countries accounted for 29% and 63% of the world female and male population, respectively, and included both sexes in Russia and Egypt, and males in China, India, and Brazil. Decadal changes saw a deterioration (ie, smaller decline, larger increase, or reversal of a decline) in the remaining 110 (59%) countries for females and 112 (61%) countries for males, including in both sexes in the USA, Nigeria, and Papua New Guinea, and females in China, India, and Brazil. Change from 2010 to 2019 saw deterioration in direction or size compared with the preceding decade for both sexes in most high-income western countries, most countries in Latin America and the Caribbean, and in east and southeast Asia, and for females in south Asia. There was a decadal improvement in the direction or size of change for many countries in central and eastern Europe (eg, Russia) and central Asia, and in parts of the Middle East and north Africa. Improvements or deteriorations in the direction or size of change in NCD mortality between the two decades resulted from multiple NCD causes of death. Among causes of death, the decline in mortality from circulatory diseases was smaller from 2010 to 2019 than from 2001 to 2010 in most countries, except in countries in central and eastern Europe and some countries in central Asia, where these declines were larger from 2010 to 2019 than from 2001 to 2010. Change in lung cancer saw a decadal improvement in many countries, especially for males, and many other cancers saw a mix of improvement and deterioration.

Interpretation From 2010 to 2019, NCD mortality declined in four of every five countries in the world. These improvements were not as large as the preceding decade for most countries, driven by smaller declines in mortality from multiple NCDs.

	Data quality	Probability of dying from an NCD between birth and age 80 years (percent)			Change in probability of dying from an NCD between birth and age 80 years (percentage points)	
		2001	2010	2019	2001–10	2010–19
Faster decline from 2010 to 2019 compared with from 2001 to 2010						
Azerbaijan	Very low	62·1	60·1	42·1	−2·1	−18·0
Qatar	Very low	64·9	58·9	43·4	−6·1	−15·5
Uzbekistan	Medium	77·3	73·8	58·6	−3·6	−15·2
Moldova	High	67·0	62·1	47·4	−4·9	−14·8
Mongolia	High	66·3	61·1	49·7	−5·2	−11·3
Kuwait	Low	35·5	31·6	20·4	−3·9	−11·2
Tajikistan	Low	60·4	60·4	49·3	−0·0	−11·1
Kazakhstan	High	61·1	55·0	44·4	−6·1	−10·6
Kyrgyzstan	High	60·9	54·2	44·0	−6·7	−10·2
Palestine	Low	55·5	55·2	45·7	−0·3	−9·5
Russia	High	57·8	50·7	41·5	−7·0	−9·2
Belarus	High	54·8	48·6	39·4	−6·1	−9·2
Oman	Very low	52·9	52·4	43·6	−0·5	−8·8
Armenia	High	51·6	47·2	38·7	−4·5	−8·4
Ukraine	High	55·4	51·6	43·7	−3·8	−7·9
Serbia	Medium	56·0	50·7	43·1	−5·3	−7·6
Slovakia	High	46·1	39·7	32·6	−6·5	−7·1
Denmark	High	41·2	34·3	27·3	−6·9	−6·9
Latvia	High	48·2	42·6	35·7	−5·6	−6·9
Colombia	High	40·6	34·7	28·5	−5·9	−6·2
Croatia	High	43·6	37·7	31·8	−5·8	−6·0
Türkiye	Medium	42·3	40·7	34·9	−1·6	−5·8
Lithuania	High	42·2	38·5	32·8	−3·7	−5·7
Ecuador	Medium	37·8	34·8	29·6	−3·1	−5·2
Guyana	Medium	59·7	59·0	54·1	−0·7	−5·0
Ghana	Very low	55·2	53·9	49·7	−1·2	−4·2
Chile	High	33·2	31·2	27·2	−1·9	−4·0
Sri Lanka	Medium	42·6	39·5	35·5	−3·1	−3·9
Indonesia	Very low	57·5	56·4	52·7	−1·1	−3·7
Iceland	High	29·9	27·3	23·8	−2·6	−3·5
Mexico	High	41·9	41·0	37·6	−0·9	−3·4
Bangladesh	Very low	45·6	44·4	41·2	−1·2	−3·2
Algeria	Very low	41·4	39·0	35·9	−2·4	−3·1
Guinea-Bissau	Very low	60·9	58·1	55·0	−2·8	−3·1
Bolivia	Very low	53·6	51·5	48·6	−2·1	−3·0
DR Congo	Very low	59·2	59·2	56·5	−0·0	−2·6
Haiti	Very low	73·8	71·8	69·2	−2·0	−2·6
Iraq	Low	52·9	50·5	48·0	−2·3	−2·6
Benin	Very low	52·1	52·0	49·7	−0·0	−2·3
Morocco	Very low	55·0	54·7	52·7	−0·3	−2·1
Togo	Very low	57·6	56·9	55·0	−0·7	−1·9
Namibia	Very low	52·1	51·7	49·9	−0·3	−1·8
Cameroon	Very low	55·4	55·3	53·6	−0·0	−1·7
Timor-Leste	Very low	52·5	52·1	50·4	−0·4	−1·6
Eritrea	Very low	63·3	62·1	60·5	−1·2	−1·6
Burkina Faso	Very low	55·1	54·7	53·4	−0·4	−1·3
Declining from 2010 to 2019 after increasing from 2001 to 2010						
Albania	Low	36·3	43·8	29·6	7·6	−14·2
Botswana	Very low	42·0	55·4	46·1	13·4	−9·3
Georgia	Medium	49·4	49·6	40·3	0·1	−9·3
Eswatini	Very low	63·2	69·9	62·8	6·7	−7·0
South Africa	Medium	41·0	52·3	45·5	11·3	−6·8
North Korea	Very low	50·9	52·8	47·4	1·9	−5·4
Egypt	Low	55·3	56·0	51·6	0·7	−4·4
Zimbabwe	Very low	55·3	70·1	66·8	14·8	−3·2
Fiji	Low	66·4	66·8	64·0	0·5	−2·8
Liberia	Very low	55·3	57·3	54·7	1·9	−2·6
Sierra Leone	Very low	55·5	59·9	57·3	4·3	−2·6
Viet Nam	Very low	43·1	43·9	39·4	0·8	−2·5
Côte d'Ivoire	Very low	43·1	52·5	50·6	9·4	−1·9
Nicaragua	High	34·1	35·0	33·1	0·9	−1·9
Paraguay	Medium	37·0	39·1	37·2	2·1	−1·8
Guinea	Very low	55·7	58·1	56·3	2·4	−1·8
Kiribati	Low	68·7	68·8	67·2	0·1	−1·6
Chad	Very low	54·0	55·6	54·1	1·6	−1·5
Solomon Islands	Low	61·9	66·5	65·1	4·6	−1·5
Tonga	Very low	49·5	49·8	48·6	0·3	−1·3
Barbados	Low	42·3	42·7	42·2	0·3	−0·5
Libya	Very low	47·6	48·6	48·5	1·0	−0·1
Slower increase from 2010 to 2019 compared with from 2001 to 2010						
Kenya	Very low	39·2	47·2	48·2	8·1	1·0
Lesotho	Very low	45·7	68·2	69·7	22·5	1·5
Honduras	Very low	49·6	51·8	53·7	2·2	1·9
Dominican Republic	Low	33·7	34·3	36·4	2·6	2·1
Grenada	Medium	45·0	47·8	49·9	2·8	2·1
Guatemala	High	36·2	40·8	43·1	4·6	2·3
Mozambique	Very low	44·0	53·5	56·5	9·5	3·0

Central Asia, Middle East and north Africa
Central and eastern Europe
East and southeast Asia
High-income western
Latin America and the Caribbean
Pacific Island nations
South Asia
Sub-Saharan Africa

Figure 1: **Countries showing improvements in the direction or size of change from 2010 to 2019 compared with from 2001 to 2010 for females**
Estimates are shown for all countries and territories in eight reporting regions. Countries are divided into three categories of changes observed across two timeframes (2001–10 and 2010–19). Within each of the three categories, countries are ordered by percentage point change from 2010 to 2019 (ie, the first country listed in each category had the largest decrease or smallest increase from 2010 to 2019 within its category). For the estimated probabilities and change in probabilities with uncertainty intervals see the appendix (pp 44–53). For results based on cancers, cardiovascular diseases, chronic respiratory diseases, and diabetes in ages 30–70 years see the appendix (pp 13–14). NCD=non-communicable disease.

Panel 1: Key findings

- NCD mortality declined in approximately 80% of the world's countries, where more than 70% of the world population resided, from 2010 to 2019
- In approximately 60% of countries, the decline from 2010 to 2019 was smaller than it had been in the preceding decade or there was a reversal of the earlier decline
- Within all regions, there were substantial performance gaps between the regional frontrunner and other countries in terms of how much NCD mortality declined from 2010 to 2019
- National performance in reducing NCD mortality from 2010 to 2019 was rarely dominated by one NCD and often resulted from a combination of changes in multiple NCDs
- In some countries, NCD mortality in working and older ages changed in the same direction, leading to large overall declines or increases; in others, it changed in opposite directions, diminishing the magnitude of the overall change

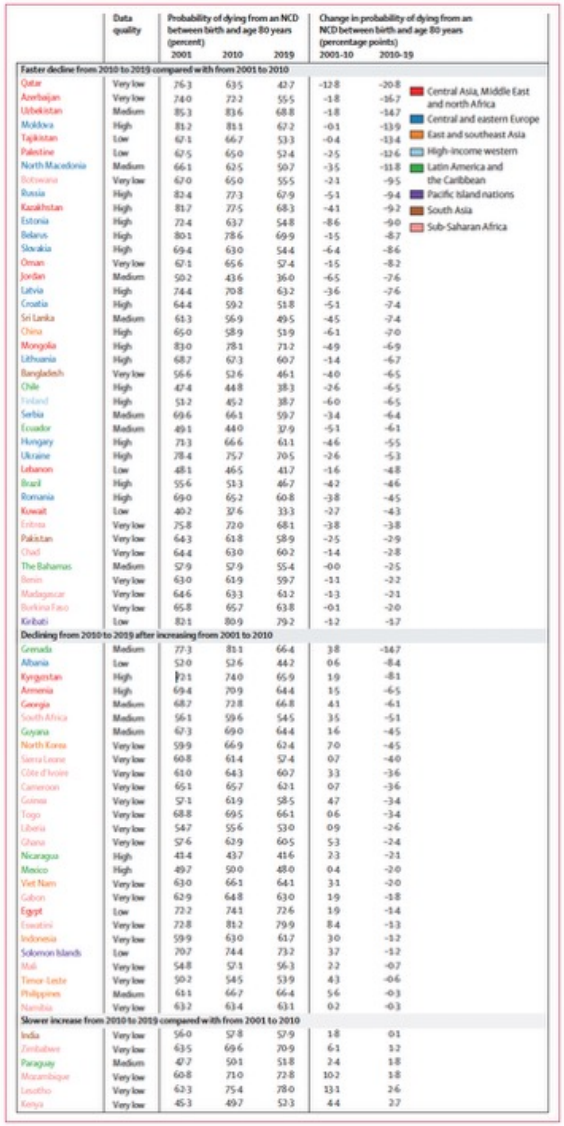

	Data quality	Probability of dying from an NCD between birth and age 80 years (percent)			Change in probability of dying from an NCD between birth and age 80 years (percentage points)	
		2001	2010	2019	2001–10	2010–19
Faster decline from 2010 to 2019 compared with from 2001 to 2010						
Qatar	Very low	76·3	63·5	42·7	-12·8	-20·8
Azerbaijan	Very low	74·0	72·2	55·5	-1·8	-16·7
Uzbekistan	Medium	85·3	83·6	68·8	-1·8	-14·7
Moldova	High	81·2	81·1	67·2	-0·1	-13·9
Tajikistan	Low	67·1	66·7	53·3	-0·4	-13·4
Palestine	Low	67·5	65·0	52·4	-2·5	-12·6
North Macedonia	Medium	66·1	62·5	50·7	-3·5	-11·8
Botswana	Very low	67·0	65·0	55·5	-2·1	-9·5
Russia	High	82·4	77·3	67·9	-5·1	-9·4
Kazakhstan	High	81·7	77·5	68·3	-4·1	-9·2
Estonia	High	72·4	63·7	54·8	-8·6	-9·0
Belarus	High	80·1	78·6	69·9	-1·5	-8·7
Slovakia	High	69·4	63·0	54·4	-6·4	-8·6
Oman	Very low	67·1	65·6	57·4	-1·5	-8·2
Jordan	Medium	50·2	43·6	36·0	-6·5	-7·6
Latvia	High	74·4	70·8	63·2	-3·6	-7·6
Croatia	High	64·4	59·2	51·8	-5·1	-7·4
Sri Lanka	Medium	61·3	56·9	49·5	-4·5	-7·4
China	High	65·0	58·9	51·9	-6·1	-7·0
Mongolia	High	83·0	78·1	71·2	-4·9	-6·9
Lithuania	High	68·7	67·3	60·7	-1·4	-6·7
Bangladesh	Very low	56·6	52·6	46·1	-4·0	-6·5
Chile	High	47·4	44·8	38·3	-2·6	-6·5
Finland	High	51·2	45·2	38·7	-6·0	-6·5
Serbia	Medium	69·6	66·1	59·7	-3·4	-6·4
Ecuador	Medium	49·1	44·0	37·9	-5·1	-6·1
Hungary	High	71·3	66·6	61·1	-4·6	-5·5
Ukraine	High	78·4	75·7	70·5	-2·6	-5·3
Lebanon	Low	48·1	46·5	41·7	-1·6	-4·8
Brazil	High	55·6	51·3	46·7	-4·2	-4·6
Romania	High	69·0	65·2	60·8	-3·8	-4·5
Kuwait	Low	40·2	37·6	33·3	-2·7	-4·3
Eritrea	Very low	75·8	72·0	68·1	-3·8	-3·8
Pakistan	Very low	64·3	61·8	58·9	-2·5	-2·9
Chad	Very low	64·4	63·0	60·2	-1·4	-2·8
The Bahamas	Medium	57·9	57·9	55·4	-0·0	-2·5
Benin	Very low	63·0	61·9	59·7	-1·1	-2·2
Madagascar	Very low	64·6	63·3	61·2	-1·3	-2·1
Burkina Faso	Very low	65·8	65·7	63·8	-0·1	-2·0
Kiribati	Low	82·1	80·9	79·2	-1·2	-1·7
Declining from 2010 to 2019 after increasing from 2001 to 2010						
Grenada	Medium	77·3	81·1	66·4	3·8	-14·7
Albania	Low	52·0	52·6	44·2	0·6	-8·4
Kyrgyzstan	High	72·1	74·0	65·9	1·9	-8·1
Armenia	High	69·4	70·9	64·4	1·5	-6·5
Georgia	Medium	68·7	72·8	66·8	4·1	-6·1
South Africa	Medium	56·1	59·6	54·5	3·5	-5·1
Guyana	Medium	67·3	69·0	64·4	1·6	-4·5
North Korea	Very low	59·9	66·9	62·4	7·0	-4·5
Sierra Leone	Very low	60·8	61·4	57·4	0·7	-4·0
Côte d'Ivoire	Very low	61·0	64·3	60·7	3·3	-3·6
Cameroon	Very low	65·1	65·7	62·1	0·7	-3·6
Guinea	Very low	57·1	61·9	58·5	4·7	-3·4
Togo	Very low	68·8	69·5	66·1	0·6	-3·4
Liberia	Very low	54·7	55·6	53·0	0·9	-2·6
Ghana	Very low	57·6	62·9	60·5	5·3	-2·4
Nicaragua	High	41·4	43·7	41·6	2·3	-2·1
Mexico	High	49·7	50·0	48·0	0·4	-2·0
Viet Nam	Very low	63·0	66·1	64·1	3·1	-2·0
Gabon	Very low	62·9	64·8	63·0	1·9	-1·8
Egypt	Low	72·2	74·1	72·6	1·9	-1·4
Eswatini	Very low	72·8	81·2	79·9	8·4	-1·3
Indonesia	Very low	59·9	63·0	61·7	3·0	-1·2
Solomon Islands	Low	70·7	74·4	73·2	3·7	-1·2
Mali	Very low	54·8	57·1	56·3	2·2	-0·7
Timor-Leste	Very low	50·2	54·5	53·9	4·3	-0·6
Philippines	Medium	61·1	66·7	66·4	5·6	-0·3
Namibia	Very low	63·2	63·4	63·1	0·2	-0·3
Slower increase from 2010 to 2019 compared with from 2001 to 2010						
India	Very low	56·0	57·8	57·9	1·8	0·1
Zimbabwe	Very low	63·5	69·6	70·9	6·1	1·2
Paraguay	Medium	47·7	50·1	51·8	2·4	1·8
Mozambique	Very low	60·8	71·0	72·8	10·2	1·8
Lesotho	Very low	62·3	75·4	78·0	13·1	2·6
Kenya	Very low	45·3	49·7	52·3	4·4	2·7

Central Asia, Middle East and north Africa
Central and eastern Europe
East and southeast Asia
High-income western
Latin America and the Caribbean
Pacific Island nations
South Asia
Sub-Saharan Africa

Figure 2: **Countries showing improvements in the direction or size of change from 2010 to 2019 compared with from 2001 to 2010 for males**
Estimates are shown for all countries and territories in eight reporting regions. Countries are divided into three categories of changes observed across two timeframes (2001–10 and 2010–19). Within each of the three categories, countries are ordered by percentage point change from 2010 to 2019 (ie, the first country listed in each category had the largest decrease or smallest increase from 2010 to 2019 within its category). For the estimated probabilities and change in probabilities with uncertainty intervals see the appendix (pp 44–53). For results based on cancers, cardiovascular diseases, chronic respiratory diseases, and diabetes in ages 30–70 years see the appendix (pp 13–14). NCD=non-communicable disease.

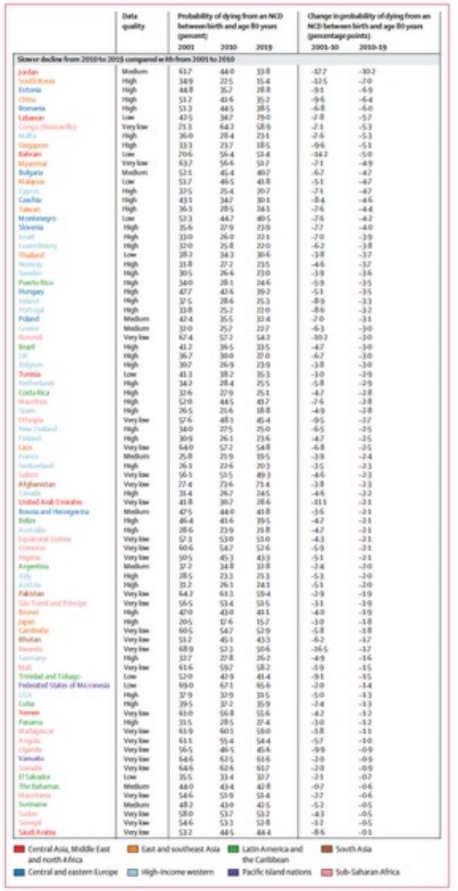

	Data quality	Probability of dying from an NCD between birth and age 80 years (percent)			Change in probability of dying from an NCD between birth and age 80 years (percentage points)	
		2001	2010	2019	2001–10	2010–19
Slower decline from 2010 to 2019 compared with from 2001 to 2010						
Jordan	Medium	63·7	44·0	33·8	−19·7	−10·2
South Korea	High	34·9	22·5	15·4	−12·5	−7·0
Estonia	High	44·8	35·2	28·8	−9·5	−6·4
China	High	53·2	43·6	35·2	−9·6	−8·4
Romania	High	53·3	44·5	38·5	−8·8	−6·0
Lebanon	Low	47·5	34·7	29·0	−12·8	−5·7
Congo (Brazzaville)	Very low	71·3	64·2	58·9	−7·1	−5·3
Malta	High	36·0	28·4	23·1	−7·6	−5·3
Singapore	High	33·1	23·7	18·5	−9·4	−5·1
Bahrain	Low	70·6	56·4	53·4	−14·2	−3·0
Myanmar	Very low	63·7	56·6	53·7	−7·1	−4·9
Bulgaria	Medium	52·1	45·4	40·7	−6·7	−4·7
Malaysia	Low	53·7	46·5	41·8	−5·1	−4·7
Cyprus	High	37·5	25·4	20·7	−7·1	−4·7
Czechia	High	43·1	34·7	30·5	−8·4	−4·6
Taiwan	High	36·1	28·5	24·1	−7·6	−4·4
Montenegro	Low	52·3	44·7	40·5	−7·6	−4·2
Slovenia	High	35·6	27·9	23·9	−7·7	−4·0
Israel	High	33·0	26·0	22·1	−7·0	−3·9
Luxembourg	High	32·0	25·8	22·0	−6·2	−3·8
Thailand	Low	38·2	34·3	30·6	−3·8	−3·7
Norway	High	31·8	27·2	23·5	−4·6	−3·7
Sweden	High	30·5	26·4	23·0	−3·9	−3·4
Puerto Rico	High	34·0	28·1	24·6	−5·9	−3·5
Hungary	High	47·7	42·6	39·2	−5·1	−3·5
Ireland	High	37·5	28·6	25·3	−8·9	−3·3
Portugal	High	33·8	25·2	22·0	−8·6	−3·2
Poland	Medium	42·4	35·5	32·4	−7·0	−3·1
Greece	Medium	32·0	25·7	22·7	−6·3	−3·0
Burundi	Very low	67·4	57·3	54·2	−10·2	−3·0
Brazil	High	43·2	36·5	33·5	−6·7	−3·0
UK	High	36·7	30·0	27·0	−6·7	−3·0
Belgium	High	30·7	26·9	23·9	−3·8	−3·0
Tunisia	Low	41·3	38·2	35·3	−3·0	−2·9
Netherlands	High	34·2	28·4	25·5	−5·8	−2·9
Costa Rica	High	32·6	27·9	25·1	−4·7	−2·8
Mauritius	High	52·0	44·5	41·7	−7·6	−2·8
Spain	High	26·5	21·6	18·8	−4·9	−2·8
Ethiopia	Very low	52·6	48·1	45·4	−9·5	−2·7
New Zealand	High	34·0	27·5	25·0	−6·5	−2·5
Finland	High	30·9	26·1	23·6	−4·7	−2·5
Laos	Very low	64·0	57·2	54·8	−6·8	−2·5
France	Medium	25·8	21·9	19·5	−3·9	−2·4
Switzerland	High	26·1	22·6	20·3	−3·5	−2·3
Gabon	Very low	56·1	51·5	49·3	−4·6	−2·3
Afghanistan	Very low	77·4	73·6	71·4	−3·8	−2·3
Canada	High	33·4	29·7	24·5	−4·6	−2·2
United Arab Emirates	Very low	41·8	39·7	28·6	−11·1	−2·1
Bosnia and Herzegovina	Medium	47·5	44·0	41·8	−3·6	−2·1
Belize	High	46·4	43·6	39·5	−4·7	−2·1
Australia	High	28·6	23·9	21·8	−4·7	−2·1
Equatorial Guinea	Very low	57·3	53·0	51·0	−4·3	−2·1
Comoros	Very low	60·6	54·7	52·6	−5·9	−2·1
Nigeria	Very low	50·5	45·3	43·3	−5·1	−2·1
Argentina	Medium	37·2	34·8	32·8	−2·4	−2·0
Italy	High	28·5	23·3	21·3	−5·3	−2·0
Austria	High	31·2	26·1	24·1	−5·1	−2·0
Pakistan	Very low	64·2	61·1	59·4	−3·9	−1·9
São Tomé and Príncipe	Very low	56·5	53·4	53·5	−3·1	−1·9
Brunei	High	47·0	43·0	41·1	−4·0	−1·9
Japan	High	20·5	17·6	15·7	−3·0	−1·8
Cambodia	Very low	60·5	54·7	52·9	−5·8	−1·8
Bhutan	Very low	51·2	45·1	43·3	−6·2	−1·7
Rwanda	Very low	68·9	57·3	56·4	−11·5	−1·7
Germany	High	32·7	27·8	26·2	−4·9	−1·6
Mali	Very low	61·6	59·7	58·2	−1·9	−1·5
Trinidad and Tobago	Low	52·0	47·9	46·4	−9·1	−1·5
Federated States of Micronesia	Low	69·0	67·1	65·6	−2·0	−1·4
USA	High	37·9	30·9	29·5	−5·0	−1·3
Cuba	High	39·5	37·2	35·9	−2·4	−1·3
Yemen	Very low	61·0	56·8	55·6	−4·2	−1·2
Panama	High	31·5	28·5	27·4	−3·0	−1·2
Madagascar	Very low	61·9	60·5	59·0	−1·8	−1·1
Angola	Very low	61·1	55·4	54·4	−5·7	−1·0
Uganda	Very low	56·5	49·5	48·4	−9·9	−0·9
Vanuatu	Very low	64·6	62·5	61·6	−2·0	−0·9
Somalia	Very low	64·6	62·6	61·7	−2·0	−0·9
El Salvador	Low	35·5	33·4	32·7	−2·1	−0·7
The Bahamas	Medium	44·0	43·4	42·8	−0·7	−0·6
Mauritania	Very low	58·6	53·9	53·4	−3·7	−0·6
Suriname	Medium	48·2	43·0	42·5	−5·2	−0·5
Sudan	Very low	58·0	53·7	53·2	−4·3	−0·5
Senegal	Very low	54·6	53·3	52·8	−1·2	−0·5
Saudi Arabia	Very low	53·2	48·5	48·4	−8·6	−0·1

Central Asia, Middle East and north Africa; East and southeast Asia; Latin America and the Caribbean; South Asia; Central and eastern Europe; High-income western; Pacific Island nations; Sub-Saharan Africa

(Figure 3 continues on next page)

	Data quality	Probability of dying from an NCD between birth and age 80 years (percent)			Change in probability of dying from an NCD between birth and age 80 years (percentage points)	
		2001	2010	2019	2001–10	2010–19
Increasing from 2010 to 2019 after declining from 2001 to 2010						
Uruguay	Medium	37·8	34·3	34·3	−3·4	0·0
Syria	Low	57·5	49·3	49·3	−8·2	0·0
Iran	Medium	44·1	37·1	37·2	−7·0	0·2
Jamaica	High	48·4	42·2	42·6	−6·2	0·5
Nepal	Very low	48·0	48·0	48·4	−0·1	0·5
Turkmenistan	Very low	59·3	54·3	54·8	−5·1	0·5
Saint Lucia	High	42·1	32·5	33·0	−9·7	0·5
Zambia	Very low	53·9	49·2	49·7	−4·7	0·6
Djibouti	Very low	52·3	50·8	51·5	−1·5	0·7
The Gambia	Very low	53·4	52·6	53·4	−0·8	0·8
Papua New Guinea	Very low	61·9	60·1	61·0	−1·8	0·9
Seychelles	Medium	45·0	42·9	43·9	−2·1	0·9
Samoa	Very low	59·8	59·5	60·8	−0·3	1·3
Central African Republic	Very low	65·7	62·1	63·5	−3·6	1·4
North Macedonia	Medium	53·5	49·1	50·5	−4·4	1·4
Malawi	Very low	57·4	51·8	53·6	−5·6	1·8
Niger	Very low	52·1	50·7	52·6	−1·4	1·8
Cabo Verde	Low	38·7	35·8	37·7	−2·9	1·9
Venezuela	High	36·8	33·3	35·3	−3·5	2·0
India	Very low	46·7	46·6	48·7	−0·2	2·1
Peru	Medium	29·7	28·1	30·7	−1·6	2·6
Saint Vincent and the Grenadines	High	46·0	41·0	45·3	−5·0	4·3
Antigua and Barbuda	Medium	43·6	40·1	44·7	−3·6	4·7
South Sudan	Very low	47·0	44·4	51·4	−2·6	7·0
Faster increase from 2010 to 2019 compared with from 2001 to 2010						
Philippines	Medium	41·9	44·1	46·8	2·2	2·7
Tanzania	Very low	43·6	43·8	46·6	0·2	2·8

Central Asia, Middle East and north Africa; East and southeast Asia; Latin America and the Caribbean; South Asia; Central and eastern Europe; High-income western; Pacific Island nations; Sub-Saharan Africa

***Figure 3*: Countries showing deteriorations in the direction or size of change from 2010 to 2019 compared with from 2001 to 2010 for females**

Estimates are shown for all countries and territories in eight reporting regions. Countries are divided into three categories of changes observed across two timeframes (2001–10 and 2010–19). Within each of the three categories, countries are ordered by percentage point change from 2010 to 2019 (ie, the first country listed in each category had the largest decrease or smallest increase from 2010 to 2019 within its category). For the estimated probabilities and change in probabilities with uncertainty intervals see the appendix (pp 44–53). For results based on cancers, cardiovascular diseases, chronic respiratory diseases, and diabetes in ages 30–70 years see the appendix (pp 13–14). NCD=non-communicable disease.

	Data quality	Probability of dying from an NCD between birth and age 80 years (percent)			Change in probability of dying from an NCD between birth and age 80 years (percentage points)	
		2001	2010	2019	2001–10	2010–19
Slower decline from 2010 to 2019 compared with from 2001 to 2010						
Jordan	Medium	63·7	44·0	33·8	−17·7	−10·2
South Korea	High	34·9	22·5	15·4	−12·5	−7·0
Estonia	High	44·8	35·7	28·8	−9·1	−6·9
China	High	51·2	41·6	35·2	−9·6	−6·4
Romania	High	51·3	44·5	38·5	−6·8	−6·0
Lebanon	Low	42·5	34·7	29·0	−7·8	−5·7
Congo (Brazzaville)	Very low	71·3	64·2	58·9	−7·1	−5·3
Malta	High	36·0	28·4	23·1	−7·6	−5·3
Singapore	High	33·3	23·7	18·5	−9·6	−5·1
Bahrain	Low	70·6	56·4	51·4	−14·2	−5·0
Myanmar	Very low	63·7	56·6	51·7	−7·1	−4·9
Bulgaria	Medium	52·1	45·4	40·7	−6·7	−4·7
Malaysia	Low	51·7	46·5	41·8	−5·1	−4·7
Cyprus	High	32·5	25·4	20·7	−7·1	−4·7
Czechia	High	43·1	34·7	30·1	−8·4	−4·6
Taiwan	High	36·1	28·5	24·1	−7·6	−4·4
Montenegro	Low	52·3	44·7	40·5	−7·6	−4·2
Slovenia	High	35·6	27·9	23·9	−7·7	−4·0
Israel	High	33·0	26·0	22·1	−7·0	−3·9
Luxembourg	High	32·0	25·8	22·0	−6·2	−3·8
Thailand	Low	38·2	34·3	30·6	−3·8	−3·7
Norway	High	31·8	27·2	23·5	−4·6	−3·7
Sweden	High	30·5	26·6	23·0	−3·9	−3·6
Puerto Rico	High	34·0	28·1	24·6	−5·9	−3·5
Hungary	High	47·7	42·6	39·2	−5·1	−3·5
Ireland	High	37·5	28·6	25·3	−8·9	−3·3
Portugal	High	33·8	25·2	22·0	−8·6	−3·2
Poland	Medium	42·4	35·5	32·4	−7·0	−3·1
Greece	Medium	32·0	25·7	22·7	−6·3	−3·0
Burundi	Very low	67·4	57·2	54·2	−10·2	−3·0
Brazil	High	43·2	36·5	33·5	−4·7	−3·0
UK	High	36·7	30·0	27·0	−6·7	−3·0
Belgium	High	30·7	26·9	23·9	−3·8	−3·0
Tunisia	Low	43·3	38·2	35·3	−3·0	−2·9
Netherlands	High	34·2	28·4	25·5	−5·8	−2·9
Costa Rica	High	32·6	27·9	25·1	−4·7	−2·8
Mauritius	High	52·0	44·5	41·7	−7·6	−2·8
Spain	High	26·5	21·6	18·8	−4·9	−2·8
Ethiopia	Very low	57·6	48·1	45·4	−9·5	−2·7
New Zealand	High	34·0	27·5	25·0	−6·5	−2·5
Finland	High	30·9	26·1	23·6	−4·7	−2·5
Laos	Very low	64·0	57·2	54·8	−6·8	−2·5
France	Medium	25·8	21·9	19·5	−3·9	−2·4
Switzerland	High	26·1	22·6	20·3	−3·5	−2·3
Gabon	Very low	56·1	51·5	49·3	−4·6	−2·3
Afghanistan	Very low	77·4	73·6	71·4	−3·8	−2·3
Canada	High	31·4	26·7	24·5	−4·6	−2·2
United Arab Emirates	Very low	43·8	30·7	28·6	−13·1	−2·1
Bosnia and Herzegovina	Medium	47·5	44·0	41·8	−3·6	−2·1
Belize	High	46·4	41·6	39·5	−4·7	−2·1
Australia	High	28·6	23·9	21·8	−4·7	−2·1
Equatorial Guinea	Very low	57·3	53·0	51·0	−4·3	−2·1
Comoros	Very low	60·6	54·7	52·6	−5·9	−2·1
Nigeria	Very low	59·5	45·3	43·3	−5·1	−2·1
Argentina	Medium	37·2	34·8	32·8	−2·4	−2·0
Italy	High	28·5	23·3	21·3	−5·3	−2·0
Austria	High	31·2	26·1	24·1	−5·1	−2·0
Pakistan	Very low	64·2	61·3	59·4	−2·9	−1·9
São Tomé and Príncipe	Very low	56·5	53·4	51·5	−3·1	−1·9
Brunei	High	47·0	43·0	41·1	−4·0	−1·9
Japan	High	20·5	17·6	15·7	−3·0	−1·8
Cambodia	Very low	60·5	54·7	52·9	−5·8	−1·8
Bhutan	Very low	51·2	45·1	43·3	−6·2	−1·7
Rwanda	Very low	68·9	52·3	50·6	−16·5	−1·7
Germany	High	32·7	27·8	26·2	−4·9	−1·6
Mali	Very low	63·6	59·7	58·2	−3·9	−1·5
Trinidad and Tobago	Low	52·0	42·9	41·4	−9·1	−1·5
Federated States of Micronesia	Low	69·0	67·1	65·6	−2·0	−1·4
USA	High	37·9	32·9	31·5	−5·0	−1·3
Cuba	High	39·5	37·2	35·9	−2·4	−1·3
Yemen	Very low	63·0	56·8	55·6	−6·2	−1·2
Panama	High	31·5	28·5	27·4	−3·0	−1·2
Madagascar	Very low	63·9	60·1	59·0	−3·8	−1·1
Angola	Very low	61·1	55·4	54·4	−5·7	−1·0
Uganda	Very low	56·5	46·5	45·6	−9·9	−0·9
Vanuatu	Very low	64·6	62·5	61·6	−2·0	−0·9
Somalia	Very low	64·6	62·6	61·7	−2·0	−0·9
El Salvador	Low	35·5	33·4	32·7	−2·1	−0·7
The Bahamas	Medium	44·0	43·4	42·8	−0·7	−0·6
Mauritania	Very low	54·6	51·9	51·4	−2·7	−0·6
Suriname	Medium	48·2	43·0	42·5	−5·2	−0·5
Sudan	Very low	58·0	53·7	53·2	−4·3	−0·5
Senegal	Very low	54·6	53·3	52·8	−1·2	−0·5
Saudi Arabia	Very low	53·2	44·5	44·4	−8·6	−0·1

Central Asia, Middle East and north Africa; East and southeast Asia; Latin America and the Caribbean; South Asia; Central and eastern Europe; High-income western; Pacific Island nations; Sub-Saharan Africa

	Data quality	Probability of dying from an NCD between birth and age 80 years (percent)			Change in probability of dying from an NCD between birth and age 80 years (percentage points)	
		2001	2010	2019	2001–10	2010–19
Slower decline from 2010 to 2019 compared with from 2001 to 2010						
South Korea	High	56·2	42·1	31·1	−14·1	−11·0
Denmark	High	55·1	46·1	38·1	−9·0	−8·0
Norway	High	48·8	39·8	31·8	−9·0	−7·9
Malta	High	51·8	42·7	34·9	−9·1	−7·8
Singapore	High	47·1	36·8	29·1	−10·4	−7·7
Netherlands	High	52·2	41·3	33·9	−10·9	−7·4
Belgium	High	50·4	42·9	36·2	−7·5	−6·7
Sweden	High	44·8	38·0	31·4	−6·8	−6·6
Slovenia	High	59·6	48·0	41·5	−11·5	−6·5
Czechia	High	63·1	54·5	48·6	−8·5	−5·9
France	Medium	47·7	40·1	34·3	−7·6	−5·8
Spain	High	48·1	40·8	35·1	−7·3	−5·7
Bahrain	Low	77·4	62·4	56·9	−15·0	−5·6
Poland	Medium	66·6	59·8	54·3	−6·8	−5·5
Switzerland	High	43·6	35·8	30·3	−7·9	−5·4
Luxembourg	High	49·8	38·8	33·6	−11·0	−5·2
Italy	High	47·8	38·4	33·5	−9·4	−4·8
Austria	High	49·6	42·6	37·8	−7·0	−4·8
Iceland	High	41·8	36·2	31·4	−5·6	−4·8
UK	High	51·8	41·7	37·0	−10·0	−4·8
Ireland	High	54·2	40·4	35·8	−13·8	−4·6
Israel	High	45·7	37·1	32·6	−8·5	−4·5
Colombia	High	48·7	42·0	37·5	−6·8	−4·5
Afghanistan	Very low	79·8	73·4	68·9	−6·4	−4·5
Portugal	High	53·0	44·0	39·6	−8·9	−4·5
Argentina	Medium	59·4	53·8	49·3	−5·6	−4·4
Taiwan	High	49·9	44·7	40·4	−5·2	−4·4
Cyprus	High	47·2	38·3	34·0	−9·0	−4·3
Mauritius	High	70·2	62·8	58·5	−7·4	−4·3
Türkiye	Medium	62·2	56·9	52·7	−5·2	−4·2
New Zealand	High	48·3	37·5	33·5	−10·8	−3·9
Costa Rica	High	42·0	37·6	34·0	−4·4	−3·6
Australia	High	43·6	35·6	32·0	−8·0	−3·6
Japan	High	38·5	34·1	30·7	−4·4	−3·5
Canada	High	46·2	37·7	34·3	−8·5	−3·5
Germany	High	51·6	44·0	40·8	−7·6	−3·3
Nigeria	Very low	57·1	52·1	48·9	−5·0	−3·1
Algeria	Very low	47·2	42·0	38·9	−5·2	−3·1
Congo (Brazzaville)	Very low	73·0	62·0	58·9	−11·0	−3·0
Uganda	Very low	70·9	62·6	59·7	−8·3	−2·9
Bulgaria	Medium	70·3	67·0	64·1	−3·3	−2·9
Ethiopia	Very low	59·0	51·6	48·8	−7·4	−2·8
Guinea-Bissau	Very low	74·6	68·1	65·3	−6·5	−2·8
Puerto Rico	High	51·2	41·4	38·7	−9·8	−2·7
Greece	Medium	47·0	41·8	39·3	−5·2	−2·6
Belize	High	56·1	46·9	44·4	−9·2	−2·5
Tonga	Very low	69·2	65·6	63·1	−3·6	−2·5
Laos	Very low	72·2	67·1	64·8	−5·1	−2·3
Tunisia	Low	53·3	49·9	47·6	−3·4	−2·3
Uruguay	Medium	61·3	56·0	53·9	−5·4	−2·1
Somalia	Very low	75·3	73·0	71·1	−2·3	−2·0
Bolivia	Very low	54·9	53·2	49·2	−3·7	−1·9
Saudi Arabia	Very low	58·5	46·4	44·7	−12·1	−1·7
Iran	Medium	51·2	46·0	44·4	−5·2	−1·6
Bhutan	Very low	53·3	49·6	48·0	−3·7	−1·6
Panama	High	44·2	41·6	40·1	−2·6	−1·6
Brunei	High	51·3	49·7	48·2	−1·7	−1·5
Comoros	Very low	62·0	56·7	55·3	−5·3	−1·4
Fiji	Low	81·2	76·6	75·2	−4·6	−1·4
Cambodia	Very low	69·4	66·9	65·6	−2·4	−1·3
Rwanda	Very low	77·6	60·4	59·3	−17·2	−1·2
Vanuatu	Very low	77·6	75·8	74·7	−1·8	−1·2
Federated States of Micronesia	Low	77·5	76·1	75·0	−1·5	−1·1
Samoa	Very low	69·6	66·2	65·3	−3·4	−1·0
DR Congo	Very low	66·9	64·8	63·9	−2·1	−0·9
Trinidad and Tobago	Low	63·7	55·7	54·8	−8·0	−0·9
Thailand	Low	47·6	44·6	43·7	−3·1	−0·9
Burundi	Very low	69·5	61·7	61·0	−7·7	−0·8
Senegal	Very low	60·6	58·2	57·5	−2·4	−0·7
Myanmar	Very low	70·4	66·7	66·0	−3·7	−0·7
Sudan	Very low	59·5	55·3	54·6	−4·2	−0·7
Iraq	Low	62·7	60·4	59·8	−2·3	−0·6
Malaysia	Low	59·0	54·2	53·7	−4·8	−0·5
Bosnia and Herzegovina	Medium	60·0	58·3	57·8	−1·7	−0·5
USA	High	50·2	43·4	43·0	−6·7	−0·5
Seychelles	Medium	64·5	61·8	61·4	−2·7	−0·4
Suriname	Medium	60·0	55·9	55·6	−4·1	−0·3
Yemen	Very low	66·9	62·5	62·3	−4·4	−0·2
Saint Lucia	High	56·7	50·6	50·5	−6·1	−0·1
Zambia	Very low	64·4	63·1	63·0	−1·3	−0·0

Central Asia, Middle East and north Africa; East and southeast Asia; Latin America and the Caribbean; South Asia; Central and eastern Europe; High-income western; Pacific Island nations; Sub-Saharan Africa

	Data quality	Probability of dying from an NCD between birth and age 80 years (percentage)			Change in probability of dying from an NCD between birth and age 80 years (percentage points)	
		2001	2010	2019	2001–10	2010–19
Increasing from 2010 to 2019 after declining from 2001 to 2010						
Antigua and Barbuda	Medium	55·2	49·7	49·7	−5·5	0·0
Angola	Very low	70·7	63·9	64·0	−6·9	0·1
Turkmenistan	Very low	73·7	68·5	68·6	−5·2	0·1
The Gambia	Very low	62·3	60·3	60·5	−2·0	0·2
Montenegro	Low	64·3	59·7	59·9	−4·6	0·2
Niger	Very low	53·6	53·3	53·6	−0·3	0·2
Syria	Low	62·6	56·4	56·9	−6·2	0·5
Central African Republic	Very low	76·3	74·9	75·8	−1·4	1·0
Cuba	High	48·3	47·9	49·6	−0·3	1·6
United Arab Emirates	Very low	35·0	30·4	32·2	−4·6	1·8
Tanzania	Very low	53·9	49·7	52·0	−4·2	2·3
Morocco	Very low	55·3	54·6	57·2	−0·7	2·5
Mauritania	Very low	46·7	44·1	46·8	−2·6	2·7
Papua New Guinea	Very low	61·7	60·0	62·7	−1·7	2·7
Peru	Medium	33·8	32·4	35·3	−1·4	2·8
São Tomé and Príncipe	Very low	55·6	54·0	57·3	−1·6	3·3
Libya	Very low	56·2	51·0	54·3	−5·3	3·3
Equatorial Guinea	Very low	65·1	51·3	54·6	−13·9	3·3
Djibouti	Very low	57·0	55·7	59·1	−1·2	3·4
El Salvador	Low	47·7	44·4	47·9	−3·4	3·5
Barbados	Low	49·3	46·0	50·3	−3·3	4·3
Saint Vincent and the Grenadines	High	56·3	48·2	52·6	−8·1	4·3
Venezuela	High	48·6	47·1	51·6	−1·5	4·5
Malawi	Very low	65·3	60·9	65·9	−4·4	5·0
South Sudan	Very low	59·7	55·3	63·1	−4·3	7·7
Jamaica	High	56·7	51·8	59·7	−4·9	7·8
Cabo Verde	Low	51·9	44·4	60·2	−7·6	15·9
Faster increase from 2010 to 2019 compared with from 2001 to 2010						
Haiti	Very low	65·5	65·7	66·6	0·1	1·0
Guatemala	High	44·6	45·9	48·7	1·2	2·8
Dominican Republic	Low	43·7	44·9	48·3	1·2	3·4
Nepal	Very low	46·8	47·2	54·0	0·4	6·7
Honduras	Very low	46·8	48·6	57·2	1·8	8·6

Central Asia, Middle East and north Africa; East and southeast Asia; Latin America and the Caribbean; South Asia; Central and eastern Europe; High-income western; Pacific Island nations; Sub-Saharan Africa

Figure 4: Countries showing deteriorations in the direction or size of change from 2010 to 2019 compared with from 2001 to 2010 for males

Estimates are shown for all countries and territories in eight reporting regions. Countries are divided into three categories of changes observed across two timeframes (2001–10 and 2010–19). Within each of the three categories, countries are ordered by percentage point change from 2010 to 2019 (ie, the first country listed in each category had the largest decrease or smallest increase from 2010 to 2019 within its category). For the estimated probabilities and change in probabilities with uncertainty intervals see the appendix (pp 44–53). For results based on cancers, cardiovascular diseases, chronic respiratory diseases, and diabetes in ages 30–70 years see the appendix (pp 13–14). NCD=non-communicable disease.

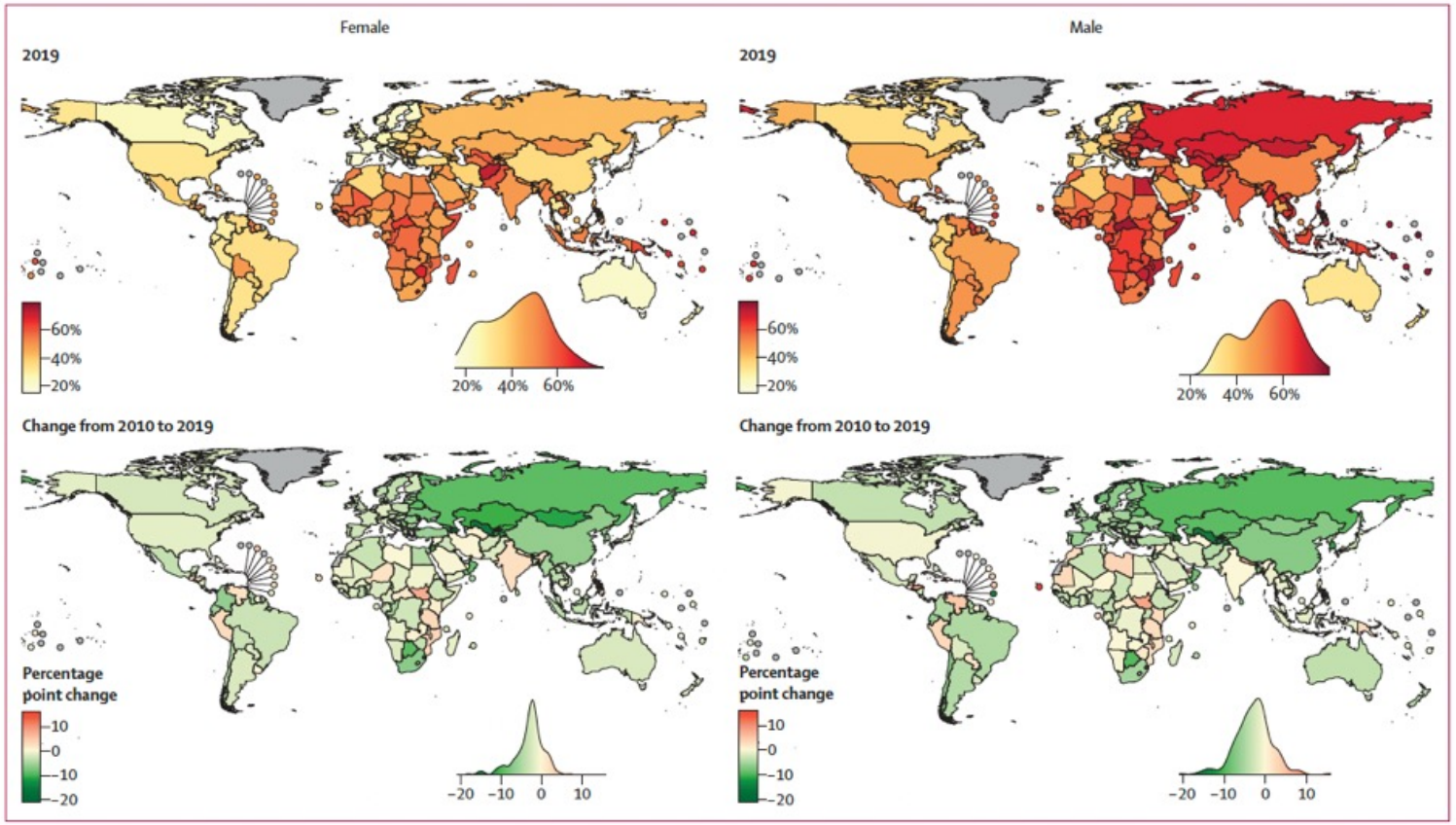

Figure 5: **Probability of dying from an NCD between birth and age 80 years in 2019 and change in probability from 2010 to 2019**
For change from 2010 to 2019, green indicates a decline in NCD mortality and red indicates an increase. The density plot alongside each map shows the smoothed distribution of estimates across countries. Countries and territories with no mortality estimates are shown in grey. For the estimated probabilities and change in probabilities with uncertainty intervals see the appendix (pp 44–53). For results based on cancers, cardiovascular diseases, chronic respiratory diseases, and diabetes in ages 30–70 years see the appendix (pp 54–55). NCD=non-communicable disease.

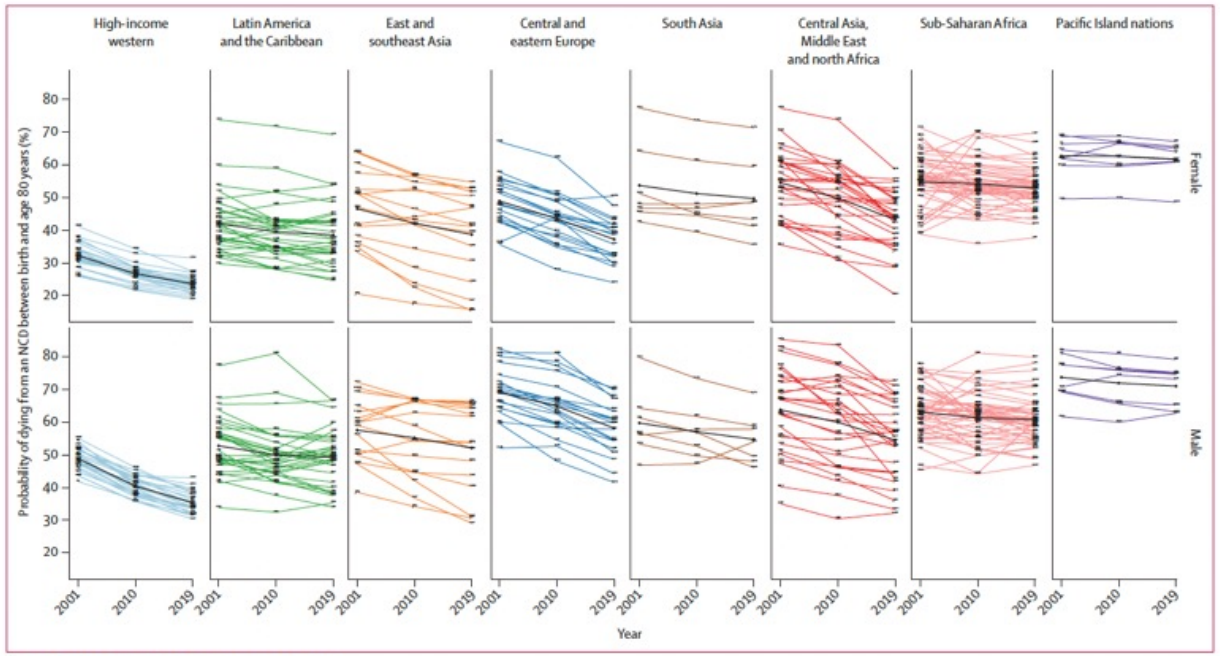

Figure 6: **Change in NCD mortality from 2001 to 2019**

Each line connects the probability of dying between birth and age 80 years from an NCD for 2001, 2010, and 2019 for one country. For each country, the difference in level between consecutive pairs of years respectively represents change over the intervals from 2001 to 2010 and from 2010 to 2019. Data are shown for 185 countries and territories, divided into eight reporting regions. Lines are coloured by region and labelled with ISO3 codes for each country. The bold black line in each panel connects the mean levels (across countries in that panel, unweighted for population) in 2001, 2010, and 2019. Regions are ordered by increasing mean probability of dying of the countries in each region for females in 2001. For results based on cancers, cardiovascular diseases, chronic respiratory diseases, and diabetes in ages 30–70 years see the appendix (pp 56–57). NCD=non-communicable disease. High-income western countries: AUS=Australia, AUT=Austria, BEL=Belgium, CAN=Canada, CHE=Switzerland, CYP=Cyprus, DEU=Germany, DNK=Denmark, ESP=Spain, FIN=Finland, FRA=France, GBR=United Kingdom, GRC=Greece, IRL=Ireland, ISL=Iceland, ISR=Israel, ITA=Italy, LUX=Luxembourg, MLT=Malta, NLD=Netherlands, NOR=Norway, NZL=New Zealand, PRT=Portugal, SWE=Sweden, USA=United States of America. Latin America and the Caribbean: ARG=Argentina, ATG=Antigua and Barbuda, BHS=The Bahamas, BLZ=Belize, BOL=Bolivia, BRA=Brazil, BRB=Barbados, CHL=Chile, COL=Colombia, CRI=Costa Rica, CUB=Cuba, DOM=Dominican Republic, ECU=Ecuador, GRD=Grenada, GTM=Guatemala, GUY=Guyana, HND=Honduras, HTI=Haiti, JAM=Jamaica, LCA=Saint Lucia, MEX=Mexico, NIC=Nicaragua, PAN=Panama, PER=Peru, PRI=Puerto Rico, PRY=Paraguay, SLV=El Salvador, SUR=Suriname, TTO=Trinidad and Tobago, URY=Uruguay, VCT=Saint Vincent and the Grenadines, VEN=Venezuela. East and southeast Asia: BRN=Brunei, CHN=China, IDN=Indonesia, JPN=Japan, KHM=Cambodia, KOR=South Korea, LAO=Laos, MMR=Myanmar, MYS=Malaysia, PHL=Philippines, PRK=North Korea, SGP=Singapore, THA=Thailand, TLS=Timor-Leste, TWN=Taiwan, VNM=Viet Nam. Central and eastern Europe: ALB=Albania, BGR=Bulgaria, BIH=Bosnia and Herzegovina, BLR=Belarus, CZE=Czechia, EST=Estonia, HRV=Croatia, HUN=Hungary, LTU=Lithuania, LVA=Latvia, MDA=Moldova, MKD=North Macedonia, MNE=Montenegro, POL=Poland, ROU=Romania, RUS=Russia, SRB=Serbia, SVK=Slovakia, SVN=Slovenia, UKR=Ukraine. South Asia: AFG=Afghanistan, BGD=Bangladesh, BTN=Bhutan, IND=India, LKA=Sri Lanka, NPL=Nepal, PAK=Pakistan. Central Asia, Middle East and north Africa: ARE=United Arab Emirates, ARM=Armenia, AZE=Azerbaijan, BHR=Bahrain, DZA=Algeria, EGY=Egypt, GEO=Georgia, IRN=Iran, IRQ=Iraq, JOR=Jordan, KAZ=Kazakhstan, KGZ=Kyrgyzstan, KWT=Kuwait, LBN=Lebanon, LBY=Libya, MAR=Morocco, MNG=Mongolia, OMN=Oman, PSE=Palestine, QAT=Qatar, SAU=Saudi Arabia, SYR=Syria, TJK=Tajikistan, TKM=Turkmenistan, TUN=Tunisia, TUR=Türkiye, UZB=Uzbekistan, YEM=Yemen. Sub-Saharan Africa: AGO=Angola, BDI=Burundi, BEN=Benin, BFA=Burkina Faso, BWA=Botswana, CAF=Central African Republic, CIV=Côte d'Ivoire, CMR=Cameroon, COD=DR Congo, COG=Congo (Brazzaville), COM=Comoros, CPV=Cabo Verde, DJI=Djibouti, ERI=Eritrea, ETH=Ethiopia, GAB=Gabon, GHA=Ghana, GIN=Guinea, GMB=The Gambia, GNB=Guinea-Bissau, GNQ=Equatorial Guinea, KEN=Kenya, LBR=Liberia, LSO=Lesotho, MDG=Madagascar, MLI=Mali, MOZ=Mozambique, MRT=Mauritania, MUS=Mauritius, MWI=Malawi, NAM=Namibia, NER=Niger, NGA=Nigeria, RWA=Rwanda, SDN=Sudan, SEN=Senegal, SLE=Sierra Leone, SOM=Somalia, SSD=South Sudan, STP=São Tomé and Príncipe, SWZ=Eswatini, SYC=Seychelles, TCD=Chad, TGO=Togo, TZA=Tanzania, UGA=Uganda, ZAF=South Africa, ZMB=Zambia, ZWE=Zimbabwe. Pacific Island nations: FJI=Fiji, FSM=Federated States of Micronesia, KIR=Kiribati, PNG=Papua New Guinea, SLB=Solomon Islands, TON=Tonga, VUT=Vanuatu, WSM=Samoa.

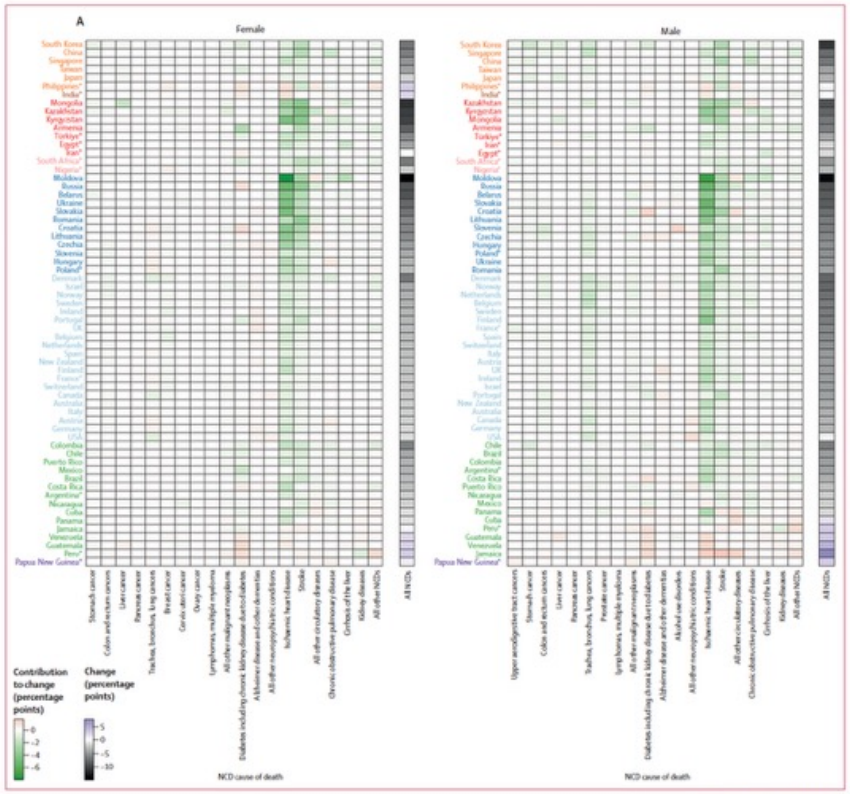

(Figure 7 continues on next page)

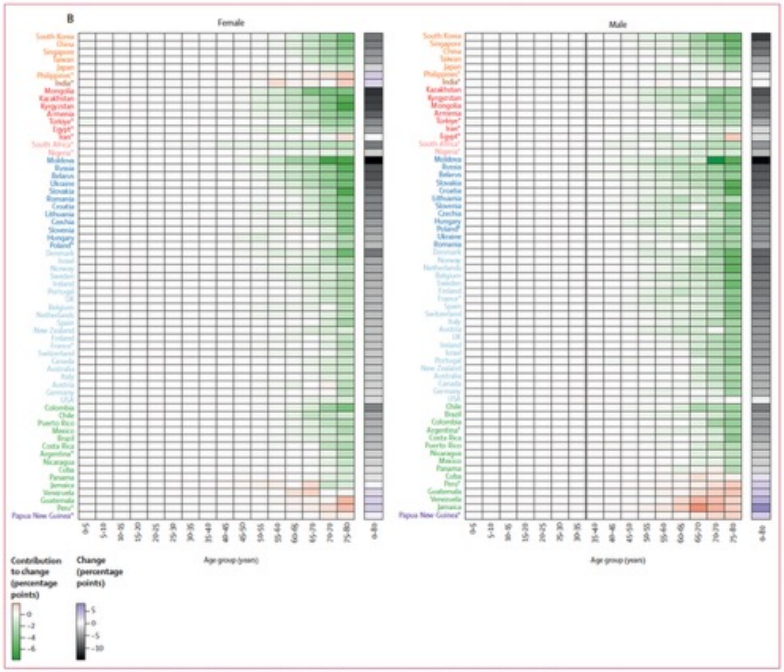

Figure 7: **Contributions of mortality from different NCD causes of death and in different age groups to overall change in NCD mortality from 2010 to 2019**
(A) The contribution of 20 mutually exclusive, collectively exhaustive NCD causes of death to the change in the probability of dying from an NCD between birth and age 80 years from 2010 to 2019. Each column represents a cause of death, as stated in the appendix (pp 11–12), with causes arranged by disease category. Results are presented for aggregated cause groups in the appendix (pp 35–36). (B) The contribution of 5-year age groups to the change in this probability over the same period, with each column representing a 5-year age group. In both panels, each row represents a country. Results are shown for 63 countries, of which 51 were identified as having high-quality data and 12 were selected based on population size. Countries are grouped and coloured by region and ordered from the largest decrease to the smallest decrease or largest increase in the probability of dying from an NCD between birth and age 80 years from 2010 to 2019. Each tile shows the absolute contribution of an NCD cause of death or age group to the total change in this probability for one country. Two colour palettes are used: one for the overall change in NCD mortality from 2010 to 2019, and one for contributions of individual NCD causes of death or age groups. For overall change, black indicates a decrease, purple an increase, and white no change. For contributions to change, green indicates a contribution to lowering NCD mortality, red a contribution to increasing it, and white a contribution of zero. For numerical results see the appendix (pp 26–28). For results based on cancers, cardiovascular diseases, chronic respiratory diseases, and diabetes in ages 30–70 years see the appendix (pp 58–60). NCD=non-communicable disease. *12 countries selected based on population size.

Panel 2: Country case studies*

Varying performance in high-income western countries

Females and males in the USA had the smallest declines in the probability of dying from a non-communicable disease (NCD) before age 80 years from 2010 to 2019 of any high-income western country; those in Germany had the second smallest for females and third smallest for males. These countries' poor performance was a consequence of having had some of the largest slowdowns in NCD mortality decline compared with the first decade of the millennium, reaching near-stagnation in the case of males in the USA.

In the USA, NCD mortality declined in most age groups from 2010 to 2019 but increased in ages 20–45 years, a rare phenomenon in high-income western countries. For almost all age groups, regardless of whether mortality decreased or increased from 2010 to 2019, the change was a deterioration compared with the previous decade. The combination of small reductions in mortality in older ages and its stagnation or rise in young adults and working ages underlies the USA's particularly poor performance among high-income western countries.

Epidemiologically, the poor performance of the USA from 2010 to 2019 can be summarised as a rise in the probability of dying from neuropsychiatric conditions, which was not offset by the continued declines in cancers and circulatory diseases. Specifically, although mortality from most cancers, ischaemic heart disease, and chronic obstructive pulmonary disease (COPD) declined from 2010 to 2019, most of these declines were smaller than the preceding decade. Lung cancer and some other cancers and kidney diseases were among the few exceptions, and had larger declines from 2010 to 2019 than in the preceding decade, but did not compensate for the deterioration in changes over time for other causes of death. Mortality from some neuropsychiatric conditions (comprising Alzheimer disease and other dementias, alcohol use disorders, and the aggregate group of all other neuropsychiatric conditions [which include drug use disorders that were not analysed separately in this work]), diabetes and its kidney complications, liver cirrhosis, and liver and pancreatic cancers increased more from 2010 to 2019 than in the previous decade or deteriorated from a decrease to an increase.

In Germany, NCD mortality declined from 2010 to 2019 from adolescence up to age 80 years, except for females aged 30–40 years and 65–75 years, who had small increases. As in the USA, these changes were a deterioration compared with the previous decade in most age groups. In terms of causes of death, circulatory diseases and neuropsychiatric conditions had a similar role as in the USA, where a rise in neuropsychiatric conditions was not offset by the decline in circulatory diseases, which was smaller from 2010 to 2019 compared with the previous decade. Furthermore, changes in cancer mortality showed greater deterioration over time in Germany than in the USA; in both countries, cancers contributed to a decrease in mortality from 2010 to 2019, but less than in the previous decade. Among cancers, mortality from lung cancer, which declined in the USA, increased in German females from 2010 to 2019 to a larger extent than in most other high-income western countries.

In contrast with the USA and Germany, Norway and Sweden had two of the largest declines in the probability of dying from an NCD before age 80 years from 2010 to 2019, and there was relatively little slowdown in their mortality decline compared with the preceding decade. The strong and sustained success in Norway and Sweden arose from a few factors. In these countries, NCD mortality generally declined throughout working and older ages from 2010 to 2019. In some adolescent and working age groups, there was an acceleration of NCD mortality decline, which is in contrast to the slowdown or even reversal of progress seen in the USA and Germany. Most NCD causes of death contributed to the sustained decrease in overall NCD mortality in Norway and Sweden. There were a few exceptions, for example Alzheimer disease and other dementias, and pancreatic and liver cancers for one or both sexes. Although the decline in mortality from some causes of death was smaller than in the previous decade, the extent of slowdown in Norway and Sweden was less pronounced than in the USA and Germany, and was compensated for by the acceleration of declines in mortality from lung, colorectal, breast, cervical, prostate, and some other cancers, and from diabetes and its kidney complications.

Progress at low levels of NCD mortality in east Asia

In 2010, Japan had the lowest probability of dying from an NCD between birth and age 80 years for both sexes (appendix pp 15–16). South Korea also had very low NCD mortality compared with high-income western countries due to a very large reduction in NCD mortality from 2001 to 2010, greater than that of all high-income western countries for both sexes. NCD mortality in Japan and South Korea continued to decline from 2010 to 2019. While the declines in NCD mortality from 2010 to 2019 in Japan and South Korea were smaller than in the preceding decade for most age groups and causes, South Korea's reduction remained greater than that of any high-income western country. The continued decline reinforces the fact that low mortality is not an obstacle to continued progress and substantial progress is possible even at low mortality. In 2019, Japan ranked second lowest in the world for females and third lowest for males in the probability of dying from an NCD between birth and age 80 years, and South Korea ranked lowest in the world for females and fourth lowest in the world for males.

Japan and South Korea achieved reductions in mortality in every age group from adolescence up to age 80 years for both sexes, and in most causes of death from 2010 to 2019. For example, mortality from liver cancer, which increased in most high-income western countries, decreased in both Japan and South Korea, and mortality from Alzheimer disease and other

(Continues on next page)

(Panel 2 continued from previous page)

Unlike Chile, Jamaica and Peru had increases in NCD mortality from 2010 to 2019. These increases resulted from a rise in mortality from most NCD causes of death, including most cardiometabolic and renal diseases and many cancers, in both countries for males and in Peru for females. Both countries had experienced a decline in NCD mortality from 2001 to 2010, and saw a reversal from 2010 to 2019, with a particularly large swing from reduction to increase among males in Jamaica. This was the result of a deterioration of trends (ie, larger increase, smaller decline, or a reversal from a decline to an increase) for most NCD causes of death from the first to the second decade of the millennium.

*Countries in case studies are selected from those used for analysis of specific NCD causes of death in figures 7–9.

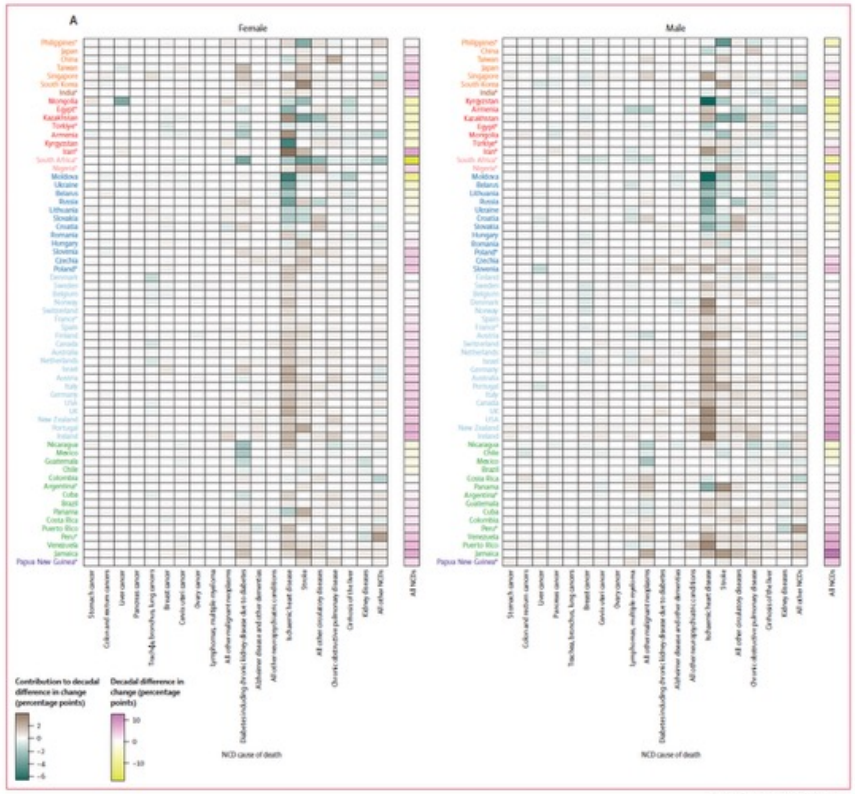

(Figure 8 continues on next page)

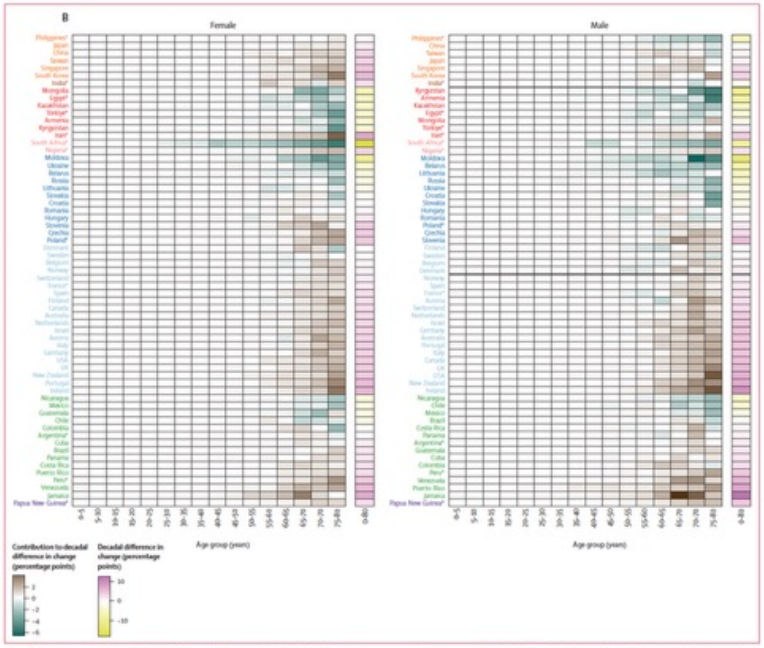

Figure 8: **Contributions of mortality from different NCD causes of death and in different age groups to slowdown or acceleration of change in NCD mortality from 2010 to 2019 compared to change from 2001 to 2010**

(A) The contribution of 20 mutually exclusive, collectively exhaustive NCD causes of death to the difference in change in the probability of dying from an NCD between birth and age 80 years between two decades (2010–19 and 2001–10). Each column represents a cause of death, as stated in the appendix (pp 11–12), with causes arranged by disease category. Results are presented for aggregated cause groups in the appendix (pp 37–38). (B) The contribution of 5-year age groups to this decadal difference in change, with each column representing a 5-year age group. In both panels, each row represents a country. Results are shown for 63 countries, of which 51 were identified as having high-quality data and 12 were selected based on population size. Countries are grouped and coloured by region and ordered from the largest improvement in NCD mortality from 2010 to 2019 compared with the preceding decade to the largest deterioration. Each tile shows the absolute contribution of a specific NCD cause of death or age group to the decadal difference in change in NCD mortality (ie, difference in change between the two decades) for one country. Two-colour palettes are used: one for the overall decadal difference in change, and one for contributions of individual NCD causes of death or age groups. For overall decadal difference in change, yellow indicates improvement (a larger decline, smaller increase, or reversal of an increase), pink indicates deterioration (a smaller decline, reversal of a decline, or a larger increase), and white indicates no difference in the magnitude of change. For contributions to decadal difference in change, green indicates a contribution to improvement of change (a larger decline, smaller increase, or reversal of an increase), brown indicates a contribution to deterioration of change (a smaller decline, reversal of a decline, or a larger increase), and white indicates a contribution of zero. For numerical results see the appendix (pp 29–31). For results based on cancers, cardiovascular diseases, chronic respiratory diseases, and diabetes in ages 30–70 years see the appendix (pp 61–63). NCD=non-communicable disease. *12 countries selected based on population size.

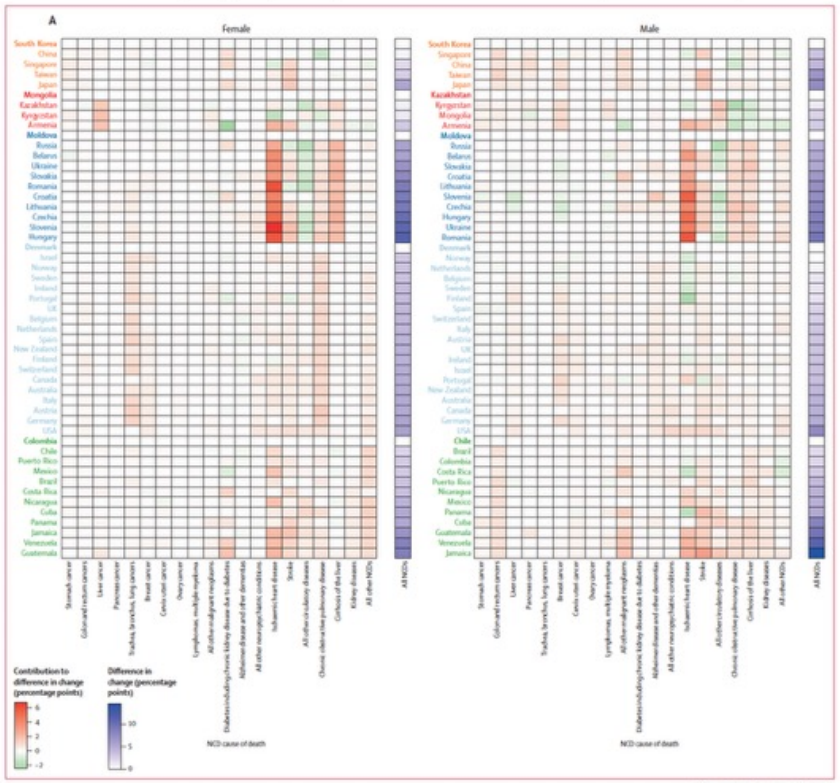

(Figure 9 continues on next page)

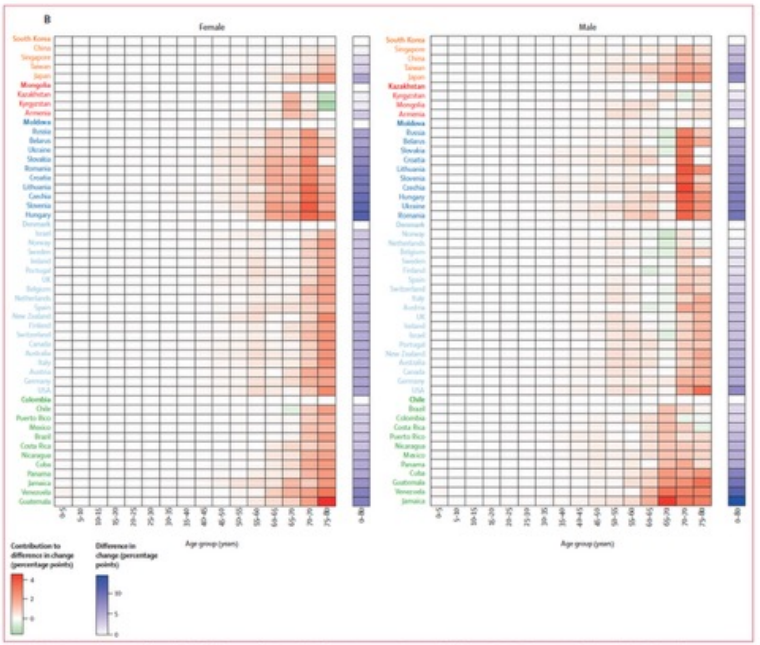

Figure 9: **Contributions of mortality from different NCD causes of death and in different age groups to how much NCD mortality in each country lags its regional benchmark**
(A) The contribution of 20 mutually exclusive, collectively exhaustive NCD causes of death to the difference in the change in the probability of dying from an NCD between birth and age 80 years from 2010 to 2019, compared with a country benchmark within each region. Benchmarks are identified as the country in each region with the largest reduction in NCD mortality over this period. Each column represents a cause of death, as stated in the appendix (pp 11–12), with causes arranged by disease category. Results are presented for aggregated cause groups in the appendix (pp 39–40). (B) The contribution of 5-year age groups to this difference, with each column representing a 5-year age group. In both panels, each row represents a country. Results are shown for 51 countries identified as having high-quality data. Countries are grouped and coloured by region and ordered from the largest decrease to the smallest decrease or largest increase in the probability of dying from an NCD between birth and age 80 years from 2010 to 2019. The benchmark for each region is the country in the first row of its region grouping and is shown in bold font. Each tile shows the absolute contribution of a specific NCD cause of death or age group to the difference in change compared with the benchmark country for one country. Two colour palettes are used: one for the overall difference in change compared with the benchmark, and one for contributions of individual NCD causes of death or age groups compared with those of the benchmark. For overall difference in change, black indicates a decrease compared with the benchmark, purple indicates an increase compared with the benchmark, and white indicates no difference in change. For contributions to difference in change, green indicates a contribution towards a larger decline or smaller increase compared with the benchmark, red indicates a contribution towards a smaller decline or larger increase compared with the benchmark, and white indicates a contribution of zero. For numerical results see the appendix (pp 32–34). For results based on cancers, cardiovascular diseases, chronic respiratory diseases, and diabetes in ages 30–70 years see the appendix (pp 64–66). NCD=non-communicable disease.

Research in context

Evidence before this study

We searched MEDLINE (via PubMed) for articles published from database inception up to May 1, 2025, with no language restrictions, using the following search terms: ("Noncommunicable Diseases"[MAJR] OR "NCD"[Title/Abstract] OR "Non-communicable disease*"[Title/Abstract]) AND ("Mortality"[MAJR] OR "Probability of Death"[Title/Abstract] OR "Death rate*"[Title/Abstract]) AND ("Trend*"[Title/Abstract] OR "Change*"[Title/Abstract]) AND ("Global Health"[mh] OR "Country"[Title/Abstract] OR "Countries"[Title/Abstract] OR "National"[Title/Abstract] OR "Global"[Title/Abstract] OR "Population-based"[Title/Abstract]) NOT (Comment[ptyp] OR Editorial[ptyp] OR Letter[ptyp] OR Case Reports[ptyp]). We identified studies that reported changes over time in non-communicable disease (NCD) mortality using national vital registration data or multicountry and global estimates of mortality. These studies used several metrics to measure NCD mortality. Most of these studies analysed one country or focused on one NCD or a group of related NCDs, and some were only at one point in time. Few evaluated contributions of different causes of death or age groups to changes in overall NCD mortality. Two previous NCD Countdown 2030 papers reported change in NCD mortality from 2010 to 2016. One of these attributed changes in NCD mortality to broad groups of causes of deaths (eg, all circulatory diseases and all cancers). The other used simulation analysis to calculate how much NCD mortality would decline if deaths from different conditions changed at the same rate as in well performing countries. The primary outcome of these analyses excluded deaths outside the age range of 30–70 years or from causes other than cardiovascular diseases, cancers, diabetes, and chronic respiratory diseases. Some papers from the Global Burden of Diseases, Injuries and Risk Factors Study reported mortality for NCD causes of death alongside other (non-NCD) conditions. We did not identify any global study that systematically compared recent trends in NCD mortality with those in preceding decades or benchmarked country-level changes against comparator countries, especially with attribution to specific NCD causes of death.

Added value of this study

To our knowledge, this is the first analysis not only to report change in NCD mortality at the national level across time for all countries but also to benchmark national performance against each country's own historical performance and against regional best performers. We systematically attributed change in overall NCD mortality, and its variations between time periods and countries, to specific causes of death and age groups.

Implications of all the available evidence

NCD mortality has improved for most countries, with heterogeneous magnitudes of change across the world. Many countries showed a slowdown or reversal of progress earlier in the millennium. Performance in reducing NCD mortality was rarely dominated by one NCD cause of death, and often resulted from a combination of changes in multiple diseases. Many NCDs with well established interventions and with large declines in the first decade of the millennium saw a slowdown or reversal of their decline after 2010. These patterns point towards underinvestment in and underutilisation of effective interventions that were rolled out late in the 20th century, or towards these interventions not reaching people most in need.

Typhoid fever is a life-threatening infection caused by the bacterium Salmonella Typhi. It is usually spread through contaminated food or water. Once Salmonella Typhi bacteria are ingested, they multiply and spread into the bloodstream.

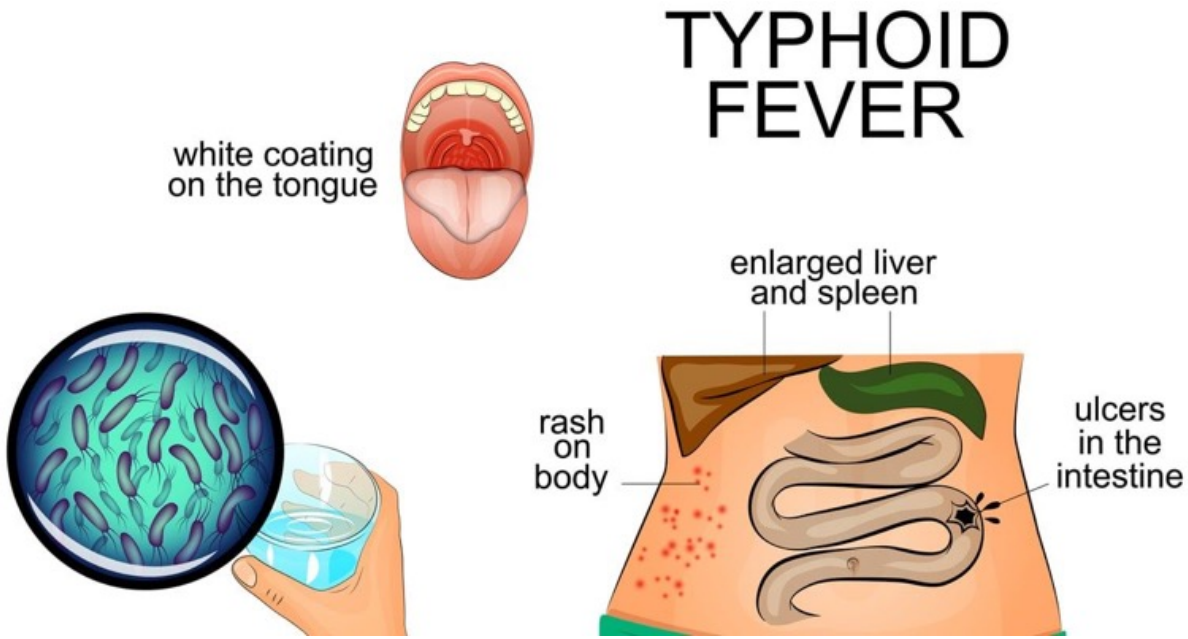

Enteric (typhoid and paratyphoid) fever

Enteric fever, caused by the human-restricted bacteria *Salmonella enterica* serovar Typhi (typhoid) and *Salmonella enterica* serovar Paratyphi A, B, and C (paratyphoid), affects persons residing in, or travelling from, areas lacking safe water, sanitation, and hygiene infrastructure. Transmission is by the faecal–oral route. A gradual fever onset over 3–7 days with malaise, headache, and myalgia is typical. Symptoms can be altered by previous antimicrobial use. Life-threatening complications can arise in the second week of untreated illness. Differentiation from other febrile illnesses is challenging. Blood or bone marrow culture remain reference standard diagnostic methods, despite the low sensitivity of blood culture. Azithromycin, ciprofloxacin (excepting cases originating in south Asia due to drug resistance), or ceftriaxone are recommended treatment options for both typhoid and paratyphoid; however, choice should be guided by local resistance patterns. Ciprofloxacin-resistant and ceftriaxone-resistant typhoid is common in Pakistan. Three vaccine types are available for prevention of typhoid disease, including the newer, more effective typhoid Vi-conjugate vaccines. Vaccination as well as water, sanitation, and hygiene measures are cornerstones of prevention.

Panel 1: **Terminology and definitions**

Definitions of drug resistance patterns

- Multidrug resistant: resistant to chloramphenicol, amoxycillin, and trimethoprim–sulphamethoxazole
- Fluoroquinolone non-susceptible: reduced susceptibility to ciprofloxacin (minimum inhibitory concentration >0·06 mg/L); resistance to nalidixic acid or pefloxacin is a marker
- Extensively drug resistant: resistant to chloramphenicol, amoxycillin, trimethoprim–sulphamethoxazole, ciprofloxacin, and ceftriaxone

WHO case definitions

- Acute typhoid fever: laboratory confirmation by culture or molecular methods of *Salmonella enterica* serotype Typhi (S Typhi) or detection of S Typhi DNA from a normally sterile site
- Relapse of typhoid fever: laboratory confirmation of S Typhi from a normally sterile site within 1 month of completing an appropriate course of antimicrobial treatment and resolution of symptoms
- Chronic typhoid carrier: evidence of shedding of S Typhi (positive stool culture or PCR) at least 12 months after finishing an appropriate course of antimicrobial treatment and the resolution of symptoms following a laboratory-confirmed episode of acute disease or two stool samples 12 months apart positive for S Typhi
- Convalescent carrier: evidence of shedding of S Typhi (positive stool culture or PCR) 1–12 months after finishing an appropriate course of antimicrobial treatment and the resolution of symptoms following a laboratory-confirmed episode of acute typhoid fever
- Suspected case of typhoid: fever for at least 3 out of 7 consecutive days in an endemic area or following travel from an endemic area, or fever for a least 3 out of 7 consecutive days within 28 days of being in household contact with a confirmed case of typhoid fever

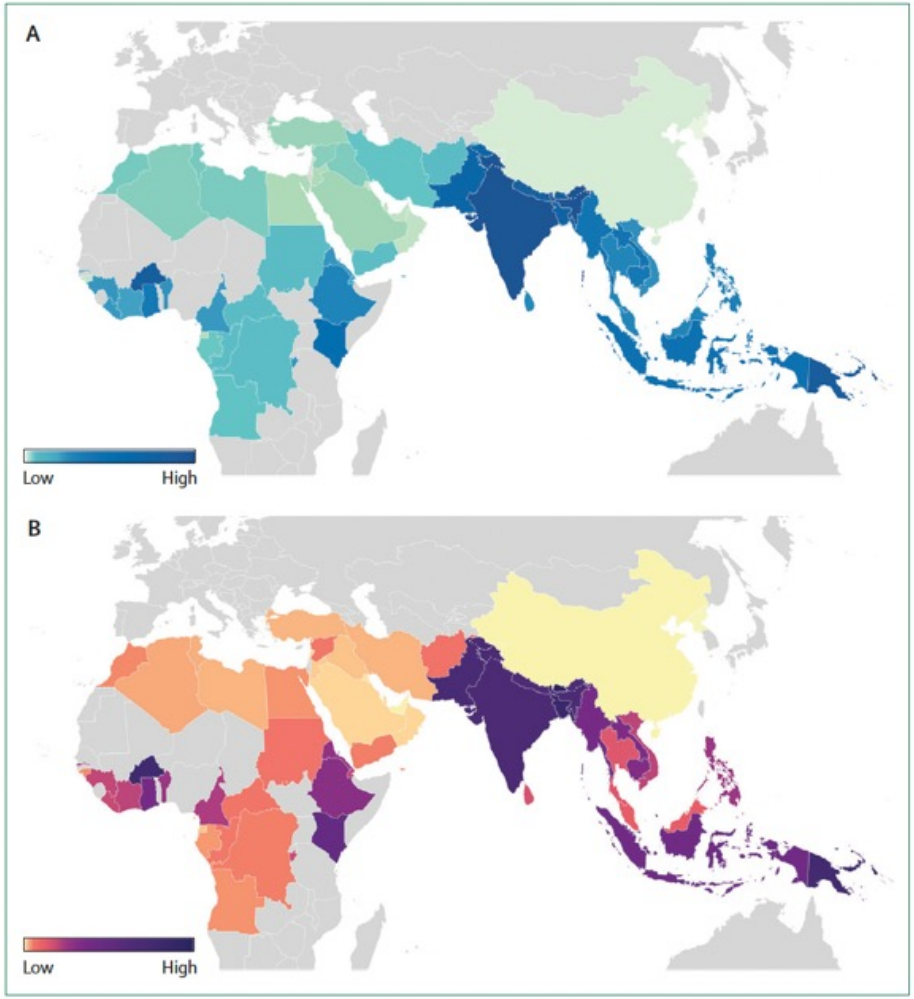

Figure 1: **Age-standardised incidence and mortality of enteric fever**
Age-standardised incidence (panel A) and mortality (panel B) of enteric fever in 75 endemic countries, per data from 2021. Reproduced from Piovani et al,[4] by permission of the authors.

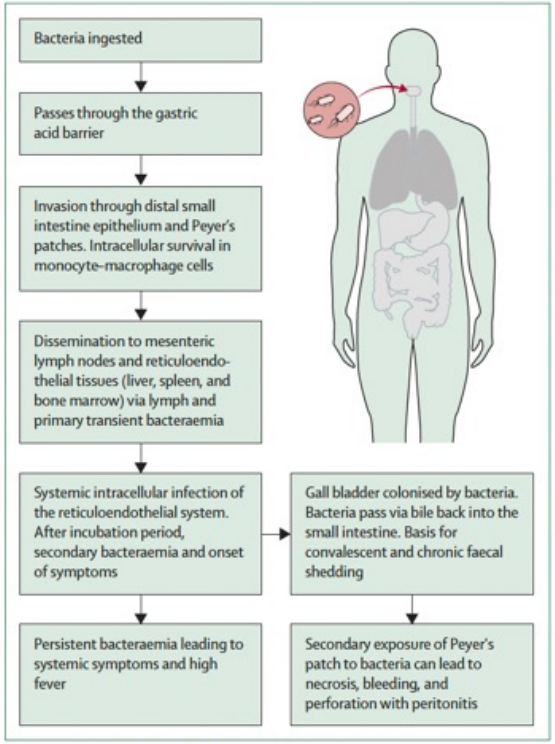

Figure 2: Stages in the pathophysiology of enteric fever

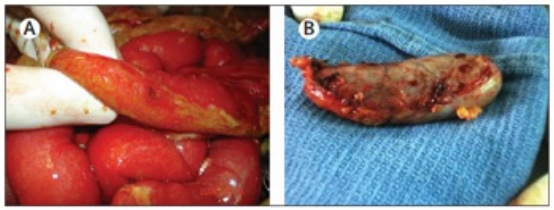

Figure 3: Typhoid-related intestinal perforation and diseased gall bladder
(A) A single perforation in the terminal ileum of a child in Viet Nam seen at laparotomy due to typhoid fever infection. (B) Diseased gall bladder removed from a Nepalese patient with chronic faecal carriage; *Salmonella enterica* serovar Typhi was isolated from the gall bladder contents.

General features
- Fever
- Malaise
- Myalgia
- Arthralgia
- Poor appetite

Respiratory
- Dry cough
- Wheeze
- Bronchitis
- Pneumonia

Gastrointestinal
- Abdominal pain
- Abdominal distension
- Nausea
- Vomiting
- Anorexia
- Constipation
- Diarrhoea
- Intestinal perforation
- Gastrointestinal bleeding

Liver, spleen, and gall bladder
- Hepatosplenomegaly
- Hepatitis
- Jaundice
- Cholecystitis
- Chronic faecal carriage

CNS
- Headache
- Mental dullness
- Delirium
- Encephalopathy
- Febrile seizures
- Meningitis
- Psychosis
- Movement disorders

Cardiovascular
- Asymptomatic ECG changes
- Relative bradycardia
- Myocarditis
- Haemodynamic shock
- Endocarditis

Renal
- Cystitis
- Nephritis
- Acute kidney injury

Haematological
- Anaemia
- Thrombocytopenia
- Disseminated intravascular coagulation

Other
- Rose spots
- Septic arthritis
- Osteomyelitis
- Focal abscess (eg, parotitis, brain, spleen, and kidney)

Figure 4: Signs, symptoms, and complications in enteric fever
Common signs and symptoms in black, complications in red.
ECG=electrocardiogram.

Panel 2: Clinical case

A male health-care worker in India, aged 34 years and previously well, presented to a hospital in south India with 5 days of fever up to 39°C, rigors, myalgia, and anorexia. There was no history of abdominal pain, nausea, vomiting, diarrhoea, cough, dyspnoea, altered sensorium, seizure, or focal neurological deficits. He had no recent travel and had not consumed street food. His temperature on admission was 37·7°C, pulse 110 beats per minute, blood pressure 110/80 mm Hg, respiratory rate 20 breaths per minute, and Glasgow Coma Scale score of 15. Systems examination was normal, with the exception of a coated tongue. The patient was admitted, started on empirical treatment with 1 g of azithromycin once daily and intravenous paracetamol. His laboratory testing reported C-reactive protein of 92·5 mg/L (normal range <5 mg/L) and normal complete blood count, liver transaminases, urea, and creatinine. Rapid diagnostic tests for scrub typhus, malaria, microfilariae, and dengue were negative. A chest x-ray and abdominal pelvic ultrasound were normal. His blood culture was positive after 14 h with a Gram-negative bacillus seen on microscopy; the isolate was subsequently confirmed to be *Salmonella enterica* serovar Typhi, susceptible to azithromycin and ceftriaxone and resistant to ciprofloxacin. The patient continued with azithromycin and remained febrile until day 4 of admission. Azithromycin was continued for a total of 7 days, at which point the patient was discharged having made a full recovery.

	First-line treatment	Alternative treatment
Uncomplicated enteric fever		
Unknown susceptibility	Azithromycin, 20 mg/kg per day, 7–10 days	--
Fully susceptible	Ciprofloxacin, 20 mg/kg per day, 7–10 days	Chloramphenicol*, 50–75 mg/kg per day, 14–21 days; amoxicillin, 75–100 mg/kg per day, 14–21 days; trimethoprim-sulphamethoxazole†, 8–40 mg/kg per day‡, 14–21 days; cefixime, 20 mg/kg per day, 7–14 days; ofloxacin 10–15 mg/kg per day, 7–10 days; levofloxacin 10–15 mg/kg per day, 7–10 days
Multidrug resistant§	Ciprofloxacin, 20 mg/kg per day, 7–10 days	Cefixime, 20 mg/kg per day, 7–14 days; azithromycin, 20 mg/kg per day, 7–10 days; ofloxacin 10–15 mg/kg per day, 7–10 days; levofloxacin 10–15 mg/kg per day, 7–10 days
Fluoroquinolone non-susceptible¶	Azithromycin, 20 mg/kg per day, 7–10 days	--
Extensively drug resistant||	Azithromycin, 20 mg/kg per day, 7–10 days	--
Severe enteric fever requiring parenteral treatment†† **		
Unknown susceptibility	Ceftriaxone, 50–75 mg/kg per day, 10–14 days	--
Fully susceptible	Ciprofloxacin‡‡, 20 mg/kg per day, 10–14 days	Ceftriaxone, 50–75 mg/kg per day, 10–14 days
Multidrug resistant§	Ciprofloxacin‡‡, 20 mg/kg per day, 10–14 days	Ceftriaxone, 50–75 mg/kg per day, 10–14 days
Fluoroquinolone non-susceptible¶	Ceftriaxone, 50–75 mg/kg per day, 10–14 days	Azithromycin§§, 20 mg/kg per day, 10–14 days
Extensively drug resistant||	Meropenem, 60 mg/kg per day, 10–14 days	Azithromycin§§, 20 mg/kg per day, 10–14 days

Culture and susceptibility result often unavailable; empirical treatment should be based on regional knowledge of susceptibility patterns.[91,104,105,107–109] *Can cause bone marrow suppression, oral route preferred. †Inexpensive, can cause allergic reactions and nephrotoxicity, not suitable during pregnancy or for children younger than 2 years. ‡8 mg/kg trimethoprim and 40 mg/kg sulphamethoxazole. §Resistant to chloramphenicol, amoxycillin, trimethoprim–sulphamethoxazole. ¶Non-susceptible to ciprofloxacin (nalidixic acid or pefloxacin resistant or ciprofloxacin resistant by disk testing). ||Resistant to chloramphenicol, amoxycillin, trimethoprim-sulphamethoxazole, ciprofloxacin, and ceftriaxone. **In intestinal perforation, antimicrobial therapy should cover other aerobic and anaerobic gastrointestinal bacteria. ††In severe typhoid (characterised by delirium, obtundation, coma, or shock) dexamethasone can be beneficial; one 3 mg/kg dose dexamethasone infused intravenously over 30 min, followed by eight doses of 1 mg/kg every 6 h. ‡‡Ofloxacin and levofloxacin are effective alternatives. §§Consider combining meropenem with azithromycin.

Table 1: **Antimicrobial treatment options for enteric (typhoid and paratyphoid) fever**

	Mechanism and type	Dose and route	Eligible persons	Protective efficacy*
Ty21a	Live attenuated, Ty2 strain of S Typhi	3 or 4 oral doses on alternate days†	Age ≥6 years; immunocompetent non-pregnant	43% (30–55) at 1–5 years‡
Vi-PS	Purified Vi capsular polysaccharide of Ty2 S Typhi strain	Single injection	Age ≥2 years	58% (44–69) at 1–3 years‡
TCV (Vi-TT)	Subunit, Vi capsular polysaccharide linked to tetanus toxoid	Single injection	Age 6 months to 65 years	83% (77–88) at 1–2 years§; 78% (66–86) at 4 years¶; 54% (13–76) at 3–5 years‖
TCV (Vi-DT)	Subunit Vi capsular polysaccharide linked to diphtheria toxoid	Single injection	Age 6 months to 45 years	Pre-approval based on immunogenicity data**
TCV (Vi-CRM_{197})	Subunit Vi capsular polysaccharide linked to CRM_{197}	Single injection	Age 6 months to 45 years	Pre-approval based on immunogenicity data**

S Typhi=*Salmonella enterica* serotype Typhi. *Data are percentage (95% CI). †Canada and the USA recommend a 4-capsule course. ‡Systematic review and meta-analysis, calculated as: (1–risk ratio) × 100%.[5] §Randomised controlled trials and adjusted cluster randomised controlled trial, calculated as: (1–incidence rate ratio) ×100%.[5] ¶Randomised controlled trial in children in Malawi.[139] ‖Extrapolated medium-term efficacy from a cluster randomised controlled trial in Bangladesh.[140] **WHO prequalified vaccines.[135]

Table 2: **Current prequalified vaccines for typhoid fever**

Conclusions

Case management of enteric fever remains challenging. Current diagnostic tests for acute enteric fever do not have the diagnostic accuracy to be reliably used at the point of care, resulting in overuse of antimicrobials and empiric treatment.[8] A cheap, reliable, and accurate enteric fever diagnostic would provide a step change in treatment and disease control.[147] There is a looming threat of further antimicrobial resistance, and steps to prepare with data on the efficacy of alternative antimicrobials for treatment are needed.[9,10,129] Effective antimicrobial treatments are needed that cure symptoms but also stop shedding of bacteria in faeces that drives onward transmission.[21] Considering the high level of adaptation of these bacteria to a narrow niche, with humans the only natural host and reservoir,[33] the deployment of typhoid conjugate vaccines, strengthening of WASH infrastructure, development of accurate point of care diagnostics, provision of effective antimicrobial regimens, and novel approaches to the detection and treatment of chronic carriers, could make the elimination of enteric fever an achievable goal.[148]

An oncolytic virus is a virus, naturally occurring or genetically modified, that selectively infects and destroys cancer cells while leaving healthy cells unharmed. This process, known as oncolysis, triggers an immune response against the tumor cells, acting as an "in situ" or tumor vaccine. Oncolytic viruses can be used in conjunction with other cancer therapies, and their ability to deliver therapeutic agents or stimulate the immune system makes them a promising approach in cancer treatment.

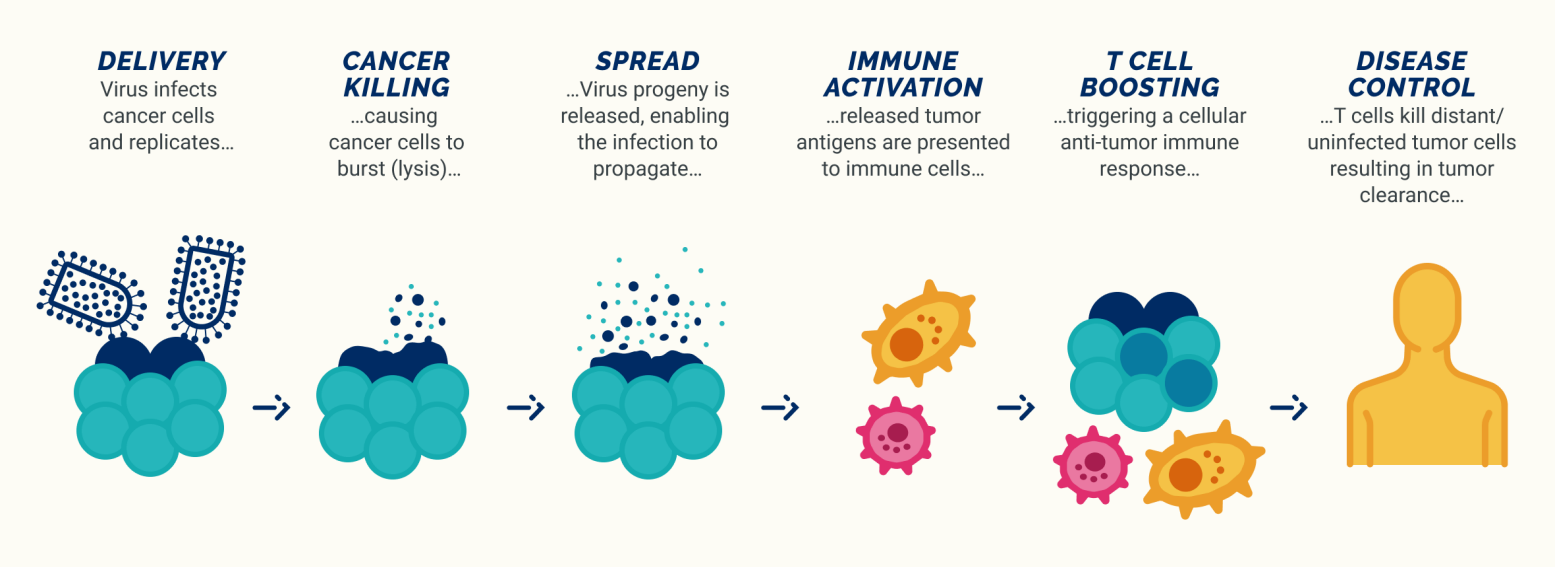

Oncolytic viruses as anticancer agents: clinical progress and remaining challenges

Immunotherapy has transformed the treatment of cancer, yet many patients do not have response or lasting benefit. Strategies to overcome resistance remain of crucial importance. Oncolytic viruses offer a promising approach, with the unique ability to selectively replicate within (and to destroy) cancer cells, remodel the immunosuppressive tumour microenvironment, and stimulate antitumour immunity. Interest in the potential of oncolytic viruses has grown steadily over the past two decades, fuelled by advances in cancer immunology and viral engineering. However, clinical translation has not kept pace, and although a plethora of promising new constructs have entered clinical testing, several barriers continue to restrict widespread clinical implementation. This Therapeutics paper highlights key milestones in oncolytic virus clinical development, discusses the challenges that remain, and, through clinical reflection, considers how future research might be streamlined to achieve meaningful benefit for patients.

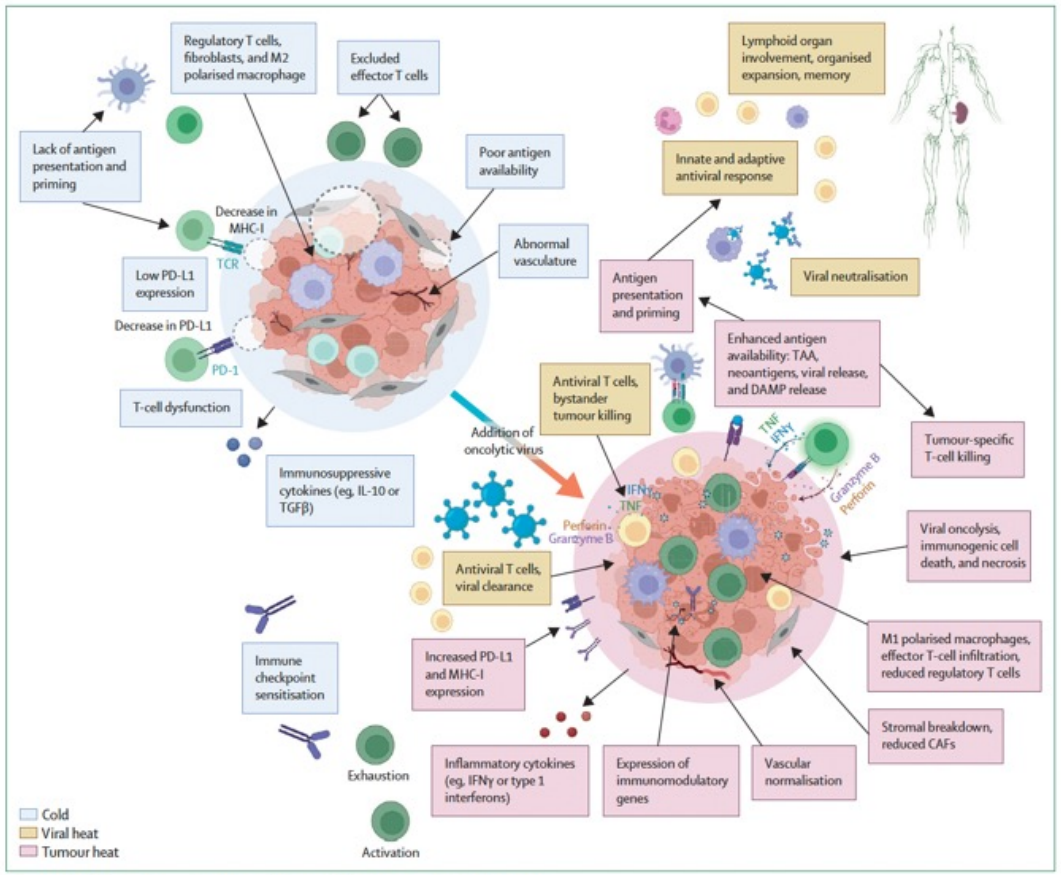

Figure 1: **Oncolytic viruses—increasing the heat of the tumour microenvironment**

Cold refers to low immune infiltration. Viral heat is the enrichment of components of the viral response including antiviral T cells. Tumour heat is the enrichment of components of an antitumour immune response including antitumour T cells. Oncolytic viruses can exert anticancer effects through direct infection and viral oncolysis, and by stimulation of an anticancer immune response through inflammatory modification of the tumour microenvironment, and priming of T cells against tumour antigens released through oncolytic virus-mediated immunogenic cell death. Delivery of oncolytic viruses, either via intratumoural or intravenous injection has been shown to lead to diverse inflammatory changes within the tumour microenvironment, including T-cell infiltration, inflammatory cytokine production, dendritic maturation, enhanced antigen presentation and priming, stromal remodelling, and vascular normalisation. However, there is complex interaction and competition within an oncolytic virus-treated tumour microenvironment between antitumour and antiviral immunity. Elements of antiviral immunity might be beneficial, including bystander killing, trafficking of immune cells to or from lymphoid organs, inflammatory cytokine secretion and cross-priming; however, viral antigens are commonly immunodominant, and might eclipse true antitumour immunity. CAF=cancer associated fibroblasts. DAMP=damage-associated molecular patterns. MHC-I=major histocompatibility complex class 1 molecules. TAA=tumour associated antigens. TCR=T-cell receptor.

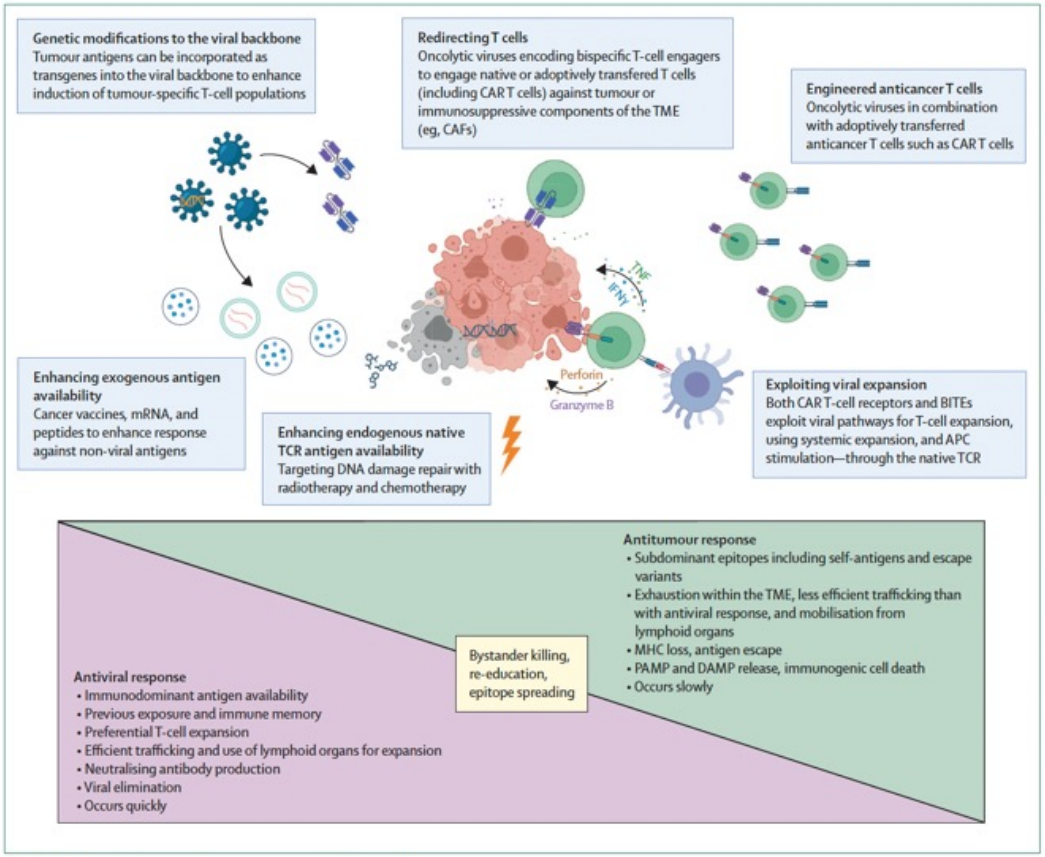

***Figure 2*: Antiviral versus antitumour immunity—redirecting the antiviral immune response**
Oncolytic viruses are, primarily, viruses rather than inert immunotherapeutic agents. To generate a response within a tumour there is a delicate balance between the adaptive immune response against the virus, and the tumour. The antiviral response is heavily evolved and efficient and often occurs quickly to facilitate pathogen clearance. It is associated with often immunodominant viral antigens, rapid expansion of CD4 and CD8 T cells and initiation of a B-cell or antibody response. Antitumour immunity classically occurs more slowly, is often associated with subdominant tumour antigens (many of which are tolerised, self-antigens) and escape variants. There is frequent T-cell exhaustion within the tumour microenvironment, and trafficking and systemic expansion might be less efficient than viral immunity. There are elements of overlap, where an antiviral immune response might promote expansion of tumour-specific T cells, such as bystander killing of tumour cells and T-cell re-education and epitope spreading. Several strategies aim to exploit the oncolytic virus-induced dominant antiviral response to promote more effective tumour-cell killing. These strategies include redirection of T cells (such as with engineered CAR T-cell receptors, or BITEs) enhancement of antigen availability in vaccine strategies, that use the oncolytic virus-inflamed tumour microenvironment for more effective priming. APC=antigen-presenting cells. BITE=bispecific T-cell engager. CAF=cancer associated fibroblasts. CAR=chimeric antigen receptors. DAMP=damage-associated molecular patterns. MHC=major histocompatibility complex. PAMP=pathogen-associated molecular patterns. TCR=T-cell receptor. TME=tumour microenvironment.

	Delivery	Backbone	Modifications
T-VEC	Intratumoural	HSV-1	*ICP34.5* deletion; *ICP47* deletion; *GM-CSF* insertion
Teserpaturev	Intratumoural	HSV-1	*ICP34.5* deletion; *ICP47* deletion; *ICP6* inactivation
RP1	Intratumoural	HSV-1	*ICP34.5* deletion; *ICP47* deletion; *GM-CSF* insertion; *GALV* insertion
RP2	Intratumoural	HSV-1	*ICP34.5* deletion; *ICP47* deletion; *GM-CSF* insertion; *GALV* insertion; encodes *CTLA-4*
CAN-3110	Intratumoural	HSV-1	Retains one copy of *ICP34.5* under control of nestin promoter
T3011	Intratumoural	HSV-1	One copy of *ICP34.5* deleted; retains *ICP47*; *IL12* and anti-PD-1 monoclonal antibody insertion
CAN-2409	Intratumoural	Replication-defective adenovirus	Encodes HSV-thymidine kinase
Nadofaragene firadenovec	Intravesical	Replication-defective adenovirus	Delivers *IFNα2b*
Cretostimogene grenadorepvec	Intravesical	Adenovirus (Ad5)	Promoter for viral replication under control of *E2F*; *GM-CSF* insertion
Tasadenoturev	Intratumoural	Adenovirus (Ad5)	*RGD* insertion; *E1A* deletion
Igrelimogene litadenorepvec	Intratumoural or intravenous	Adenovirus (chimeric Ad5–Ad3)	Modified fibre protein to avoid neutralisation; encodes TNF and IL-2
CAdVEC	Intratumoural	Adenovirus and HD-Ad	Encodes IL-12 and anti-PD-L1 antibody
Vocimagene amiretropvec	Intratumoural	Replication-competent retrovirus	Encodes yeast cytosine deaminase (prodrug activating)
Pelareorep	Intratumoural	Reovirus	Unmodified
Pexastimogene devacirepvec	Intratumoural	Vaccinia virus	Thymidine kinase gene-inactivated; *GM-CSF* insertion
H-1 parvovirus	Intratumoural or intravenous	Parvovirus	Unmodified

Ad3=adenovirus serotype 3. Ad5=adenovirus serotype 5. HD-Ad=helper-dependent adenoviral vectors. HSV-1=herpes simplex virus type 1. T-VEC=talimogene laherparepvec.

Table 1: **Examples of viral agents under clinical development**

Panel 1: **Clinical considerations—lessons learned from the approval of talimogene laherparepvec and beyond**

Treatment earlier in the course of disease

Subgroup analysis of the OPTiM phase 3 study evaluating talimogene laherparepvec (T-VEC) in advanced melanoma showed that 92% of patients with complete response had earlier stage disease (stage IIIb to stage IVM1a *vs* stage IVM1b or IVM1c), providing rationale for the use of oncolytic viruses earlier in the disease course.[20,21] Clinically, adenoviral vector nadofaragene firadenovec (Adstiladrin; Ferring Pharmaceuticals, Bridgewater, NJ, USA) has been approved for the treatment of early non-muscle invasive bladder cancer, and neoadjuvant T-VEC has shown promise in melanoma and triple negative breast cancer, with several other neoadjuvant oncolytic virus studies underway. With well documented safety and tolerability, including in combination with chemotherapy and immunotherapy (which are now established pillars of neoadjuvant therapy), further evaluation of the efficacy of oncolytic viruses in early stage disease is warranted.

Treatment for patients at high risk of therapeutic morbidity

The approval of T-VEC has enabled real-word studies evaluating oncolytic virotherapy in patients who would conventionally not be represented in trial cohorts (eg, advanced age or significant comorbidities). Therapeutic regimens such as dual immune checkpoint inhibitors are associated with substantial morbidity, and older age (age >75 years), or poor Eastern Cooperative Oncology Group performance status (>2) are negative prognostic indicators. Real-world studies of T-VEC have shown safety in older cohorts (eg, median age 83)[37] with low rates of adverse events, and case reports have shown safety of T-VEC in patients with heart and renal transplants. Oncolytic herpes simplex virus-1 RP1 was also shown to be well tolerated in recipients of solid organ transplants with advanced cutaneous malignancies. Oncolytic viruses could therefore be an appealing therapeutic option for those with comorbidities, older age, or poor performance status.

Consideration of dose scheduling and choice of combination

T-VEC did not show clinical benefit in combination with anti-PD-1 agent pembrolizumab in the phase 3 MASTERKEY-265 study, despite promise in early-phase studies.[1] This (and other trials of immune checkpoint inhibitors in combination with oncolytic viruses) highlighted the potential importance of dose scheduling. In this study, agents were delivered concomitantly, whereas previous early-phase trials used a sequential approach. Few preclinical studies (and no clinical studies) have evaluated scheduling comparisons; however, concomitant therapy could favour a dominant viral response, or lead to inhibitory inflammation. Optimal scheduling is also a consideration for incorporation of immunomodulatory transgenes, leading to expression at the same time in the same biological space. Further, MASTERKEY-265 opted for a combination with pembrolizumab (anti-PD-1), while T-VEC in combination with ipilimumab had also shown promise in a comparative phase 2 study versus ipilimumab alone. The right immune checkpoint inhibitor in the right context remains to be elucidated, and a focus on deeper translational understanding of complex combinations within early phase studies will be imperative to streamline effective clinical translation.

	Viral agent	Approval location (year)	Approval context	Registry studies
Andtbacka et al (2015);[29] Andtbacka et al (2019)[36]	Talimogene laherparepvec (T-VEC)	USA (2015); Europe (2015); and Israel (2017)	Unresectable stage IIIb to stage IV melanoma	Phase 3; DRR 19·3% (57 of 295 patients) for T-VEC *vs* 1·4% (2 of 141 patients) for GM-CSF (unadjusted odds ratio 16·6; 95% CI 4·0–69·2; p<0·0001); ORR 31·5% for T-VEC *vs* 6·4% for GM-CSF; median OS 23·3 months (95% CI 19·5–29·6) *vs* 18·9 months for GM-CSF (95% CI 16·0–23·7)
Todo et al (2022)[50]	Teserpaturev	Japan (2021)	Refractory high-grade glioma	Phase 2; median PFS 4·7 months (95% CI 3·3–6·1); 1-year survival 84·2% (16 of 19 patients, 95% CI 60·4–96·6); median OS 20·2 months (95% CI 16·8–23·6)
Boorjian et al (2021)[51]	Nadofaragene firadenovec (Adstiladrin)	USA (2022)	BCG-non-responsive NMIBC	Phase 3; CR 53·4% (55 of 103 patients) at 3 months; maintained in 25 (45·5%) of 55 patients at 12 months

CR=complete response. DRR=durable response rate. NMIBC=non-muscle invasive bladder cancer. ORR=objective response rate. OS=overall survival. PFS=progression-free survival.

Table 2: **T-VEC and beyond—viral agents approved since 2015**

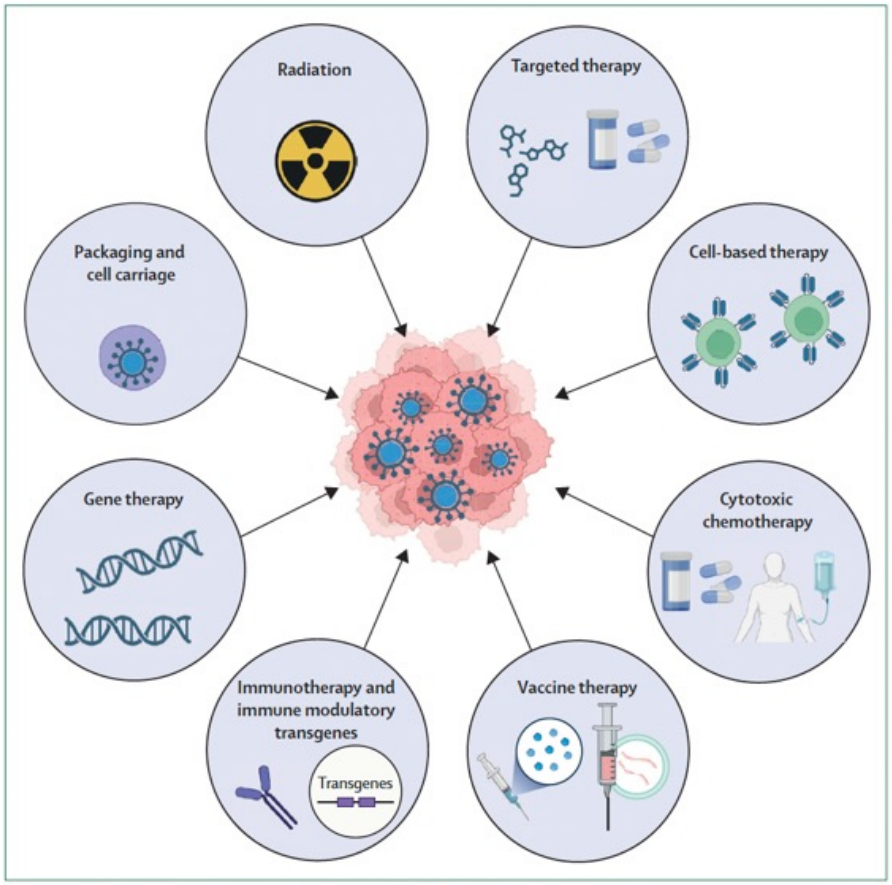

Figure 3: **Oncolytic viruses in combination with other treatment modalities**
Oncolytic viruses do not have universal therapeutic potency as single agents; however, they are well tolerated, with non-overlapping side-effects, and have diverse effects on the tumour microenvironment, making them an appealing addition to the therapeutic armoury when used in combination with other treatments. Combinatorial strategies currently under investigation include immunotherapy, conventional chemotherapy, cancer vaccines, cell therapy, and targeted therapy. More research is needed, including translational mechanistic readouts from clinical trials of combinations, to evaluate where oncolytic viruses as a tool might be applied most effectively. With broad and ever-complex combinations, questions such as scheduling become of paramount importance, and testing this huge variety of constructs, combinations, and schedules in a clinical setting remains a challenge.

	Agent	Phase	Disease setting	Key outcomes
Oncolytic viruses as monotherapies				
HSV-1				
Senzer et al (2009)[58]	T-VEC	2	Stage IIIc to stage IVM1c melanoma	ORR was 26% (13 of 50 patients); OS was 58% at 1 year; 92% responses maintained for between 7 months and 31 months
Andtbacka et al (2015);[26] Andtbacka et al (2019)[30]	T-VEC	3	Stage IIIb to IV melanoma	DRR was 19·3% (57 of 295 patients) for T-VEC vs 1·4% (two of 141 patients) for subcutaneous GM-CSF (unadjusted odds ratio, 16·6; 95% CI 4·0–69·2; p<0·0001); ORR 31·5% for T-VEC vs 6·4% for GM-CSF; median OS was 23·3 months for T-VEC (95% CI 19·5–29·6) vs 18·9 months for subcutaneous GM-CSF (95% CI 16·0–23·7); median time to CR was 8·6 months
Stahlie et al (2022)[60]	T-VEC	Meta-analysis (eight studies)	Stage III to stage IV melanoma	For stage IIIb to stage IVM1a disease, CR was 41% (141 of 344 patients; 95% CI 25–58) and ORR was 64% (181 of 283 patients; 95% CI 41–82); for stage IVM1b to stage IVM1c disease, CR was 4% (six of 151 patients; 95% CI 2–9) and ORR was 9% (12 of 135 patients; 95% CI 3–27); 0–11% of participants across all studies had severe adverse events (grade 3–4)
Dummer et al (2021)[61]	T-VEC	2	Neoadjuvant; resectable stage IIIb to stage IVM1a melanoma	pCR was 17·1% for T-VEC (n=76); 2-year RFS was 29·5% for T-VEC vs 16·5% for surgery alone (HR 0·75, 80% CI 0·58–0·96); benefit maintained at 3 years; response correlated with increased CD8 density
Todo et al (2022)[62]	Teserpaturev	1/2	High-grade glioma	n=13 patients; median OS was 7·3 months (95% CI 6·2–15·2); median PFS was 8 days from last G47 administration; 1-year survival from last G47 administration was 38%
Ling et al (2023)[63]	CAN-3110	1	Recurrent glioblastoma	Single arm, n=41 patients; median OS was 11·6 months (95% CI 7·8–14·9); enhanced survival in baseline seropositive patients (14·2 months in HSV-1 seropositive patients [95% CI 9·5–15·7] vs 7·8 months in HSV-1 seronegative)
Adenovirus				
Klaassen (2024)[64]	Cretostimogene grenadorepvec	3	BCG-unresponsive high-risk non-muscle invasive bladder cancer	CR was 75·2% (75 of 102 patients) at any time in the study
Boorjian et al (2021)[31]	Nadofaragene firadenovec	3	BCG-unresponsive non-muscle invasive bladder cancer	CR was 53·4% (55 of 103 patients with carcinoma in situ) within 3 months, maintained in 45·5% (25 of 55 patients) patients at 12 months; micturition urgency was the most common grade 3 or grade 4 TRAE (2 of 157 patients)
van Putten et al (2022)[65]	Tasadenoturev	1	Recurrent glioblastoma	Median PFS was 82 days (range 28–287); median OS was 129 days (range 68 days to >7 years); OS >6 months was 32% (six of 19 patients), one patient was alive at 2·5 years and another at 7·5 years
Replication-competent retrovirus				
Cloughesy et al (2020)[7]	Vocimagene amiretrorepvec	2 or 3	High-grade glioma	No significant improvement on physicians' choice therapy
Reovirus				
Samson et al (2018)[66]	Pelareorep	1	Primary and metastatic brain tumours	Infection of tumour cells after intravenous delivery; upregulation of IFNγ gene expression and PD-1–PDL-1 axis
Vaccinia virus				
Samson et al (2022)[68]	Pexa-Vec	Biological endpoint	Neoadjuvant; metastatic colorectal cancer or melanoma liver lesions, before resection	9 patients; pexastimogene devacirepvec found in tumours; 22% (two of nine patients) had tumour necrosis
Oncolytic viruses in combination therapy				
Checkpoint blockade				
Ribas et al (2017)[69]	T-VEC plus pembrolizumab	2b	Advanced melanoma	ORR was 62% (13 of 21 patients); CR was 33% (7 of 21 patients); response was associated with IFNγ gene expression, PD-L1 expression, and CD8 infiltration was elevated after treatment
Chesney et al (2023)[70]	T-VEC plus pembrolizumab	3	Stage IIIb to stage IVM1c melanoma	No significant improvement in OS or PFS; ORR was 48·6% (168 of 346 patients) for combination therapy vs 41·3% (143 of 346 patients) for pembrolizumab alone; grade 3 or higher TRAE in 20·7% patients who had combination therapy vs 19·5% patients who had pembrolizumab alone
Chesney et al (2018)[29]	T-VEC plus ipilimumab	2	Stage IIIb to stage IV melanoma	ORR was 39% (38 of 98 patients) for combination therapy vs 18% (18 of 100 patients) for ipilimumab alone; decrease in visceral lesions in 52% patients in the combination group vs 23% of patients treated with ipilimumab alone; grade 3 or higher TRAE in 45% patients who had combination therapy vs 35% patients who had ipilimumab alone
Harrington et al (2020)[28]	T-VEC plus pembrolizumab	1b	Head and neck squamous cell carcinoma	PR was 13·9% (5 of 36 patients); median PFS was 3 months (95% CI 2·0–5·8); phase 3 was not pursued
Robert et al (2024)[24]	T-VEC plus pembrolizumab	2	Anti-PD-1 refractory melanoma (primary and acquired resistance in unresectable or metastatic, and progression following adjuvant therapy)	ORR 3·8% (primary resistance; 95% CI 0·1–19·6), 6·7% (acquired resistance; 95% CI 0·2–32·0), 53·3% (recurrence <6 months after adjuvant anti-PD-1; 95% CI 26·6–78·7), 46·7% (recurrence ≥6 months after adjuvant anti-PD-1; 95% CI 21·3–73·4)

(Table 3 continues on next page)

(Continued from previous page)

	Agent	Phase	Disease setting	Key outcomes
Wong et al (2025)[67]	RP1 plus nivolumab	1/2	PD-1 refractory melanoma	n=140 patients; ORR was 32·9% (95% CI 25·2–41·3); CR was 15·0%; median duration of response 33·7 months; OS at 2 years 63·3% (95% CI 53·6–71·5);
Nassiri et al (2023)[18]	Tasadenoturev plus pembrolizumab	1/2	Recurrent glioblastoma	n=49 patients; ORR was 10·4% (95% CI 4·2–20·7); OS at 12 months was 52·7%; median OS was 12·5 months (95% CI 10·1–69·2)
Sacco et al (2023)[83]	RP2 plus nivolumab	1	Refractory uveal melanoma	ORR was 28·6% (4 of 14 patients); favourable safety profile compared to historical studies of dual checkpoint blockaged in a similar cohort
Cytokines				
Ji et al (2023)[84]	T3011 (expressing IL-12 and anti-PD-1 monoclonal antibody)	1	Advanced solid tumours	ORR was 11% (six of 55 patients); no dose-limiting toxic effects; grade 3 or higher TRAE in 2·2% (two of 90 patients)
Santos et al (2023)[85]	Igrelimogene litadenorepvec (encoding IL-2 and TNF)	1	Advanced solid tumours	Disease control in 22% (two of nine patients), including PR in 11% (one of nine patients)
Chemotherapy or radiotherapy				
Arnold et al (2023)[86]	Palareorep plus gemcitabine-nab-paclitaxel in combination with atezolizumab	1/2	Pancreatic cancer	ORR was 62% (eight of 13 patients); confirmed OR 53%
Soliman et al (2023)[48]	T-VEC plus neoadjuvant chemotherapy	2	Neoadjuvant, stage II or stage III triple negative breast cancer	pCR rate was 45·9%; 2-year disease-free rate was 89%
Clark et al (2025)[87]	Palareorep plus paclitaxel and avelumab	2	Hormone receptor positive breast cancer	n=48 (15 patients in paclitaxel group, 16 patients in paclitaxel plus palareorep group, 14 patients in paclitazel plus palareorep plus avelumab group, and three patients in safety run-in group); median PFS was 6·4 months (paclitaxel), 12·1 months (paclitaxel plus palareorep), and 5·8 months (paclitaxel plus palareorep plus avelumab); ORR was 20% (three of 15 patients in paclitaxel group), 31% (five of 16 patients in paclitaxel plus palareorep group), and 14% (two of 14 patients in paclitaxel plus palareorep plus avelumab group)
Candel Therapeutics (2024)[45]	CAN-2409 plus valacyclovir plus chemoradiotherapy	2	Neoadjuvant borderline resectable pancreatic ductal adenocarcinoma	Survival benefit was 28·8 months in patients who had combination therapy vs 12·5 months in patients who received standard of care
Monga et al (2021)[88]	T-VEC plus external beam radiation therapy	2b or 2	Neoadjuvant, soft tissue sarcoma	No dose-limiting toxic effects; no increase in proposed rate of pathological necrosis
Gállego Pérez-Larraya et al (2022)[89]	Tasadenoturev plus radiotherapy	1	Diffuse intrinsic pontine glioma; paediatric (patients aged 3–18 years)	Median OS was 17·8 months
Toulmonde et al (2022)[90]	Pexastimogene devacirepvec plus cyclophosphamide	2	Advanced soft tissue sarcoma	Evidence of systemic immune activation but no patients were progression-free at 6 months; tumour shrinkage on MRI in 75% (nine of 12 patients)
Targeted agents				
Abou-Alfa et al (2023)[91]	Pexastimogene devacirepvec plus sorafenib	3	Advanced hepatocellular carcinoma	Median OS was 12·7 months (95% CI 9·89–14·95) in patients who had combination therapy vs 14·0 months (94% CI 11·01–18·00) in patients who had sorafenib alone; early termination of the study due to futility; 53·7% (117 of 218 patients) had serious adverse events with combination therapy vs 35·5% (77 of 217 patients) had serious adverse events with sorafenib alone
Cell carriage				
Fares et al (2021)[92]	Adenovirus Ad5 NSC-CRAd-S-pk7	1	Malignant glioma, after neurosurgical resection; treatment with radiotherapy and temozolomide was initiated within 10–14 days	Delivered by use of neural stem cells; median PFS was 9·05 months; median OS was 18·4 months; PR in 8% (one of 12 patients)

CR=complete response. DRR=durable response rate. HR=hazard ratio. OR=overall response. ORR=overall response rate. OS=overall survival. pCR=pathological complete response. PFS=progression-free survival. PR=partial response. RFS=relapse-free survival. TRAE=treatment-related adverse events.

Table 3: **Examples of viral agents as monotherapy and in combination**

Panel 2: Optimising patient selection: Tumour subtype and biomarkers—patient selection

Predicting which patients will have dramatic and durable responses to oncolytic virus therapy remains a challenge. However, subgroup analysis of clinical trials is beginning to elucidate select populations who might benefit. This warrants further trials based on individualised tumour phenotype rather than broad cancer type, with deep, translational readouts to aid biomarker discovery and patient selection. For example, patients with head and neck melanoma were seen to have greater benefit with talimogene laherparepvec therapy than the overall study cohort,[20,38] and patients with IDH1 mutant high-grade glioma had a higher rate of response to vocimagene amiretrorepvec (Toca 511) than patients with IDH1 wild type high-grade glioma.[29] Interferon signalling defects have also been associated with resistance to checkpoint therapy, but susceptibility to oncolytic viruses such as herpes simplex virus-1 and vesicular stomatitis virus in preclinical models.[117] More research is needed to understand mechanisms of response and resistance to begin to better stratify patient selection.

Conclusions and future directions

Despite considerable challenges over the last two decades, oncolytic viruses continue to offer considerable promise to the field of oncology. Established and emerging data from the use of T-VEC, along with other virus platforms and encoded transgenes, are providing new insights into patient response, and the number of strategies under development is growing exponentially. Oncolytic viruses continue to be safe and well tolerated, and there is increasing evidence to support their application in particular settings, including in earlier-stage disease.

Methods for seamlessly integrating basket-style trial design into the evaluation of novel agents has been proposed in other settings and could help shorten oncolytic virus clinical timelines. However, this should proceed alongside a preclinical and translational commitment to deeper understanding of the biology of viral therapies in patients. Thus, future careful integration of artificial intelligence, machine learning, and biomarker modelling will be helpful in the analysis of multiomic, longitudinal translational data from clinical trials, to enable construction of cross-tumour biomarker classifiers which might lead towards adaptive personalisation of virotherapy-based treatment schedules.

Solid-state hydrogen storage

involves binding hydrogen within a solid material, such as metal hydrides, carbonaceous materials, or metal-organic frameworks (MOFs), rather than compressing it as a gas or liquefying it. This method offers enhanced safety by eliminating the risk of leaks, high hydrogen storage density through volumetric packing of individual hydrogen atoms, and the potential for lower energy consumption and simpler infrastructure compared to conventional methods. The stored hydrogen can be released by altering temperature and pressure, allowing for a reversible process with broad applications in transportation, energy, and beyond

Ein Hydridion ist ein negativ geladenes Wasserstoffion mit der Formel H^-, das ein zusätzliches Elektron zu einem neutrale Wasserstoffatom aufgenommen hat. Es ist ein starkes Reduktionsmittel und findet sich hauptsächlich in ionischen Hydriden, die durch die Reaktion von Wasserstoff mit stark elektropositiven Metallen wie Natrium oder Kalium gebildet werden. Beispiele für ionische Hydride sind Natriumhydrid (NaH) und Kaliumhydrid (KH).

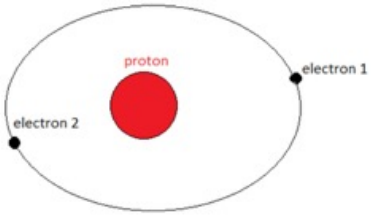

Solid-state hydrogen storage goes electric

A solid electrolyte is a solid-state material, like a polymer, oxide, or sulfide, that conducts ions while being an electron insulator and a mechanical separator.

Broad adoption of hydrogen as a versatile energy carrier is primarily hampered by a lack of safe and compact hydrogen storage. Hydrogen is often stored as compressed gas or cryogenic liquid, which requires high pressures or extremely low temperatures. Metal hydrides—compounds in which hydrogen is chemically bonded to solid metallic or intermetallic hosts—can store hydrogen with a high volumetric density. The inherent thermodynamic stability of these solidstate storage compounds provides safety but also requires impractically high temperatures for hydrogen release. Hirose et al. report an approach that electrochemically “pumps” hydrogen in the form of hydride ions (H–) through a solid electrolyte into or out of a metal hydride. This elegantly circumvents the requirement of high temperature to free hydrogen from the metal hydride, offering a pathway to harness high-capacity hydrogen storage under practical release conditions.

The Nernst equation—a central formula for calculating electrochemical cell potential under a given condition—also illustrates how a small voltage equates to many orders of magnitude change in hydrogen gas pressure, generating a large driving force for hydrogen exchange

Hirose et al. developed a solid electrolyte by compositional tuning of a pseudo-ternary system in which barium, calcium, and sodium atoms form a compound with hydrogen atoms. This electrolyte exhibited good hydride ion conductivity (~2 × 10–5 S/cm) at room temperature, low electronic conductivity (1.3 × 10–9 S/cm), and stability over a suitably wide voltage range. The hydride-conducting electrolyte was sandwiched between a hydrogen-storage electrode and a counter electrode that delivered hydrogen gas to a reservoir (see the figure). This solid-state electrolyte could reversibly insert and extract hydride ions into and out of a diverse array of metal hydrides (such as TiH_2, MgH_2, $NaAlH_4$, $LiAlH_4$, $NaBH_4$, and NaH) at moderate temperatures (60° to 100°C). Notably, magnesium hydride and sodium aluminum hydride electrodes achieved reversible hydrogen adsorption capacities that are close to their theoretical values, maximizing the full storage potential offered by these materials. At 90°C, the electrochemical cell with a magnesium hydride electrode achieved reversible hydrogen storage over 10 cycles (charge and discharge) at >99% of theoretical capacity (~2020 mA·hour/g), although at rather low charge and discharge rates. This achievement demonstrates the feasibility of the electrochemical approach to metal hydride hydrogen storage.

Electrochemical delivery of hydrogen

Metal hydrides can store hydrogen safely with a large volumetric density, but their inherent stability requires impractically high temperatures to release the stored hydrogen for use. A solid-state electrolyte can reversibly insert or extract hydrogen from the hydride at moderate temperatures (60° to 100°C) under an electric potential.

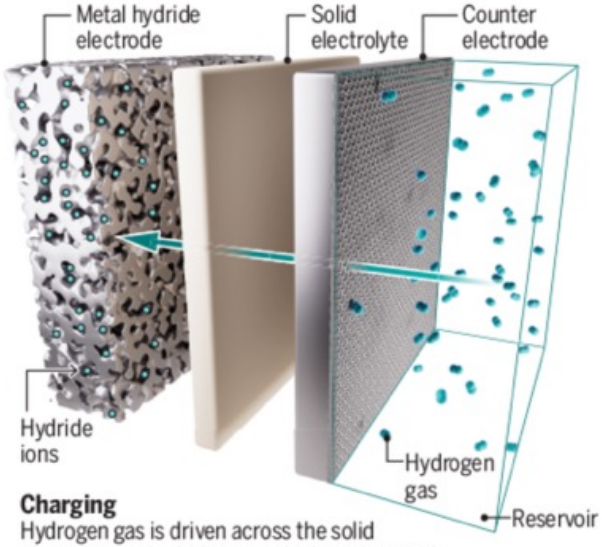

Charging

Hydrogen gas is driven across the solid electrolyte as hydride ions, which are inserted into the metal hydride electrode for storage.

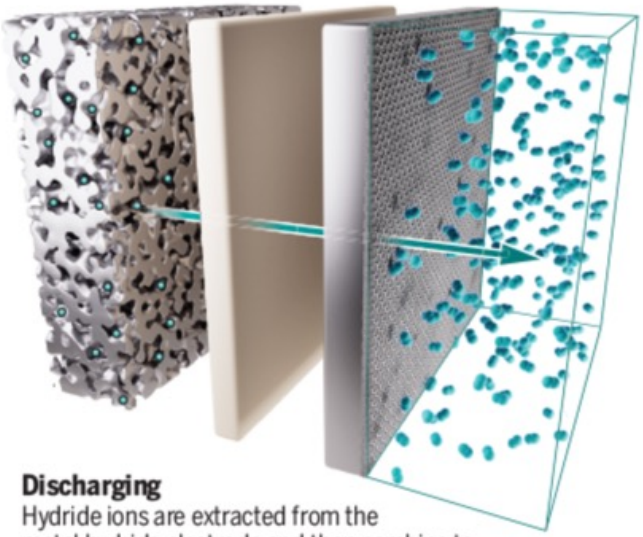

Discharging
Hydride ions are extracted from the metal hydride electrode and then combine to form hydrogen gas at the counter electrode.

The study of Hirose et al. opens new directions to overcome the impractically high temperature requirements imposed by high-capacity metal hydride–based hydrogen-storage systems. Magnesium hydride has a theoretical gravimetric hydrogen-storage capacity (the amount of hydrogen that can be held per total mass) of 7.6 wt %, and much of this capacity was successfully accessed. However, the overall electrochemical cell configuration achieved a capacity of only 0.11 wt %. This is due, in part, to the thick, heavy solid-electrolyte layer (~450 μm) and a low active material ratio (20 wt % metal hydride) in the electrode. Furthermore, Hirose et al. acknowledged that voids in the cold-pressed solid electrolyte permit hydrogen-gas crossover. This leakage leads to a mixed storage mechanism in which the desired electrochemical hydride-ion insertion occurs simultaneously with an uncontrolled thermochemical reaction between the permeated hydrogen gas and the magnesium hydride electrode. The energy efficiency of the electrochemical system is also presently lower than that of thermal methods. The device of Hirose et al. required an energy input of ~81 kJ/mol, which is higher than that for optimized thermal desorption of hydrogen (~72 kJ/mol). The authors note that further engineering of the constituent materials and the electrochemical device (such as by decreasing the electrolyte thickness) could substantially reduce the voltage needed for charging, potentially decreasing the energy requirement down to ~45 kJ/mol, which is considerably lower than that for thermal-based metal hydride storage.

High-capacity, reversible hydrogen storage using H^--conducting solid electrolytes

Hydrogen absorption and desorption in solids are pivotal reactions involved in batteries and hydrogen storage devices. However, conventional thermodynamic and electrochemical hydrogen storage using high-capacity materials suffers from high hydrogen-desorption temperatures and instability of electrolytes. In this work, we explored electrochemical hydride ion (H^-)–driven hydrogen storage and developed a solid electrolyte, anti–α-AgI–type $Ba_{0.5}Ca_{0.35}Na_{0.15}H_{1.85}$, which exhibits excellent H^- conductivity and electrochemical stability. this electrolyte is compatible with several metal-hydrogen electrodes, such as titanim hydride and magnesium hydride (MgH_2), allowing for high-capacity, reversible hydrogen storage at low temperatures. Specifically, Mg–H_2 cells operating as hydrogen storage devices ($Mg + H_2 \rightleftarrows MgH_2$) achieved a reversible capacity of 2030 milliampere hours per gram at 90°C, offering safe and efficient hydrogen electricity conversion and hydrogen storage devices.

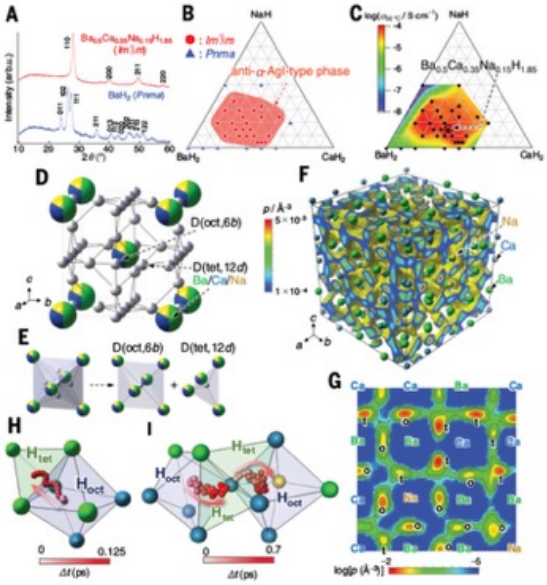

Fig. 1. Structural analysis of the BaH_2–CaH_2–NaH system. (**A**) XRD patterns of BaH_2 (blue) and $Ba_{0.5}Ca_{0.35}Na_{0.15}H_{1.85}$ (red). (**B**) Formation diagram of the cubic *Im3m* (red circles) and orthorhombic *Pnma* (blue triangles) phases in the BaH_2–CaH_2–NaH system. Arb. u., arbitrary units. ($_C$) Heat map of the logarithm of ionic conductivity (σ) at 50°C in the BaH_2–CaH_2–NaH pseudoternary diagram. (**D**) Refined crystal structure of $Ba_{0.5}Ca_{0.35}Na_{0.15}D_{1.85}$. The green, blue, yellow, and gray spheres correspond to the Ba, Ca, Na, and D atoms, respectively. (**E**) Coordination of M ($Ba_{0.5}Ca_{0.35}Na_{0.15}$) toward D(6*b*) in DM6 octahedra and D(12*d*) in DM4 tetrahedra. (**F**) Three-dimensional isosurface plots of the probability density of hydrogen in the 4 × 4 × 4 supercell obtained through MPNN–MD simulations at 600 K. The isosurface of 1×10^{-4} Å^{-3} is depicted in yellow. The heat maps displayed on the lattice sections illustrate the probability densities ranging from 1×10^{-4} to 5×10^{-3} Å^{-3}. (**G**) Contour plots showing hydrogen probability density at $z = 0.75$ in the cross-section obtained through MPNN–MD simulations. The o and t symbols denote the octahedral (6*b*) and tetrahedral (12*d*) sites, respectively. The probability densities are presented on a log scale from 10^{-2} to 10^{-5} Å^{-3}, with contour plot intervals of 0.5 in logarithmic scale. (**H** and **I**) Hydrogen migration trajectories obtained through MPNN–MD simulations at 400 K. Hydrogen atoms were visualized using a white-red color gradient corresponding to elapsed simulation time (Δt).

Try this simple, science-backed trick to fall asleep faster

I struggle with getting good sleep. What can I do about it?

Try heating up your feet at night with one of these methods:

- Take a warm bath or shower.
- Do a quick foot soak in warm water.
- Wear socks to sleep.

Warming the extremities before bed has been shown to help people fall asleep more quickly. It does so as well as many over-the-counter sleep aids.

Decades of studies have confirmed this effect. An oft-cited 1999 study published in Nature found that the degree of dilation of the blood vessels in the feet, such as occurs when we wear warm socks, was the best predictor of how quickly people would fall asleep — more so than melatonin levels or even how "sleepy" the subjects felt.

And a randomized controlled trial of 46 men over the age of 60 found that warming the feet in the bath one hour before bedtime every night for six weeks resulted in improvements in how quickly the men fell asleep and how long they slept. These findings have been supported by multiple additional studies in older adults.

If you do opt for a full-on warm bath or shower, a 2019 meta-analysis found that doing so even for as little as 10 minutes one or two hours before bed helped people fall asleep about nine minutes quicker and boosted sleep efficiency — that is, the time of objectively measured sleep compared to time spent in bed.